UNIVERSIDAD NACIONAL AUTÓNOMA DE MÉXICO

Maestría y Doctorado en Ciencias Bioquímicas

TnaA modula la expresión de los genes Hox y de algunos genes responsivos a Notch en discos de ala de *Drosophila melanogaster*

TESIS

QUE PARA OPTAR POR EL GRADO DE:
Doctor en Ciencias

PRESENTA:
M. en C. Marco Antonio Rosales Vega

TUTOR:
Dra. Martha Verónica Vázquez Laslop
Instituto de Biotecnología, UNAM.

MIEMBROS DEL COMITÉ TUTOR:
Dr. Luis Fernando Covarrubias Robles
Instituto de Biotecnología, UNAM.

Dr. Juan Rafael Riesgo Escovar
Instituto de Neurobiología, UNAM.

Cuernavaca, Morelos. Agosto, 2024.

A mis papás y mi hermano
que están para mí
incondicionalmente

AGRADECIMIENTOS INSTITUCIONALES

Este trabajo fue realizado en el Instituto de Biotecnología, en el departamento de Genética del Desarrollo y Fisiología Molecular, en el laboratorio 15 del edificio Norte, bajo la tutoría de la Dra. Martha Verónica Vázquez Laslop.

Durante mi doctorado se obtuvo apoyo económico por parte del Programa de Apoyo a los Estudios del Posgrado (**PAEP**) para la asistencia al congreso de genética de *Drosophila* con sede en San Diego, California en Marzo del 2017

Investigación realizada gracias al Programa de Apoyo a Proyectos de Investigación e Innovación Tecnológica (**PAPIIT**) de la UNAM **IN202220**. Agradezco a la DGAPA-UNAM la beca recibida.

Agradezco al Consejo Nacional de Humanidades, Ciencias y Tecnología (**CONAHCyT**) por mi beca de Doctorado No. **307929.**

El comité tutoral que asesoró el desarrollo del presente trabajo, estuvo conformado por:

Dra. Martha Verónica Vázquez Laslop
Instituto de Biotecnología, UNAM

Dr. Luis Fernando Covarrubias Robles
Instituto de Biotecnología, UNAM

Dr. Juan Rafael Riesgo Escovar
Instituto de Neurobiología, UNAM

A los sinodales que estuvieron presentes en mi examen de candidatura y que aportaron valiosos comentarios a esta tesis: la Dra. Alejandra Covarrubias, la Dra. Hilda Lomelí, la Dra. Ingrid Fetter, la Dra. Elizabeth Ortiz y el Dr. Daniel Ríos.

Durante el desarrollo de esta tesis, se recibió asesoría por parte del Dr. Mario Enrique Zurita Ortega y de la Dra. Viviana Valadez Graham.

Durante el desarrollo experimental de esta tesis, se recibió apoyo por parte de la laboratorista María del Carmen Muñoz García.

A todos mis compañeros y amigos del laboratorio durante estos diez años: Maritere, Alyeri, Silvia, Grisel, Sara, Cynthia, Adriana, Andrea, Joselyn, Juan Manuel, Samantha, Eduardo, Florencia, Irving, Bruce, Zazil y a todos los que pudiera estar omitiendo.

AGRADECIMIENTOS

A mi papá, Juan Antonio, porque siempre has tenido fe en mi y me has impulsado a seguir adelante desde que era un niño. Gracias por enseñarme disciplina, por ayudarme a tener la mente abierta y por tu apoyo durante estos tiempos difíciles tanto económica como espiritualmente.

A mi mamá Micaela, quien todos los días se esfuerza por dar lo mejor de sí misma, gracias por ser un ejemplo para que entendiera el valor de ser perseverante. Gracias por cuidarnos en la enfermedad, que es cuando mas lo necesitamos y en la salud, que es cuando menos lo valoramos.

A mi hermano mayor, Mauricio Antonio, quien me ayuda a ser un mejor hombre e hijo. Gracias por ayudarme a desarrollar mi imaginación a través del juego desde pequeño, porque es esta imaginación la que hoy me hace posible recorrer este camino. Sigue siendo tu mejor versión para inspirar a las nuevas generaciones que necesitan de tu ejemplo.

A mi mamá académica, Martha Vázquez, quien me enseñó la disciplina y el amor para recorrer el sendero de la excelencia académica. Gracias por la motivación, el apoyo y por las largas horas discutiendo nuestros datos con singular alegría.

El capitulo mas oscuro de esta tesis es el que no se cuenta, el de las horas mas oscuras y tristes del estudiante que redacta. A todos los amigos y familiares que me ayudaron a salir adelante y pudiera estar omitiendo, muchas gracias.

Dejo para el final, por ser el agradecimiento más importante a Dios, por iluminarme durante este recorrido, por darme sabiduría y paciencia durante todo este tiempo. GRACIAS.

PROTESTA UNIVERSITARIA DE INTEGRIDAD Y HONESTIDAD ACADÉMICA Y PROFESIONAL

De conformidad con lo dispuesto en los artículos 87, fracción V, del Estatuto General, 68, primer párrafo, del Reglamento General de Estudios Universitarios y 26, fracción I, y 35 del Reglamento General de Exámenes, me comprometo en todo tiempo a honrar a la Institución y a cumplir con los principios establecidos en el Código de Ética de la Universidad Nacional Autónoma de México, especialmente con los de integridad y honestidad académica.

De acuerdo con lo anterior, manifiesto que el trabajo escrito titulado:

TnaA modula la expresión de los genes Hox y de algunos genes responsivos a Notch en discos de ala de *Drosophila melanogaster.*

Que presenté para obtener el grado de Doctor es original, de mi autoría y lo realicé con el rigor metodológico exigido por mi programa de posgrado, citando las fuentes de ideas, textos, imágenes, gráficos u otro tipo de obras empleadas para su desarrollo.

En consecuencia, acepto que la falta de cumplimiento de las disposiciones reglamentarias y normativas de la Universidad, en particular las ya referidas en el Código de Ética, llevará a la nulidad de los actos de carácter académico administrativo del proceso de graduación.

ATENTAMENTE

M. en C. Marco Antonio Rosales Vega

No de cuenta. 514025177

LISTA DE SIGLAS, SÍMBOLOS Y ABREVIATURAS

A/P. Antero-Posterior
abd-A. *abdominal A*
Abd-B. *Abdominal B*
Antp. *Antennapedia*
BAP. "Brahma Associated Proteins"
brm. *brahma*
DNA. "Deoxyribonucleic acid"
D/V. Dorso-Ventral
Dfd. *Deformed*
FGTs. Factores generales de la transcripción
IR. "Inner ring"
IRE. "Inner Ring Enhancer"
lab*. labial*
pb. *proboscipedia*
PcG. Grupo Polycomb
PRE. "Polycomb Responsive Element"
N. *Notch*
OR. "Outer ring"
PBAP. "Polybromo associated BAP"
RNA. "Ribonucleic acid"
Scr. *Sex combs reduced*
Su(H). *Suppressor of Hairless*
SUMO. "Small ubiquitin modifier"
TF. Factor transcripcional
tna. *tonalli*
trxG. Grupo trithorax
TSS. "Transcription start site"
Ubx. *Ultrabithorax*
wg**.** *wingless*

TABLA DE CONTENIDO

RESUMEN

Los genes del grupo trithorax se requieren para mantener activa la expresión de los genes Hox en *Drosophila melanogaster. tonalli* (*tna*) pertenece al grupo trithorax (trxG) y codifica para diversas isoformas que tienen un dominio SP-RING característico de un tipo de E3 ligasas de SUMO. La SUMOilación es una modificación postraduccional de proteínas que causa cambios en su función y/o localización. *tna* se identificó por su interacción genética con genes que codifican subunidades del complejo remodelador de la cromatina BRAHMA/BAP para regular la expresión de los genes homeóticos *Antennapedia, Ultrabithorax* y *Sex combs reduced*. *tna* codifica al menos dos transcritos *tna-RD* y *tna-RA* y a dos isoformas $TnaA_{123}$ y $TnaA_{130}$. Las isoformas de TnaA presentan una compartamentalización subcelular diferencial durante la embriogénesis. El análisis de las isoformas de TnaA presentes en animales con una mutación ($tna^{EY22929}$) que afecta principalmente al transcrito *RA* nos permitió determinar que los transcritos *RD* y *RA* codifican a las isoformas $TnaA_{123}$ y $TnaA_{130}$, respectivamente. Asimismo, la comparación de la sobrevivencia de individuos con una reducción selectiva de $TnaA_{123}$ con la de sus hermanos/as con dosis normales de TnaA, nos permitió determinar que $TnaA_{123}$ es necesaria para alcanzar la etapa adulta mientras que $TnaA_{130}$ es dispensable para esta función. En trabajos previos se mostró que *tna* pertenece al grupo trithorax, ya que al mutarlo se suprimen fenotipos de pérdida de función de *Polycomb* (*Pc*) en faratos y adultos. Con el mismo ensayo, durante mi doctorado, mostré que TnaA es necesaria para la expresión de *Ultrabithorax* y *Sex combs reduced* en los discos imagales de larvas de tercer instar. Datos previos del laboratorio mostraron que TnaA se localiza en sitios discretos de la cromatina de cromosomas politénicos de glándulas salivales de larvas de tercer instar. Durante mi doctorado, profundicé este análisis y encontré que TnaA está en alrededor de 100 bandas. Lo anterior nos motivó a determinar los sitios donde se encuentra TnaA en la cromatina mediante ChIP-seq en glándulas salivales y discos imagales de ala. En congruencia con lo determinado en los cromosomas politénicos, los análisis de ChIP-seq mostraron que TnaA está en alrededor de 100 sitios en la cromatina. Uno de los sitios en donde se encuentra TnaA se localiza río arriba de *wingless* (*wg*), que es un gen esencial para el desarrollo de todos los organismos multicelulares, por lo que nos enfocamos en determinar el papel de TnaA en la expresión de *wg* en discos de ala. *wg* tiene múltiples “enhancers” embrionarios y de discos imagales. Por ChIP-qPCR encontramos que TnaA se encuentra en la cromatina del “enhancer” que dirige la expresión de *wg* en el anillo interno para modular su expresión en discos de ala. Este trabajo demuestra que TnaA puede modular la expresión de sus blancos en momentos cruciales del desarrollo, puesto que al menos una de sus isoformas se encuentra en regiones regulatorias altamente específicas de la cromatina de sus genes blanco.

1. INTRODUCCIÓN

1.1 El papel de los “enhancers” en la transcripción de los genes eucariontes

El desarrollo de los organismos multicelulares está determinado en gran parte por la información genética contenida en su genoma. La información genética incluye a los genes y a los elementos regulatorios que determinan su expresión en el tiempo y el espacio.

La expresión génica comienza con la transcripción, que es el proceso de copiar una secuencia de DNA a un transcrito de RNA con ayuda de una RNA polimerasa (RNA Pol). En eucariontes, existen tres RNA polimerasas distintas y la RNA polimerasa II (RNA Pol II) es la que transcribe a los genes que codifican para las proteínas, los RNAs pequeños nucleares y los microRNAs. La transcripción de un gen inicia en un sitio denominado TSS (“Transcription Start Site”). El TSS está localizado en el extremo 5’ del gen y está rodeado por distintas secuencias que conforman la región central del promotor (también denominada región “core” del promotor). El promotor sirve como una región de anclaje para la RNA Pol y los factores generales de la transcripción (FGTs), que pueden ser de diferentes tipos de acuerdo a las secuencias que lo conforman (revisado en Sloutskin et al., 2021).

El mapeo experimental de los TSS a nivel de una sola base muestra distintos mecanismos de inicio de la transcripción, lo cual ha llevado a la clasificación de promotores como “enfocados” si tienen un solo TSS bien definido y “dispersos” si tienen múltiples TSS espaciados y cercanos entre sí. Los promotores enfocados se encuentran preferencialmente en genes con patrones de expresión tejido-específico, mientras que la iniciación dispersa es más común en genes de “housekeeping” y se expresan en múltiples tipos celulares (revisado en Sloutskin et al., 2021).

Los promotores son suficientes para dirigir la transcripción de un gen, sin embargo, la mayoría tienen una baja actividad basal. En eucariontes, existen múltiples secuencias regulatorias que pueden influir en la actividad del promotor central. Algunas de ellas son las regiones silenciadoras o “silencers” que disminuyen la actividad basal del promotor mientras que los “enhancers” o potenciadores aumentan la actividad de los promotores y ambas pueden estar cerca (a dos bases) o lejos (a megabases) y/o en las regiones 5' ó 3' del promotor que regulan.

En algunos casos los “enhancers” pueden funcionar independientemente de su orientación (revisado en Panigrahi y O'Malley, 2021) y muchos presentan especificidad por un promotor en particular (revisado en Galouzis y Furlong, 2022). Los “enhancers” son regiones de unión de múltiples factores transcripcionales (FTs), los cuales son claves para regular la expresión espacio-temporal de un gen. No todas las proteínas que se encuentran en los “enhancers” se unen directamente al DNA, sino que se unen a los FTs, enzimas modificadoras, remodeladores de la cromatina o a los nucleosomas del “enhancer”, modulando así la expresión génica.

1.2 TnaA y la vía de SUMOilación

TnaA es una E3 ligasa de SUMO (Monribot-Villanueva et al., 2013). La SUMOilación es una modificación postraduccional que puede aumentar la estabilidad, alterar la función y modificar la interacción de las proteínas SUMOiladas (revisado en Varejão et al., 2020). SUMO (Small Ubiquitin MOdifier) es una proteína pequeña estructuralmente similar a la ubiquitina. La conjugación de SUMO se lleva a cabo en residuos de lisina de la proteína blanco con motivos consenso [ψ-K-x-D/E], donde "ψ" es un aminoácido hidrofóbico, "K" una lisina, "x" es cualquier aminoácido y "E/D" puede ser un ácido aspártico o un ácido glutámico (Rodriguez et al., 2001).

La SUMOilación es un proceso reversible que inicia con la generación de una proteína SUMO madura mediante un corte proteolítico mediado por las proteasas de la familia Ulp/SENP. Posteriormente, SUMO se conjuga a una cisteína de la enzima activadora (E1) en un proceso dependiente de ATP. Después, SUMO se transfiere a la enzima Ubc9 (E2) que, a su vez, conjuga a SUMO a una lisina de su proteína blanco. Las E3 ligasas de SUMO como TnaA, juegan un papel importante en este proceso, al estimular la actividad de Ubc9 o al facilitar la formación del complejo Ubc9-sustrato. Por lo tanto, las E3 ligasas aumentan la especificidad de E2-SUMO por su sustrato (revisado en Varejão et al., 2020). TnaA es una E3 ligasa de tipo SP-RING y se ha mostrado que en *Drosophila melanogaster* (*D. melanogaster*) interacciona físicamente con la enzima E2 y con subunidades del complejo remodelador de la cromatina BRAHMA/BAP (Monribot-Villanueva et al., 2013).

La SUMOilación juega un papel importante en el desarrollo de *D. melanogaster* desde etapas embrionarias tempranas (revisado en Lomelí y Vázquez, 2011; Talamillo et al., 2020). SUMO y las enzimas de la vía de la SUMOilación se encuentran enriquecidas particularmente durante etapas tempranas del desarrollo de *D. melanogaster* (revisado en Talamillo et al., 2020).

Los estudios de proteómica en diversos modelos han evidenciado la presencia de cientos o miles de proteínas SUMOiladas en un momento dado (Hendriks y Vertegaal, 2016), a pesar de que hasta ahora solo se han identificado alrededor de una decena de E3 ligasas de SUMO. Este fenómeno aun es objeto de investigación. Se plantea la posibilidad de que la regulación fina de la expresión y la localización de las E3 ligasas permita la SUMOilación de múltiples proteínas en contextos específicos (Pichler et al., 2017).

1.3 *tna* es un gen del grupo trithorax

tna es un gen del trxG que se define como un grupo de genes necesarios para mantener la expresión correcta de los genes Hox. Los genes Hox codifican para FTs que determinan la identidad de los segmentos corporales a lo largo del eje antero-posterior desde etapas embrionarias tempranas y promueven el desarrollo de

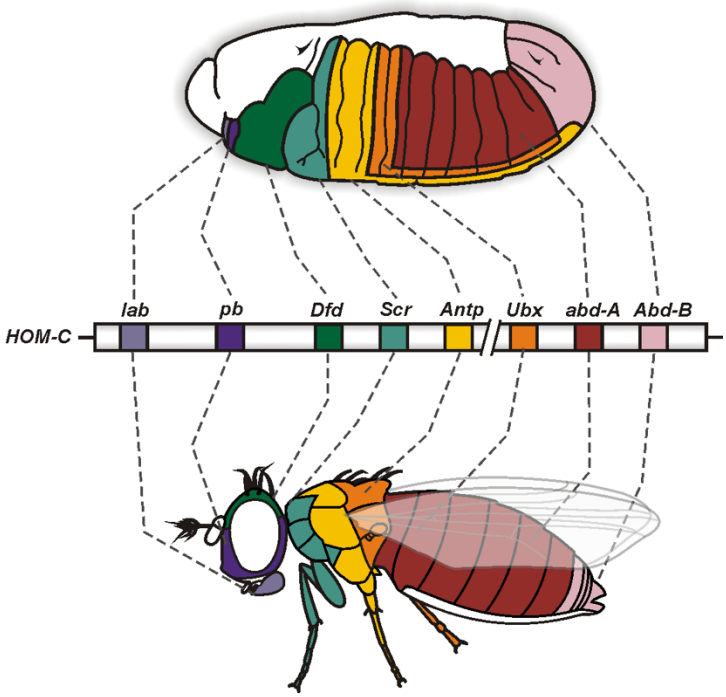

Figura 1. Los genes Hox determinan la identidad de los segmentos de *D. melanogaster*. Los genes Hox se expresan (indicados con un color distinto) en segmentos específicos desde las etapas embrionarias hasta la etapa adulta. Entre el embrión y el adulto se muestran el complejo Antennapedia (conformado por *lab, pb, Dfd, Scr y Antp*) y el complejo Bithorax (conformado por *Ubx, abd-A y Abd-B)* separados por dos líneas diagonales (//).

diferentes rasgos morfológicos mediante el control de programas genéticos específicos (Figura 1) (revisado en Pearson et al., 2005 y en Sánchez-Herrero, 2013).

La regulación de la expresión de los genes Hox en el tiempo y en el espacio debe ser muy precisa para alcanzar el desarrollo apropiado de las estructuras corporales. En el embrión temprano la expresión de los genes Hox se activa por proteínas codificadas por los genes de segmentación (revisado en Clark et al., 2019). Subsecuentemente, cuando los genes de segmentación dejan de expresarse, la expresión correcta de los genes Hox en los segmentos apropiados se mantiene gracias a las proteínas del trxG, mientras que las proteínas del grupo Polycomb (PcG) mantienen reprimida su expresión en los segmentos donde no se necesitan (revisado en Kassis et al., 2017). Esta delicada interacción entre las proteínas del PcG y trxG es esencial para mantener el patrón de expresión de los genes Hox durante el desarrollo del organismo.

Dentro del trxG existen genes que codifican para subunidades de complejos remodeladores de la cromatina. En *D. melanogaster*, se han identificado al menos dos de estos complejos BRAHMA de la familia SWI/SNF. BAP (del inglés “Brahma Associated Proteins”) y PBAP (del inglés “Polybromo Associated BAP”). Ambos complejos comparten a Brahma, que es la ATPasa dependiente de DNA, y a otras seis subunidades conocidas como Moira (Mor), Snr1, Bap60, Bap55, Bap111 y actina.

Osa es la subunidad única del BAP mientras que Polybromo y Bap170 son las subunidades características del PBAP (Mohrmann et al., 2004; Chalkley et al., 2008). *tna* se identificó porque interacciona genéticamente con subunidades del complejo BRAHMA/BAP *brahma* (*brm*) y *osa* (*osa*) para la expresión correcta de los genes Hox (Gutiérrez et al., 2003). Además, TnaA coinmunoprecipita con Osa y Brahma en embriones (Monribot-Villanueva et al., 2013).

1.4 TnaA en el desarrollo de los discos imagales en *D. melanogaster.*

Los fenotipos de falta de función de *tna* se observan en tejidos que provienen de discos imagales. Los discos imagales de *D. melanogaster* son tejidos compuestos por células no diferenciadas que se generan desde etapas embrionarias y son los precursores de algunas partes de la cabeza, el cuerpo de la mosca y sus apéndices. Los discos se forman durante la embriogénesis, a partir de un grupo de alrededor de 30-50 células que se invaginan para formar una estructura en forma de saco que prolifera rápidamente durante las etapas larvarias para formar discos maduros de alrededor de 30,000 células. Mientras que la mayor parte de los discos están formados por células epiteliales, también se encuentran unidos a neuronas, glía, mioblastos y células traqueales. Durante su desarrollo, los discos adoptan formas complejas y se subdividen en distintas regiones establecidas por la expresión controlada de múltiples vías de señalización. Finalmente, durante la etapa de pupa, los discos experimentan procesos morfogenéticos y luego se diferencian para formar tejidos específicos en los adultos.

A partir de los discos imagales de ala se forman las alas y el tórax dorsal de la mosca adulta. Durante su desarrollo, el disco se subdivide en distintos ejes cardinales (Figura 2AB). Los primeros intentos para elucidar el destino de las regiones del disco de ala fueron experimentos de corte y trasplante de fragmentos del disco (Bryant 1975). Lo anterior fue posible en parte gracias a que el disco de ala de larvas de tercer instar tiene una forma característica que hace que sus regiones sean fácilmente identificables. Por ejemplo, la asimetría del disco permite identificar fácilmente las regiones anterior y posterior. En general, el disco se subdivide en el “Pouch”, que es una región de forma ovoide que da lugar al ala, el “Hinge” que da lugar a la bisagra localizada en la base del ala y al “Notum” que da lugar a la mayor parte del tórax posterior de la mosca (revisado en Tripathi e Irvine 2022; Figura 2A).

Los discos imagales de pata darán lugar a las patas de la mosca adulta y parte del tórax de la misma. Todos los discos de pata se desarrollan de manera similar (Schubiger et al., 2012), con excepción de los discos del primer par de patas de machos, en los cuales se desarrollan los peines sexuales. En general, los discos de pata se dividen en cinco segmentos: coxa, trocánter, fémur, tibia y cinco segmentos del tarso (Figura 2B).

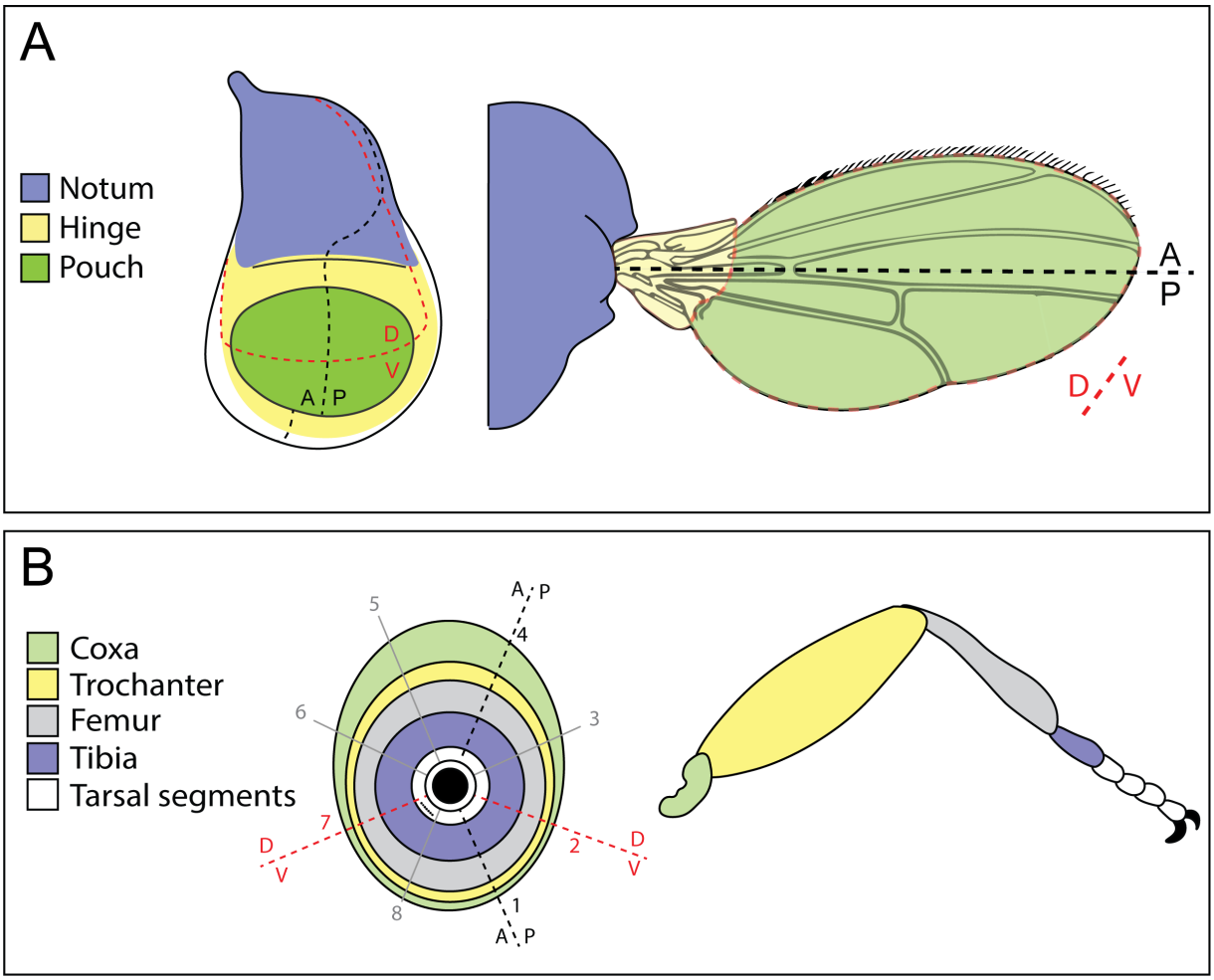

Figura 2. Mapa de destino de los discos imagales de ala y pata de *D. melanogaster.* (**A**) Mapa de destino del disco de ala. Se indican el "Pouch", el "Hinge" y el "Notum" que darán lugar al ala, a la bisagra y al tórax dorsal de la mosca adulta, respectivamente. En ambos paneles los ejes A/P (negro) y D/V (rojo) están marcados con líneas punteadas gruesas. (**B)** Mapa de destino del disco de pata T1. Los segmentos de la pata se desarrollan a partir de cada uno de los segmentos concéntricos del disco de pata del más proximal al distal. Se indican coxa, trocánter, fémur, tibia y los segmentos tarsales.

wingless (*wg*) es un gen importante para el desarrollo de los discos imagales. Nosotros encontramos a TnaA en una región localizada río arriba de *wingless* (*wg*) (ver Antecedentes) y fue objeto de estudio en uno de los dos artículos que aquí presento. *wg* codifica a una proteína que se secreta para coordinar la formación de patrones con la proliferación de ciertos tejidos (revisado en Wiese et al., 2018). En el disco de ala, *wg* se expresa en cuatro regiones distintas. En un grupo de células a lo largo del límite D/V, en dos anillos concéntricos conocidos como anillo interno (IR) y externo (OR) y en una región conocida como banda dorsal.

En el límite D/V, la expresión de *wg* está regulada por la vía de Notch, la cual se activa por la interacción del dominio extracelular de Notch con sus ligandos Delta y Serrate (de la familia DSL). Lo anterior resulta en el corte, procesamiento y maduración de una región del dominio intracelular de Notch, el cual se transporta al

núcleo para unirse con su efector Su(H) (de la familia CSL) y a otras proteínas coactivadoras o correpresoras para modular la expresión de sus genes blanco, como *wg* (Kopan e Ilagan, 2009). En el IR, la expresión de *wg* está regulada por proteínas como Nubbin y Rotund (del Alamo-Rodríguez et al., 2002). Estos FTs probablemente participen en la activación de la expresión de *wg* mediada por el "enhancer" del anillo interno (*IRE*). Sin embargo, los mecanismos que activan a este "enhancer" aún no se entienden con detalle.

2. ANTECEDENTES

tna es un gen esencial y los individuos con pérdida de función de *tna* no alcanzan la etapa adulta salvo en contadas excepciones. Sin embargo, sí llegan a etapas avanzadas de desarrollo y estos individuos presentan diversos fenotipos mutantes similares a los encontrados en individuos con la pérdida de función de algunos genes Hox (quetas ectópicas en el halterio, la pérdida de cerdas en el peine sexual de los machos y la extensión permanente de las alas) (Gutiérrez et al., 2003).

Ubx y *Scr* se requieren desde la embriogénesis temprana para determinar la identidad de los segmentos corporales y su expresión permanece en los discos imagales que provienen de dichos segmentos. Dado que los fenotipos de pérdida de función de los Hox en mutantes de *tna* se observan en tejidos adultos provenientes de los discos imagales, decidimos analizar la expresión de *Ubx* y *Scr* en discos imagales de mutantes de *tna* (ver más adelante).

tna codifica al menos dos isoformas proteicas conocidas como $TnaA_{123}$ y $TnaA_{130}$. Estas isoformas son las más abundantes a lo largo del desarrollo, aunque reportes previos muestran que existen otras isoformas que son específicas de algunas etapas de desarrollo (Monribot-Villanueva et al., 2013) o que son poco abundantes en diversos estadíos (datos no publicados). Previo a este trabajo, pensábamos que estas

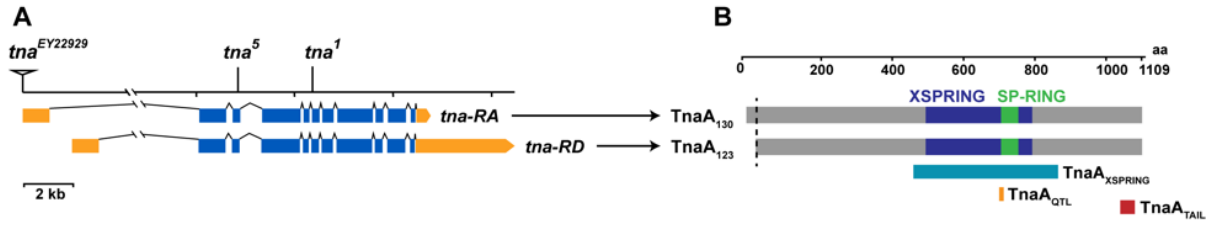

Figura 3. **Isoformas de TnaA presentes en larvas de tercer instar con diferentes genotipos mutantes *tna*.** (**A**) Región genómica de los transcritos *tna-RA* y *tna-RD* [los exones no traducidos y traducidos se muestran en amarillo y azul, respectivamente (Gutiérrez et al., 2003)], se indican las lesiones (triángulos para inserciones y líneas verticales para mutaciones puntuales). (**B**) Isoformas de TnaA (gris) y su procedencia a partir de los transcritos *RA* y *RD* (flechas que provienen del panel A), nótese que la diferencia entre las isoformas radica en la región amino terminal (línea punteada). Se indica al XSPRING (morado) y al SP-RING (verde). Se muestran las regiones blanco de los anticuerpos policlonales $TnaA_{XSPRING}$ (turquesa), $TnaA_{QTL}$ (amarillo) y $TnaA_{TAIL}$ (rojo) (Modificada de la Figura 1 de Rosales-Vega et al., 2018).

isoformas podían provenir de distintos transcritos o ser el resultado del procesamiento de una de ellas (Gutiérrez et al., 2003; Monribot-Villanueva et al., 2013). Sin embargo, ahora es claro que el transcrito *RD* codifica a la isoforma $TnaA_{123}$, mientras que el transcrito *RA* codifica a la isoforma $TnaA_{130}$ (Figura 3). Ambas isoformas se expresan de manera diferencial durante el desarrollo y su compartamentalización en embriones indica que la isoforma $TnaA_{130}$ es citoplásmica, mientras que la isoforma $TnaA_{123}$ es preferentemente nuclear (Monribot-Villanueva et al., 2013). No obstante, no podemos descartar la posibilidad de que esta compartamentalización cambie durante el desarrollo.

En el transcurso de mi maestría y doctorado continué el estudio iniciado por otros compañeros (A. Juárez, Z. Palomera, y M. Vázquez) sobre la presencia de TnaA en los cromosomas politénicos de las glándulas salivales de larvas de tercer instar. Determiné que TnaA se encuentra en alrededor de 100 bandas en estos cromosomas (de un total de 3852 bandas), lo cual sugiere que TnaA participa en la regulación de la expresión de un grupo selecto de genes. Posteriormente, junto con la M. en C. A. Hernández, montamos la técnica de ChIP-seq para determinar las regiones en las que se encuentra TnaA en la cromatina tanto en las glándulas salivales como en los discos de ala. Encontramos que, al igual que en el análisis de TnaA en cromosomas politénicos, esta proteína se encuentra en pocos sitios en la cromatina de estos tejidos (alrededor de 100). Con los datos de discos de ala, encontramos que TnaA se encuentra en una región río arriba de *wg*.

3. HIPÓTESIS

Dado que $TnaA_{123}$ es nuclear y se encuentra en sitios específicos en la cromatina, proponemos que es la isoforma esencial para la sobrevivencia y que su función se ejerce en regiones regulatorias como “enhancers” y promotores de sus genes blanco, incluidos los genes Hox y *wg*.

4. OBJETIVOS

4.1 Objetivo general

Determinar si $TnaA_{123}$ es esencial para la sobrevivencia y para regular la expresión de sus genes blanco, incluidos los genes Hox y *wg,* en discos imagales de larvas de tercer instar.

4.2 Objetivos particulares

1. Determinar la procedencia de las isoformas $TnaA_{123}$ y $TnaA_{130}$ y su papel en la supervivencia a etapa adulta.

2. Determinar si TnaA afecta la expresión de los genes *Hox* en discos imagales de larvas de tercer instar.

3. Determinar si TnaA regula la expresión de *wg* en diferentes regiones del disco de ala de larvas de tercer instar.

4. Corroborar los datos de ChIP-seq que indican que TnaA se encuentra en la cromatina de un "enhancer" de *wg* en discos de ala.

5. RESULTADOS

Para entender cómo se generan las isoformas prioritarias de TnaA estudiamos animales con una mutación (*tna*^{EY22929}) que afecta principalmente al transcrito *RA*, lo cual nos permitió determinar que los transcritos *RD* y *RA* codifican a las isoformas $TnaA_{123}$ y $TnaA_{130}$, respectivamente. Asimismo, la comparación de la sobrevivencia de individuos con una reducción selectiva de $TnaA_{123}$ con la de sus hermanos/as con dosis normales de TnaA, nos permitió determinar que $TnaA_{123}$ es necesaria para alcanzar la etapa adulta mientras que $TnaA_{130}$ dispensable en estas etapas.

Además, analizamos el papel de TnaA en la expresión de los Hox directamente en los discos imagales de larvas de tercer instar y encontramos que TnaA es importante para la regulación de la expresión de *Ubx* y *Scr*.

Este trabajo resultó en la publicación de un artículo original con arbitraje donde soy primer autor y se anexa a continuación:

Rosales-Vega, M., Hernández-Becerril, A., Murillo-Maldonado, J. M., Zurita, M. y Vázquez, M. (2018). The role of the trithorax group TnaA isoforms in Hox gene expression, and in *Drosophila* late development. *PLOS ONE* **13**, 1-22.

PLOS ONE

RESEARCH ARTICLE

The role of the trithorax group TnaA isoforms in Hox gene expression, and in *Drosophila* late development

Marco Rosales-Vega[1], Adriana Hernández-Becerril[1], Juan Manuel Murillo-Maldonado[1,2¤], Mario Zurita[1], Martha Vázquez[1]*

1 Departamento de Fisiología Molecular y Genética del Desarrollo, Instituto de Biotecnología, Universidad Nacional Autónoma de México, Cuernavaca, Morelos, México, **2** Departamento de Neurobiología del Desarrollo y Neurofisiología, Instituto de Neurobiología, Universidad Nacional Autónoma de México, Querétaro, Querétaro, México

¤ Current address: Departamento de Neurobiología del Desarrollo y Neurofisiología, Instituto de Neurobiología, Universidad Nacional Autónoma de México, Querétaro, Querétaro, México
* mvazquez@ibt.unam.mx

OPEN ACCESS

Citation: Rosales-Vega M, Hernández-Becerril A, Murillo-Maldonado JM, Zurita M, Vázquez M (2018) The role of the trithorax group TnaA isoforms in Hox gene expression, and in *Drosophila* late development. PLoS ONE 13(10): e0206587. https://doi.org/10.1371/journal.pone.0206587

Editor: Amit Singh, University of Dayton, UNITED STATES

Received: August 1, 2018

Accepted: October 16, 2018

Published: October 29, 2018

Data Availability Statement: All relevant data are within the manuscript and its Supporting Information files.

Funding: This work was supported by funds from Dirección General de Asuntos del Personal Académico (DGAPA), Programa UNAM-PAPIIT grant IN208316 (http://dgapa.unam.mx/index.php/pf-papiit) to MV. MR-V and AH-B are doctoral students from Programa de Doctorado en Ciencias Bioquímicas, Universidad Nacional Autónoma de

Abstract

Regulation of developmental gene expression in eukaryotes involves several levels. One of them is the maintenance of gene expression along the life of the animal once it is started by different triggers early in development. One of the questions in the field is when in developmental time, the animal start to use the different maintenance mechanisms. The trithorax group (TrxG) of genes was first characterized as essential for maintaining homeotic gene expression. The TrxG gene *tonalli* interacts genetically and physically with genes and subunits of the BRAHMA BAP chromatin remodeling complex and encodes TnaA proteins with putative E3 SUMO-ligase activity. In contrast to the phenocritic lethal phase of animals with mutations in other TrxG genes, *tna* mutant individuals die late in development. In this study we determined the requirements of TnaA for survival at pupal and adult stages, in different *tna* mutant genotypes where we corroborate the lack of TnaA proteins, and the presence of adult homeotic loss-of-function phenotypes. We also investigated whether the absence of TnaA in haltere and leg larval imaginal discs affects the presence of the homeotic proteins Ultrabithorax and Sex combs reduced respectively by using some of the characterized genotypes and more finely by generating TnaA defective clones induced at different stages of development. We found that, *tna* is not required for growth or survival of imaginal disc cells and that it is a fine modulator of homeotic gene expression.

Introduction

Homeotic (Hox) genes determine the segmental identity in *Drosophila*. In *Drosophila* Hox genes are in two complexes, the bithorax (BX-C) and the Antennapedia (ANTP-C) complexes. The initiation of Hox expression in specific segments occurs during embryogenesis and it is controlled by maternal and segmentation genes. Later on the activation or repression are

México (UNAM) and have scholarships 307929 and 453402 respectively from CONACyT. The funders had no role in study design, data collection and analysis, decision to publish, or preparation of the manuscript.

Competing interests: The authors have declared that no competing interests exist.

maintained in the appropriate segments by proteins encoded by genes that belong to the trithorax group (TrxG) or the Polycomb group (PcG) respectively. Several TrxG and PcG proteins are involved in chromatin dynamics (reviewed by [1]). *Drosophila* has two types of the SWI/SNF chromatin remodeling complex BRAHMA (BAP and PBAP), which have as a catalytic ATPase, the Brahma protein. These two types have common and specific subunits. Common subunits are Brahma and Moira, while Osa is a specific subunit of BAP. Brahma, Moira and Osa are encoded by TrxG genes [2–4]. *tonalli* (*tna*) is a TrxG gene that was identified because it modifies *brahma* (*brm*), *osa* (*osa*) and *moira* (*mor*) [5].

tna encodes $TnaA_{130}$ and $TnaA_{123}$, two TnaA isoforms that presumptively have E3 SUMO ligase activity (see ahead, and [6]). These isoforms are derived either from different transcripts [7] and/or as a result of the processing of some of them [6]. $TnaA_{130}$ and $TnaA_{123}$ isoforms are differentially expressed during development and have specific compartmentalization within the cell [6].

SUMOylation is a post-translational modification similar to ubiquitination that adds a SUMO moiety to target proteins through the action of common activating E1 and conjugation E2 enzymes that in *Drosophila* are represented by single proteins. In contrast, there are several types of E3 ligases that choose or help the SUMOylation of a target protein. SUMOylation of a target protein can change its sub-compartmentalization within the cell or nucleus, can favor a change of partners and/or it can label it for degradation (revised in [8]). The PIAS (Protein Inhibitors of Acivated STAT [Signal Transducers and Activators of Transcription]) family is a subgroup of E3 SUMO ligases that interact physically with E2 enzymes through a canonical 42 amino-acidic residues SP-RING (Siz/PIAS-Really Interesting) zinc finger [9]. TnaA share with the PIAS family the SP-RING [9] but this zinc finger is embedded in a unique 300 amino-acidic residues XSPRING (eXtended SP-RING) domain that is found in a few insect and vertebrate proteins and that is not present in the PIAS proteins [5]. TnaA physically interacts with *Drosophila* SUMO conjugating enzyme E2 *in vivo* and it coimmunoprecipitates with the Osa and Brm proteins from the BRM complex in embryo extracts [6].

Hox gene expression starts early at embryonic stages and prevails late in development. Therefore, it is controlled at each stage and tissue by different selected transcription factors that act on specific regulatory regions of each Hox gene (reviewed in [10]). Thus, it is probable that chromatin accessibility of these regulatory regions is under fine control involving chromatin remodelers and/or modifiers. As a TrxG gene, *tna* is required for the maintenance of expression of Hox genes [5], and adult animals with mutations in *tna* or in *tna* and *brm*, or *osa* mutations, show phenotypes that resemble Hox loss-of-function revealed in adult cuticular structures. One of the characteristics that make *tna* unique among TrxG genes is that it is required late in development [5], being the lethal phase of *tna* third instar larvae and pupal stages [5, 6]. As *tna* was identified as a *brm*-modifier gene and animals with *tna* mutant combinations reach the pharate stage and die before reaching adulthood presenting Hox loss-of-function phenotypes [5], one hypothesis is that its function is required to maintain Hox gene expression by facilitating chromatin remodeling by the BRAHMA BAP complex at these late stages of development. These facts make TnaA protein(s) interesting to study for the function they could have to ensure correct gene expression at these stages of development.

In this work we explored TnaA requirements for the expression of the Hox genes *Ultrabithorax* (*Ubx*) and *Sex combs reduced* (*Scr*), through immunostaining of the respective Hox proteins in imaginal discs of late third instar larvae with mutant *tna* genotypes, or in TnaA defective clones generated at different stages of development. We found that although animals derived from these experiments do present Hox loss-of-function adult cuticular phenotypes, the wild-type domains of Hox expression are not visibly altered in imaginal discs. In contrast, ectopic Hox expression is suppressed in *tna* mutant backgrounds, leading to the conclusion

that TnaA finely modulates Hox gene expression in imaginal cells and that its function can only be observed when Hox gene expression is not robustly regulated.

Material and methods

Ethics statement

All animals handling was approved by the Instituto de Biotecnología, UNAM, Bioethics Committee, Permit Number 359 (2018/05/04), which follows NOM-062 animal welfare Mexican law. All efforts were made to minimize animal suffering. Animals were sacrificed by CO_2 euthanasia.

Fly strains, and genetic procedures

The lesions of *tna* alleles and the target of the interference RNAs (RNAi) used in this work are represented in Fig 1A and, unless otherwise noted, they are described in Flybase [7]. Briefly, tna^1 and tna^5 are EMS-induced mutations. In tna^1 Gln 566 changed to a stop codon [5]. tna^5 was recovered after EMS mutagenesis in a genetic screen to identify *brm*-interacting mutations. The lesion is a T for A change at base 10,857,881 (genome release version 6) [11] that correspond to the limit between exon 3 and 4 (where exon 1 is UTR) from tna-RD and that affects the splicing of a 451 bp intron present in all *tna* transcripts (J. A. Kennison, personal communication). $tna^{EY22929}$ is a P{EPgy2} element insertion [12]. *tna* knockdown was achieved by expressing interference RNA (RNAi) from lines $tna^{GD12331}$ (inserted either in chromosome 2, or in chromosome 3) from Vienna GD collection (vector pGD264, construct ID 12331 Vienna *Drosophila* Resource Center, [13]), and $tna^{JF02536}$ from Perrimon's pVALIUM10-derived TRiP [14] collections using different drivers. Drivers used in this work were *Act5C-GAL4* [15] for ubiquitous expression, and *MS1096-GAL4* [16], and *A9-GAL4* [17] were used to drive gene expression to the dorsal region of the haltere pouch. Fly cultures and crosses were performed according to standard procedures. Flies were raised on yeast-molasses media at 25˚C unless otherwise noted.

Lethality of individuals carrying heteroallelic combinations of *tna* alleles was determined by counting the Tb^+ progeny from crosses between parents with *tna* alleles balanced with *In(3LR) TM6B* (tna^+) carrying the larval/pupal marker Tb^1, and the adult markers Dr^{Mio}, or Sb^1. To evaluate pupariation and adult survival rates of heteroallelic *tna* individuals, and the survival of *tna* knocked-down flies, we performed a χ^2 test (significance set at $P<0.05$), comparing the number of *tna* heteroallelic animals (*tna/tna*) with the one of their *tna*/+ siblings in each genotype. For the eclosion rate analysis, we performed a t-test ($P<0.05$), comparing the proportion of eclosed/total heteroallelic *tna/tna* pupae (non-Tubby). At least two crosses were performed for each genotype.

Loss-of-function Hox phenotypes were scored in adult animals from $tna^1/tna^{EY22029}$, with *tna* knockdown and from crosses where imaginal tna^1 clones were induced (see Induction of Mitotic Clones section), and compared their appearance on control animals derived from crosses without the tna^1 *FRT2A* chromosome and thus tna^+. Three replicas were performed for each experiment. To evaluate the *Scr* loss-of-function phenotype we scored legs from at least 15 males of each genotype. The percentage was calculated by dividing the number of legs with less than nine teeth per sex comb over the number of total male legs scored. Statistical significance was determined with a t-test ($P<0.001$).

To analyze the suppression effect of *tna* mutant alleles on ectopic Hox expression in imaginal discs, immunostaining with the respective Hox protein antibody was performed in at least 40 imaginal discs per genotype of interest, derived from at least three independent replicas per genotype. Statistical significance was determined using a t-test ($P<0.05$) to compare the

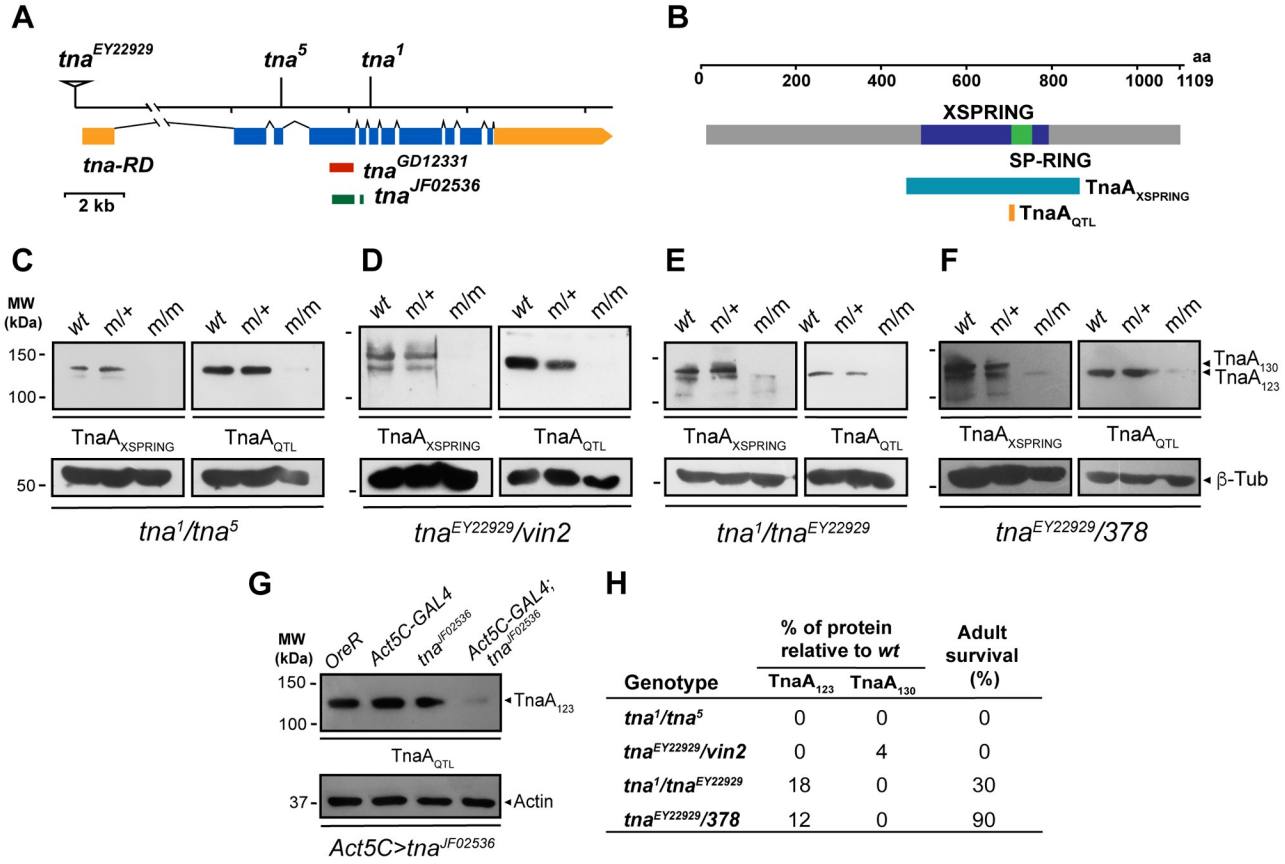

Genotype	% of protein relative to *wt*		Adult survival (%)
	$TnaA_{123}$	$TnaA_{130}$	
***tna*^{1}/*tna*^{5}**	0	0	0
tna*^{EY22929}/*vin2	0	4	0
***tna*^{1}/*tna*^{EY22929}**	18	0	30
tna*^{EY22929}/*378	12	0	90

Fig 1. TnaA isoforms present in third instar larvae with different *tna* mutant genotypes. (**A**) *tna* genomic region of the tna-RD transcript ([11], untranslated and translated exons in yellow and blue respectively) indicating the lesions (triangle for insertion and vertical black lines for point mutations) and the RNAi alleles (region targeted, red and green for *tna*^{GD12331}, and *tna*^{JF02536} respectively) used in this work. (**B**) TnaA protein (grey, 1109 residues) indicating the XSPRING (purple) and SP-RING (green). The regions targeted by the polyclonal antibodies are shown, $TnaA_{XSPRING}$ (turquoise) and $TnaA_{QTL}$ (yellow). TnaA isoforms in different third instar larvae with *tna* mutant genotypes. The genotypes are indicated at the bottom of each panel (**C**-**G**), and they are ordered according to adult survival (**H** and Table 1). The genotypes of the larvae used to prepare the protein extracts tested are *OregonR* (wt), heterozygote *tna*/+ (m/+, Tubby larvae), and heteroallelic *tna* mutant (m/m, non Tubby larvae) (upper part in each panel). Western blots of soluble protein extracts from third instar larvae were probed with $TnaA_{XSPRING}$ (dilution 1:250) and $TnaA_{QTL}$ (1:3000) antibodies as indicated. $TnaA_{XSPRING}$ often detects also a minor 95–110 kDa protein (observed for example in C and D), that it is a *bona fide* TnaA-related product (not seen with preimmune). (**G**) TnaA knockdown in third instar larvae. *tna*^{JF02536} RNAi-expression driven by *Act5C-GAL4*. Larvae were raised at 28˚C. β-tubulin (C-F), and actin (G) were used as loading controls. Note that survival is observed when $TnaA_{123}$ is present (*tna*^{1}/*tna*^{EY22929}, and *tna*^{EY22929}/*378* genotypes). (**H**) Quantification of $TnaA_{123}$ and $TnaA_{130}$ in larvae with the mutant-indicated genotypes and their adult survival according to Table 1. Note that even low amounts of $TnaA_{123}$ are enough to allow animals to reach adulthood. (*tna*^{1}/*tna*^{EY22929}, and *tna*^{EY22929}/*378* genotypes). The percentage was calculated relative to the amount of each isoform observed in the wild-type *OreR* larvae using the $TnaA_{XSPRING}$ antibody (left in each panel).

https://doi.org/10.1371/journal.pone.0206587.g001

number of discs from *tna* transheterozygous animals showing ectopic Hox suppression and the number of *Pc*^{3} discs showing ectopic Hox expression.

Antibodies, production and affinity purification of TnaA antibodies

To detect TnaA in this work, we used two polyclonal rabbit antibodies, anti-$TnaA_{XSPRING}$, and anti-$TnaA_{QTL}$ raised against regions of the $TnaA_{PD}$ isoform identified and sequenced by Gutiérrez *et al*., (2003) and reported by Flybase [11]. Rabbit anti-$TnaA_{XSPRING}$ was raised as the one from rat reported in Monribot-Villanueva *et al*., (2013) immunizing animals with a purified GST fusion protein harboring the entire XSPRING domain contained in aminoacids 433–856 of TnaA. Anti-$TnaA_{QTL}$ was raised against the 14-mer QTLHKRNLLPLEHS peptide

(aminoacids 691–704) by New England Peptide. Both antibodies (Fig 1B) were affinity-purified from total sera.

For Western blot assays, affinity-purified primary rabbit anti-$TnaA_{QTL}$ and anti-$TnaA_{X\text{-}SPRING}$ antibodies were used at 1:3000 and 1:250 dilutions respectively. Mouse anti-β-tubulin (E7, Developmental Studies Hybridoma Bank) and anti-actin (JLA20, Developmental Studies Hybridoma Bank) were used each at 1:3000 dilution. Secondary antibodies were anti-rabbit HRP goat IgG (H+L) (65–6129) and anti-mouse HRP goat IgG/IgA/IgM (H+L) (A10668) (Invitrogen).

To detect Hox proteins Ubx and Scr, we used monoclonal antibodies FP3.38 [18] for Ubx, and 6H4.1 [19] for Scr. To detect Osa we used monoclonal Osa 15A8 [20]. These three antibodies were purchased from Developmental Studies Hybridoma Bank. Secondary antibodies anti-rabbit and anti-mouse Alexafluor 568 goat (red), and anti-rat Alexafluor 594 (Invitrogen) were used for confocal microscopy.

Protein extraction and analyses

Larval soluble protein extracts for Western analyses were obtained either by homogenizing whole larvae in lysis buffer (250 mM sucrose, 50 mM Tris pH 7.5, 25 mM KCl, 5 mM $MgCl_2$, Complete protease inhibitor (ROCHE), 5 mM EDTA, 1% SDS) or by inverting the anterior part of half larvae according to Cunningham *et al*., (2012) [21] directions, where 10–20 third instar larvae were cut in half and inverted to remove trachea, gut and adipose tissue. In this case the remaining tissue including central nervous system, imaginal discs and salivary glands was homogenized in lysis buffer (PBS, 1% Triton X-100, 1 mM $MgCl_2$, 5 mM EDTA and Complete protease inhibitor from ROCHE). Extracts obtained in either way were centrifuged at 10,000 g for 10 minutes at 4˚C to remove cell debris. The proteins were separated by SDS-PAGE and electro-transferred onto nitrocellulose membranes for Western blot analyses. Immunoblots were done according to standard procedures and proteins of interest were detected with specific antibodies with the kits Supersignal West Pico, and Femto Chemiluminescent Substrates from Thermo Scientific, according to manufacturer's instructions.

Quantification of TnaA isoforms in mutant genotypes was done by using the densitometry measurement tool from ImageJ (Fiji). Raw values were normalized according to the respective loading control in each lane, and final values were expressed as a percentage of protein relative to the one found in wild-type animals.

Induction of mitotic clones

The tna^1 allele recombined into an *FRT2A* chromosome (tna^1 *FRT2A*) was a kind gift from J. A. Kennison. tna^1 clones were induced either with the *hs-FLP* [22] or the *Ubx-FLP* [23, 24] drivers as FLPase sources.

To induce clones in imaginal discs with heat shock, we basically used the protocol reported by [25]. Briefly, clones were induced in the progeny of the cross tna^1 *FRT2A/TM6B*, *Tb*, *Dr* X *hs-FLP*; +; *Ubi-GFPX2 FRT2A* that was set up at 25˚C. Clones were induced in the progeny at 24 h after egg laying (AEL) with a single 37.5˚C heat shock for 1 h. Some clones in haltere discs were induced in an egg collection of 4 h, applying a heat shock of 38.5˚C for 1 h to the progeny at 9 h AEL.

We also used the *Ubx-FLP* [24], that induces recombination through a *Ubx* enhancer that is active in all imaginal discs (IDE, Imaginal Disc Enhancer), identified in the PBX-41 segment [23]. Crosses were set with *Ubx-FLP*/Y; tna^1 *FRT2A/TM6B*/+ X +; *Ubi-GFP FRT2A*, or males +; *FRT82B* osa^{308}*/TM6B Dr*, *Tb* X *Ubx-FLP*; +; *FRT82B Ubi-mRFP* at 25˚C. Animals with induced clones either with *hs-FLP* or with *Ubx-FLP* were kept at 25˚C until they reached 110

to 115 h AEL, where discs were dissected for immunostaining with the antibodies of interest and observed using confocal microscopy as stated in the next section, or animals were allowed to reach the adult stage to estimate cuticular Hox loss-of-function phenotypes.

Immunostaining of imaginal discs and cuticle preparations

Wing and haltere discs were obtained from male and female third instar larvae. Male first leg discs were isolated from sexed third instar larvae to study *Scr* expression. Immunostaining of imaginal discs were done as described by Blair (2000) [26] with some modifications. Briefly, imaginal discs were dissected in cold 1X PBS and fixed with 4% paraformaldehyde for 30 min at room temperature. Discs were washed with PBT (1X PBS with 0.2% Triton X-100), blocked for 1 h with 0.1% bovine serum albumine in PBST 1X with 250 mM NaCl at 4˚C. Primary antibodies were added at appropriate dilutions overnight at 4˚C, and the next day discs were washed with PBT. Secondary antibodies were added together with Hoechst (0.1 ug/ml) for 2 h at room temperature washed again with PBST and after removal of PBST, discs were mounted in 80% glycerol, 4% *n*-propyl gallate in 1X PBS and stored in darkness until observation in confocal microscopy.

Fluorescent images from immunostained imaginal discs, or for detection of Hox proteins or apoptotic cells (TUNEL assay), were acquired with an Olympus Inverted FV1000, or a 2P Upright confocal FV1000 confocal microscopes with a 20X 0.75 or 60X 1.3 numerical aperture objectives. Images were processed using ImageJ (Fiji) and Adobe Photoshop CS software.

Adult cuticle preparations were processed by standard procedures by boiling flies in 10% KOH, washed in distilled water, and mounting them in glycerol 50% to observe them in a Nikkon Eclipse E600 upright microscope equipped with an Amscope MU500 digital camera.

Cell survival analyses

To assess the role of *tna* on cell survival, we compared the areas of both tna^{1}/tna^{1} ($GFP^{-/-}$), and tna^{+}/tna^{+} twin-spot ($GFP^{+/+}$) clones induced 24 h AEL. Images were analyzed with ImageJ (Fiji) to measure the area of 13 clones and their twin spots. A paired t-test was used to assess significant differences in their respective areas ($P<0.05$) (S1 Fig).

To determine whether tna^{1}/tna^{1} genotype could cause cell death, we performed a TUNEL (Terminal deoxynucleotidyl-transferase-mediated dUTP Nick end Labeling) cell-death assay, with the *In Situ* Cell Death Detection kit TMR red, (Roche, cat. no. 12156792910), according to manufacturer instructions. Apoptotic cells in wing imaginal discs of genotype *MS1096-GAL4 UAS-ras*^{V12} *UAS-dlg*^{RNAi} were used as a positive control. For the cell death assay, imaginal discs were dissected, fixed and washed as for immunostaining. Confocal images were captured as stated in the previous section.

Results

tna is required at late phases of development

Pharates deficient in *tna* present cuticular Hox loss-of-function phenotypes [5]. To further study the effect of Hox gene expression in imaginal discs lacking TnaA at larval stages, we inspected with more detail a selected *tna* allelic set of combinations producing animals that die between the third instar larval stage and adulthood (Table 1). We used the *tna* alleles (Fig 1A) tna^{1} [5], tna^{5} that is a null allele [6], and $tna^{EY22929}$ [12] that is a P{EPgy2} element insertion at 5' end of *tna*. We combined each of these alleles between them, and with two chromosomal deficiencies that uncover *tna*, *Df(3L)378* and *Df(3L)vin2*. We also knocked down *tna* expression by inducing the expression of two different RNAi constructs, $tna^{JF02536}$ from the TRiP

Table 1. Survival of animals with *tna* mutant genotypes at pupal and adult stages.

	PUPAE		ADULTS
	Pupariation Rate[b] (Observed/ Expected)[c]	**Eclosion Rate[b] (Eclosed/Total *tna/tna* Pupae)[d]**	**Survival[b] (Observed/ Expected)[c]**
Relevant Genotype[a]			
***tna*^{1}**			
tna^{5}	147/495[e] (30)	0/147 (0)	0/476[e] (0)
Df(3L)378	115/392 (29)	0/115 (0)	0/383 (0)
Df(3L)vin2	84/215 (39)	0/84 (0)	0/174 (0)
***tna*^{5}**			
Df(3L)378	129/204 (63)	0/129 (0)	0/172 (0)
Df(3L)vin2	90/155 (58)	0/90 (0)	0/112 (0)
***tna*^{EY22029}**			
tna^{1}	139/132 (105)[ns]	63/139 (45)	37/123 (30)
tna^{5}	132/153 (86)[ns]	117/132 (89)[ns]	110/144 (76)[ns]
Df(3L)378	231/253 (91)[ns]	207/231 (90)[ns]	188/207 (90)[ns]
Df(3L)vin2	307/380 (81)[ns]	0/307 (0)	0/317 (0)

[a]. Relevant genotype shows the *tna* alleles in heteroallelic animals evaluated. The alleles carried by parental males are shown in bold at the top of each section.

[b]. Puparium formation, eclosion rate, and adult survival were evaluated in progeny from the same crosses in at least two independent replicas. Statistical significance in each case was determined with a χ^2 or t-test ($P<0.05$) as stated in Material and Methods. Non-significant differences are indicated (ns).

[c]. The percentage (in parentheses) of *tna/tna* heteroallelic individuals (non-Tubby pupae or non-Sb and/or non-Dr adults) was calculated taking as 100% the *tna/* Balancer individuals in progeny (half of the Tubby pupae or half of the Sb and/or Dr adults).

[d]. Percentages of eclosed pupae (in parentheses) were calculated dividing the number of eclosed over the total number of *tna/tna* (non-Tubby) (non-eclosed plus eclosed) pupae.

[e]. The disparity between the numbers of expected pupae and adults (compare first and third columns) is caused because the balancer chromosomes from mothers and fathers have Tubby as a larval/pupal marker, and in adults one balancer chromosome carried Sb and the other one has Dr. It was not possible to distinguish which balancer chromosome carry each Tubby pupae counted, but one class carrying one of the parental balancer chromosomes is more lethal than the other. When divided by two, to calculate the expected *tna/tna* progeny we found a difference between the number of Tb eclosed pupae and Sb or Dr adult flies. e. g. first lane: Half of Tubby pupae = 495. Adults with Dr marker = 476.

https://doi.org/10.1371/journal.pone.0206587.t001

collection [14] and *tna*^{GD12331} from the Vienna GD collection [13] directed towards different regions of *tna* mRNAs (Fig 1A).

The genetic analyses we made involve the determination of pupal and adult survival of animals with heteroallelic *tna* combinations (Table 1). We evaluated the number of heteroallelic animals that reach the pupal stage, and of those we counted how many were able to eclose from their pupal cases. We found that *tna*^{1} is the strongest allele tested. This is expected because we have shown previously that *tna*^{1} is a dominant negative mutation [6]. Only between 30–40% of the expected animals with *tna*^{1} as one of the alleles in the genotype (together with *tna*^{5} or with *Df(3L)378* and *Df(3L)vin2*), reach the pupal stage. Close to 60% of the animals with *tna*^{5} (together with any of the two deficiency chromosomes) reach the pupal stage, dying before reaching adulthood. In contrast, 80–100% of the animals with *tna*^{EY22929} reach the pupal stage. None of the pupae with *tna*^{1} or *tna*^{5} were able to eclose from their pupal cases, with the notorious exception of combinations of these alleles with *tna*^{EY22929} allele where some animals survive until adulthood. 45–90% of animals with *tna*^{EY22929} eclose (with the exception of animals harboring also *Df(3L)vin2* that die as pupae), and from those 30–90% do reach adulthood. Of notice, all the adult animals of *tna*^{1}/ *tna*^{EY22929} genotype present the held-out wings phenotype (Fig 2A) that was the base for the identification of *tna* as a *brm*-modifier in our original screen [5]. Adult flies with *tna*^{1}/ *tna*^{EY22929}, or *tna*^{EY22929}/*Df(3L)378* genotypes,

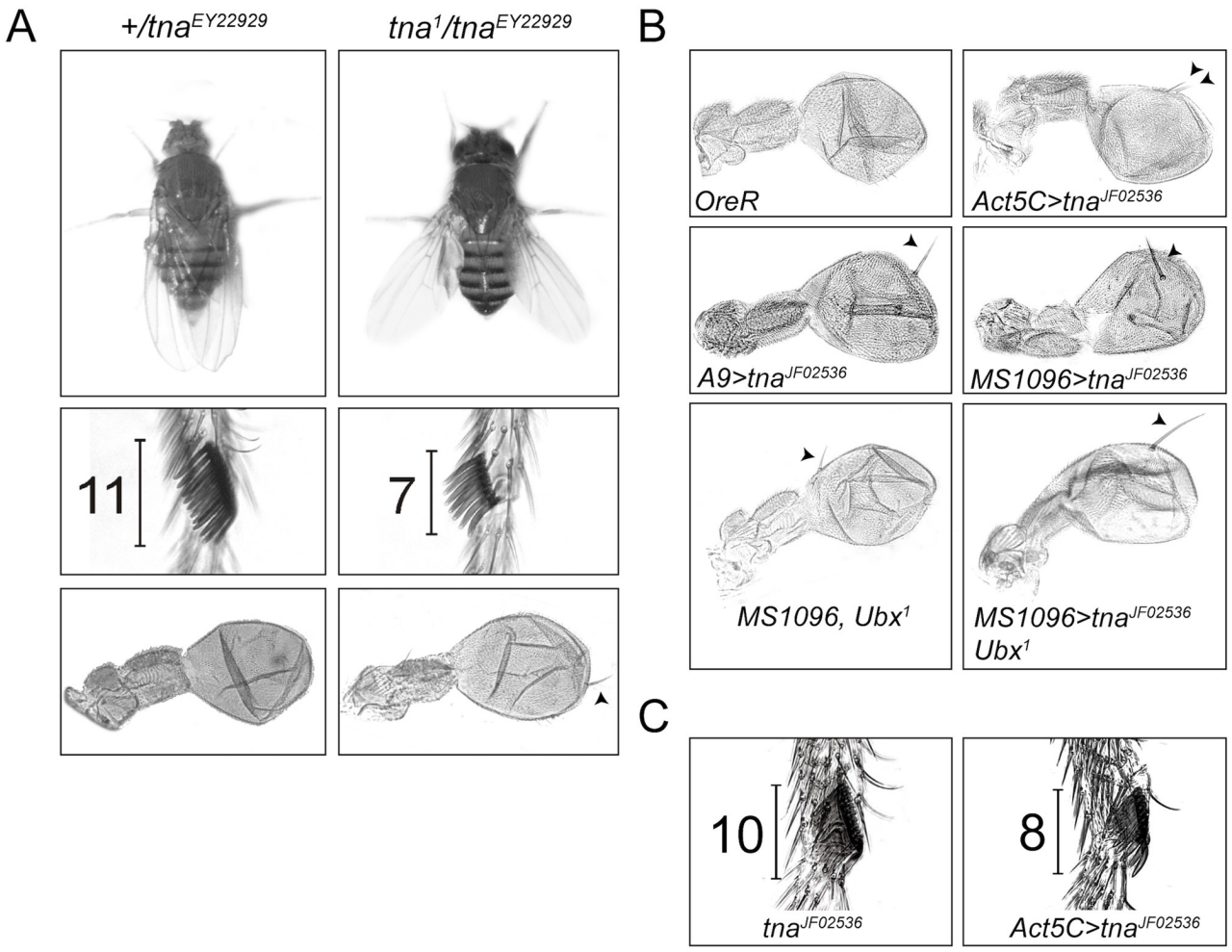

Fig 2. Hox transformations in *tna* mutant and *tna* knocked down adult animals. (**A**) Held-out wing (upper), reduction of the number of sex comb teeth in first leg of males (middle) and ectopic bristle in the haltere (lower), indicating loss-of-function of *Antennapedia* (*Antp*) *P2* promoter, *Scr*, and *Ubx* respectively, in $tna^{EY22929}/tna^{1}$ (right), compared to wild type phenotypes (left) in $tna^{EY22929}/+$ flies. (**B**) Appearance of ectopic bristles in halteres indicates a haltere-to-wing transformation in flies expressing the RNAi produced by the $tna^{JF02536}$ allele with different GAL4 drivers (*Act5C*, *A9*, *MS1096*) (right). Parental flies with the mentioned drivers (not shown) have halteres with wild-type phenotypes (*OreR* haltere in upper left picture). Note that the location of the ectopic bristle in animals with *tna* knockdown, depends on the location where the *tna* RNAi is directed. (**C**) Males with ubiquitous *tna* knockdown ($Act5C>tna^{JF02536}$), do not survive to adulthood. Presented here is the first leg of a pupal male individual with a decrease in the number of sex comb teeth (right) compared to wild type (left). For percentages of these phenotypes see Table 2.

https://doi.org/10.1371/journal.pone.0206587.g002

present Hox loss-of-function phenotypes such as loss of sex comb teeth in male first legs (*Scr*), and partial haltere to wing transformation (*Ubx*) (Fig 2A and Table 2).

As *tna locus* harbors different transcripts that produce different isoforms, mainly $TnaA_{130}$ and $TnaA_{123}$, we were interested in correlate which of them was present in larvae of the genotypes studied. We performed Western analyses with anti-TnaA antibodies (Fig 1B) that detect both $TnaA_{130}$ and $TnaA_{123}$ isoforms ($TnaA_{XSPRING}$) or $TnaA_{123}$ preferentially ($TnaA_{QTL}$) in protein soluble extracts from larvae of some of the genotypes tested and from its siblings that carried a wild type *tna* allele for comparison (Fig 1C–1F). We also tested animals with genotypes that included the tna^{-} *Df(3L)378* and *Df(3L)vin2* deficiency chromosomes (Fig 1D and 1F). Animals with combinations that include either one of these deficiencies, survive up to the third instar larvae stage in significant percentages (from 30–90% of the expected individuals, Table 1) and then die as pupae. This fact allows us to analyze protein extracts from these

Table 2. Hox phenotypes in adults with *tna* mutant genotypes, with *tna* knockdown, or where *tna*⁻ clones were induced in imaginal discs.

Relevant Genotype	*Antp P2* Held-out wings	*Ubx* Haltere to wing[a]	*Scr* < 9 teeth/sex comb[b]
OreR	0/72 (0)	0/72 (0)	0/48 (0)
$tna^{EY22929}$	0/62 (0)	0/62 (0)	0/44 (0)
$tna^{1}/tna^{EY22929}$	54/54 (100)	15/54 (28)	30/39 (77)
$tna^{EY22929}/Df(3L)378$	0/63 (0)	7/63 (11)	32/37 (87)
***tna* knockdown**[c]			
Act5-GAL4	0/85 (0)	0/85 (0)	0/43 (0)
$tna^{JF25036}$	0/96 (0)	0/96 (0)	0/32 (0)
$Act5\text{-}GAL4>tna^{JF25036}$	0/136 (0)	22/136 (16)	4/29 (14)
A9-GAL4	NA	0/110 (0)	NA
$A9\text{-}GAL4>tna^{JF25036}$	NA	53/345 (15)	NA
MS1096-GAL4	NA	0/95 (0)	NA
$MS1096\text{-}GAL4;\ Ubx^{1}$	NA	19/87 (22)	NA
$MS1096\text{-}GAL4>tna^{JF25036}$	NA	12/152 (8)	NA
$MS1096\text{-}GAL4>tna^{JF25036}/Ubx^{1}$	NA	122/142 (86)	NA
Adults from mitotic imaginal clones[NA]			
$hs\text{-}FLP;\ tna^{1}\ FRT2A/Ubi\text{-}GFP\ FRT2A$			
No heat shock	0/47 (0)	0/47 (0)	0/49 (0)
Heat shock[d]	23/159 (15)	1/55 (2)	2/49 (4)
$Ubx\text{-}FLP;\ tna^{1}\ FRT2A$	0/29 (0)	0/29 (0)	0/37 (0)
$Ubx\text{-}FLP;\ tna^{1}\ FRT2A/Ubi\text{-}GFP\ FRT2A$	34/50 (68)	7/50 (14)	0/33 (0)

Percentages are in parentheses. NA is non applicable. The number of individuals showing the indicated Hox loss-of-function phenotypes is statistically significant (t-test, $P<0.01$, see Material and methods). Statistical test was not applicable (NA) for the evaluation of phenotypes of adults from mitotic imaginal clones induction because in principle it was not known how many clones were induced in each case.

[a]. Adult individuals with at least one partially transformed haltere.

[b]. Adult ($tna^{1}/tna^{EY22929}$) or pharate ($Act5\text{-}GAL4>tna^{JF25036}$) males with less than 9 sex comb teeth per leg.

[c]. Flies expressing *tna* RNAi from $tna^{JF25036}$ were raised at 28˚C.

[d]. Heat shock was applied as established in Material and Methods at 24 AEL.

https://doi.org/10.1371/journal.pone.0206587.t002

mutant third instar larvae, making it easier to determine which TnaA isoforms were affected specifically with the *tna* mutant alleles we were testing, given that combined with the deficiency chromosomes, these alleles would be the only source of TnaA. We also analyzed soluble extracts from larvae with *tna* knockdown by the expression of $tna^{JF02536}$ at 28˚C (Fig 1G).

We found that $TnaA_{130}$ disappeared in all the mutant genotypes tested (Fig 1), particularly when one of the alleles is $tna^{EY22929}$, while $TnaA_{123}$ disappears (tna^{1}/tna^{5}, Fig 1C and 1H), or it is still detected at a much lower concentration than in a wild-type condition (see for example, $tna^{1}/tna^{EY22029}$, or $tna^{EY22929}/Df(3L)378$, Fig 1E, 1F and 1H) with antibodies ($TnaA_{QTL}$ and $TnaA_{XSPRING}$). We also found that RNAi expression from $tna^{JF02536}$ at 28˚C, knocked down *tna* expression almost 90% (see ahead, Fig 1G). In particular, we compared $tna^{EY22929}/Df(3L)vin2$ and $tna^{EY22929}/Df(3L)378$ (Fig 1D and 1F) because they give totally different results regarding survival to adulthood (Table 1). While 90% of $tna^{EY22929}/Df(3L)378$ animals survive to adult stages, none of the $tna^{EY22929}/Df(3L)vin2$ animals survive to this stage. In contrast, animals from both genotypes reach the pupal stage with the difference that 100% of $tna^{EY22929}/Df(3L)vin2$ die before they eclose (Table 1). Western analyses are in agreement with these findings given that $tna^{EY22929}/Df(3L)378$ larvae still present some detectable levels of $TnaA_{123}$ protein (Fig 1F and 1H), that may account for their 90% survival to adulthood, meanwhile in

tna^{EY22929}/*Df(3L)vin2* larvae, TnaA$_{123}$ isoform is barely detectable (Fig 1D and 1H) and they present 100% of lethality in adult stages.

These results indicate two findings. First, the presence of TnaA$_{130}$ is not required for survival to adulthood, because animals lacking it, reach this stage (*tna*^{1}/*tna*^{EY22029}, and *tna*^{EY22929}/*Df(3L)378*). We noticed that although *tna*^{1}/*tna*^{EY22929} animals present a slightly higher amount of TnaA$_{123}$ than the one found in *tna*^{EY22929}/*Df(3L)378* animals, the latter ones have a better adult survival (90% compared to 30% of *tna*^{1}/*tna*^{EY22929}). This difference may be due to the fact that *tna*^{1} is a dominant negative [6]. The second finding is that the P{EPgy2} element insertion in the *tna*^{EY22929} allele, is affecting the expression of tna-RA transcript that would be encoding TnaA$_{130}$. Moreover, one of our hypotheses was that TnaA$_{123}$ could originate from TnaA$_{130}$ processing [6], but with these data, we support the hypothesis that TnaA$_{123}$ and TnaA$_{130}$, are translated from different transcripts, being those tna-RD and tna-RA respectively.

For *tna* knockdown, two *UAS-RNAi* constructs, *tna*^{JF02536} and *tna*^{GD12331}, were expressed at 18, 25 and 28˚C with the ubiquitous driver *Act5C-GAL4*. A higher percentage of lethality is observed by increasing *tna* RNAi expression at higher temperatures (Table 3). RNAi expression from either *tna*^{JF02536} or *tna*^{GD12331} alleles caused lethality of pupae and pharates, being males more sensitive than females. *tna*^{JF02536} induction caused more lethality than *tna*^{GD12331} induction and then it was further characterized. The effectiveness of the interference, caused by the expression of the RNAi from *tna*^{JF02536}, was confirmed by the low protein levels found in these larvae (Fig 1G). Females from these experiments reached adulthood in higher percentages than males, but they die within 10 days after eclosion (Table 3). As for *tna*^{1}/ *tna*^{EY22929} animals, knocking down *tna* through RNAi, result in *Ubx* and *Scr* loss-of-function phenotypes at, albeit low, measurable penetrance (Fig 2B and 2C and Table 2). *Act5C-Gal4* is a strong ubiquitous driver. To study the effect of knocking down *tna* in a restricted spatial domain within the haltere, we induced the expression of *tna* RNAi to the dorsal region of the haltere pouch with the GAL4 drivers *MS1096* and *A9* (see Material and methods). The animals from these experiments showed ectopic bristles located mainly in the dorsal region of the haltere capitellum. To test whether this partial transformation was caused by a reduction in *Ubx* expression, we tested whether *tna* knockdown (by expressing RNAi from *tna*^{JF02536}), enhances the loss-of-function *Ubx* phenotypes observed in animals with the null *Ubx*^{1} allele [27]. The

Table 3. Survival of flies with *tna* knockdown.

Relevant Genotype		Survival to adulthood of flies bred at:		
		18˚C	25˚C	28˚C
Act5C-GAL4/+[a]				
tna^{GD12331}	F[b]	95/105 (91)[ns]	81/127 (64)	4/98 (4)
	M[b]	107/114 (94)[ns]	46/97 (47)	0/112 (0)
tna^{JF02536}	F	81/115 (70)	107/222 (48)	5/125 (4)
	M	1/109 (1)	1/183 (1)	3/169 (2)

[a]. *Act5C-GAL4* driver directs ubiquitous expression of *tna*^{GD12331} or *tna*^{JF02536} (Fig 1A).

[b]. Female (F) or male (M) adult progeny expressing the indicated RNAi. The proportion indicates the survival of adult flies expressing the indicated RNAi with respect to the survival of the healthier class in the cross (which is not expressing the RNAi) at the indicated temperature. Percentages of each proportion are in parentheses. Note that survival is more affected in males than in females and it diminishes by increasing the breeding temperature, where RNAi expression is increased. Data are from three independent crosses for each genotype, n = 3, and are statistically significant (χ^2 test, P<0.01), except the ones labeled ns (non-significant).

https://doi.org/10.1371/journal.pone.0206587.t003

result of this genetic combination (Table 2) was the appearance of a single ectopic bristle in the dorsal distal pouch region of the transformed halteres (Fig 2B). *tna* knockdown enhanced the penetrance and the expressivity of the Ubx^1 phenotype (from 22 to 86%, observed as a higher percentage of halteres with a single larger bristle than the one present in halteres of Ubx^1/+ halteres genotype) (Table 2, Fig 2B).

In conclusion, reduction of TnaA dosages caused by different *tna* null or hypomorphic alleles or by knocking down its expression, causes different grades of lethality through development and, when animals are able to form cuticles, homeotic defects caused by loss-of-function of several Hox genes are evident at different extents (penetrances and expressivities).

tna^1 mitotic clones induced either at embryonic or larval stages survive normally

Previously we showed that loss of maternal *tna* function is completely rescued paternally and loss of both maternal and zygotic functions caused lethality primarily at the third larval instar [5]. To further investigate the role of *tna* in imaginal disc cells, we generated *tna* deficient mitotic clones. We recombined the lesion in tna^1 from a tna^1*FRT2A* chromosome (gift from J. A. Kennison, see Methods), with the FLP/FRT system, expressing the FLPase either by heat shock at different times of development (Fig 3A), or under the control of an enhancer active in all discs (Imaginal Disc Enhancer, IDE) [24], identified in the *Ubx* PBX-41 segment [23]. With both methods, we were able to get tna^- GFP^- clones that we checked by immunostaining with the anti-$TnaA_{XSPRING}$ antibody (Fig 3B). We were able to induce *tna* mutant clones in all the discs and we found in general that these clones survive well in all types of imaginal discs. We

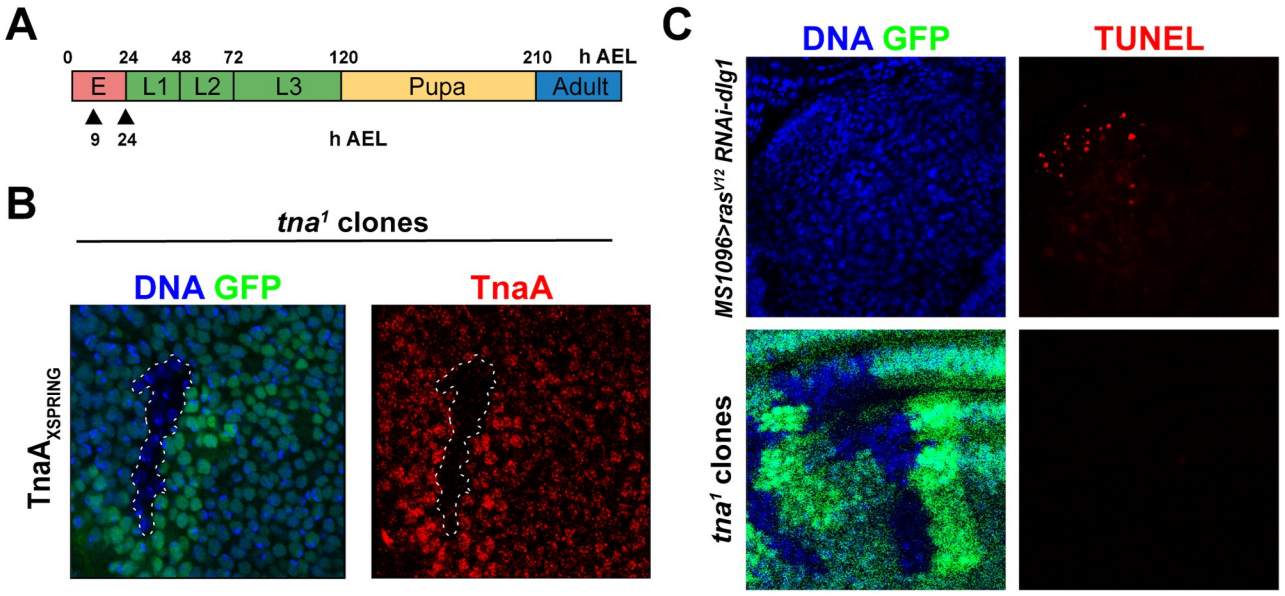

Fig 3. Induction of TnaA defective mitotic clones in third instar imaginal discs at different times of development does not cause cell death. (**A**) Timeline of heat shock pulses (black triangles After Egg Laying, AEL) applied to induce mitotic recombination in animals bearing *hs-FLP* (*hs-FLP*; +; tna^1 *FRT2A/Ubi-GFPX2 FRT2A*). (**B**) Immunostaining of TnaA with the $TnaA_{XSPRING}$ antibody in a wing disc where mitotic clones were induced. DNA was stained with Hoechst (blue) to show nuclear presence. GFP (green) marks the tna^+/tna^- and that did not recombine (medium green intensity), and the tna^+/tna^+ (strong green intensity) cells result of the recombination event. GFP^- marks the tna^-/tna^- clone, as corroborated by the absence of TnaA immunostaining (red). (**C**) TUNEL death assay (red) performed in imaginal discs with tna^- clones (GFP^-), Hoechst (blue), (tna^+ cells are GFP^+, green) (lower panels). As a positive cell death control (red), apoptotic cells were detected in larval discs of the genotype *MS1096-GAL4 UAS-*ras^{V12} *UAS-*dlg^{RNAi} (see text) (upper panels). Note also that in general here and in the next figures, the number and size of the tna^-/tna^- (GFP^-) cells compared to the ones in the tna^+/tna^+ (GFP^+) clone seems to be similar, showing that tna^-/tna^- cells do not present an obvious defect.

https://doi.org/10.1371/journal.pone.0206587.g003

did not notice any change in the size or in the frequency of appearance of the GFP$^-$ *tna*$^-$ clones compared to GFP$^+$ *tna*$^+$ twin spots in discs (GFP panels in Fig 3B, 3C and S1 Fig), with the exception of clones in haltere discs, where we noticed often that the GFP$^+$ twin spot was slightly larger than the *tna*$^-$ GFP$^-$ cells (e. g. GFP panel in Fig 4A). Neither, we observed any effect in cells in the vicinity within the border of *tna*$^-$ clones. We also evaluated cell death by TUNEL in clones made in the wing disc (Fig 3C), finding that there was no difference in survival between *tna*^{1}/*tna*$^+$, *tna*$^+$/*tna*$^+$ cells, and *tna*^{1}/*tna*^{1} mutant clones, while we detect cell death in the dorsal pouch of wing discs where apoptosis and overgrowth are induced by disrupting apical-basal cell polarity (Fig 3C) as reported by [28].

Thus, according to the results of these genetic and immunostaining assays, in general *tna* does not seem to influence cell survival, or cell number or size in imaginal discs.

Influence of TnaA in Hox expression in larval imaginal discs

Our next goal was to study Hox expression in *tna*$^-$ cells in the region of imaginal discs that will become the adult cuticle where loss-of-function homeotic transformations have been characterized. In particular, we focused on *Ubx* and *Scr* expression that is affected in pharates with *tna* mutant genotypes [5], in adults with the genotype *tna*^{1}/ *tna*^{EY22929} (Fig 2A, Table 2), or where *tna* expression has been knocked down through the expression of the RNAi from *tna*^{JF02536} (Fig 2B and 2C, Table 2).

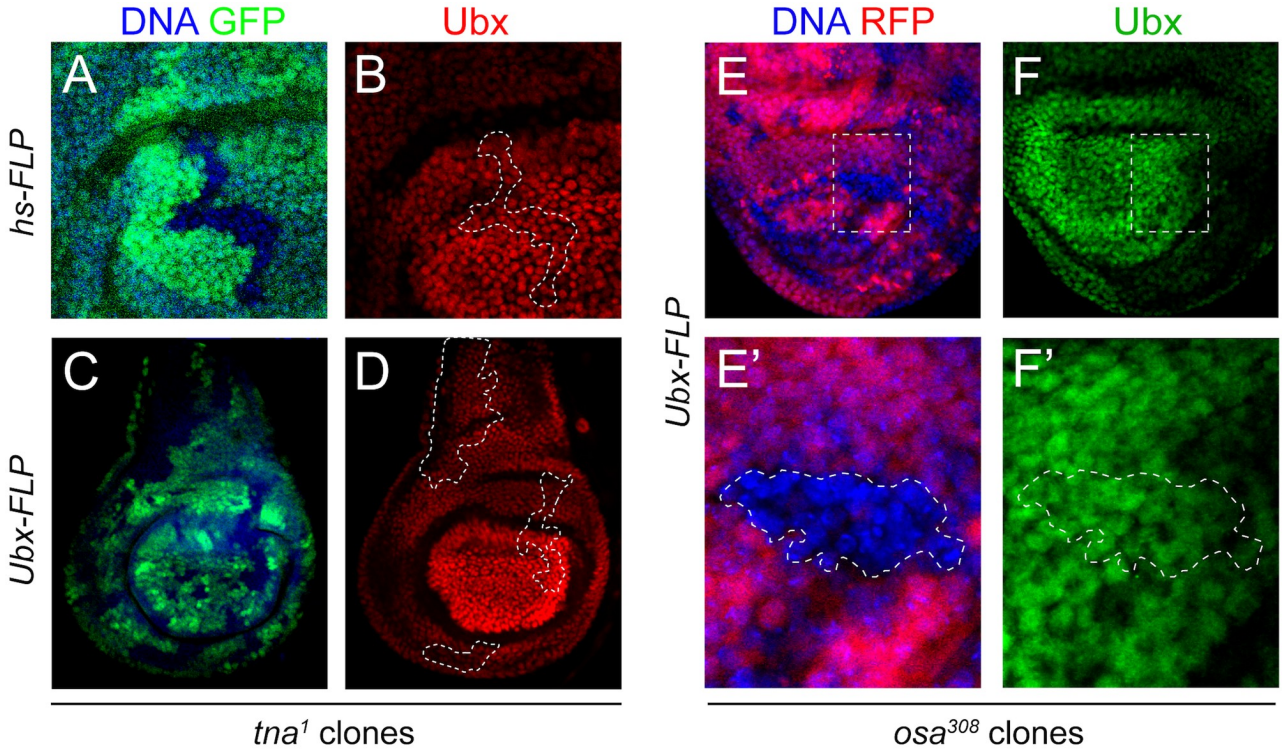

Fig 4. Ubx protein is present in TnaA or Osa defective mitotic clones in haltere discs. TnaA (GFP$^-$ in **A** and **C** and Fig 3B) and Osa (RFP$^-$ in **E** and **E'**, and S3 Fig) defective mitotic clones induced by expressing FLPase either from *hs-FLP* (**A** and **B**) or *Ubx-FLP* (**C**, **D**, **E'**, and **F'**) in haltere imaginal discs. Almost the whole disc is shown in **C** and **D** to note that the absence of TnaA (GFP$^-$) in any region of the disc does not affect the presence of Ubx, which is observed in a wild-type pattern. Ubx protein was immunostained with monoclonal antibody FP3.38 [18] (red signal in **B**, and **D**, and green in **F**, and **F'**). Note that no decrease or absence of the Hox protein Ubx is observed in any of the TnaA$^-$ or Osa$^-$ clones (labeled with pointed white shapes).

https://doi.org/10.1371/journal.pone.0206587.g004

In a wild-type haltere disc, *Ubx* is expressed strongly in the pouch (the region that will become the haltere of the adult fly), being the most prominent the posterior compartment [29] (see for example, Fig 4D). In these regions, Ubx represses several genes that direct wing development [30]. The halteres from the animals with the *tna* mutant aforementioned genotypes, present a mild haltere-to-wing transformation indicated by the presence of ectopic bristles in the haltere capitellum (Fig 2A and 2B). This resembles a loss-of-function phenotype of *Ubx* [30]. Taking into account these observations, we made tna^- (GFP^-) clones in haltere discs by inducing recombination either with an *hs-FLP* (Fig 4A), or with the *Ubx-FLP* (Fig 4C). We dissected haltere discs from animals where clones were induced, and they were immunostained for Ubx (Fig 4B and 4D, red signal). Other animals from the same experiments were allowed to reach the adult stage to evaluate the presence of the ectopic bristles in the haltere (Ubx^- phenotype) (Table 2). We found that the Ubx^- phenotype was present in the halteres of adult flies where clones were induced (2% to 14% when recombination was induced either with heat shock or with the Ubx-FLPase, respectively, Table 2). The presence of this transformation corroborate that cells producing the mutant phenotype in the haltere disc were hit by the recombination event. We tried several protocols to induce tna^- clones at different moments of development (with heat shock at 9 or 24 h AEL as stated in Fig 3A) (Fig 4A) or by getting tna^- clones in several regions of the disc (by driving recombination with the *Ubx-FLP* that is expressed widely in imaginal discs, Fig 4C). We specially looked for clones in the region of the haltere disc that produces the ectopic bristle in the adult halteres in *tna* mutant animals from the same experiments (Table 2), and we could not detect a reduction Ubx (Fig 4B and 4D) in any of the tna^- (GFP^-) clones induced with any of the treatments tested.

Scr is normally expressed in the prothoracic leg imaginal disc mostly in a crescent-shaped region in the anterior half of the disc, and in marginal regions near the disc stalk, specially on the posterior side [19] (for example, Fig 5A). *tna* mutant adults (e. g. $tna^1/tna^{EY22029}$) with decreased TnaA levels (Fig 1E), present *Scr* loss-of-function phenotype [5] (Fig 2A, and Table 2 this work). This phenotype is observed in adult males as a reduction in the number of sex comb teeth in the prothoracic T1 first leg. We immunostained for Scr, leg discs of $tna^1/tna^{EY22029}$ animals finding that decreased TnaA level does not affect immunostaining of Scr (S2 Fig).

Therefore, we generated tna^- (GFP^-) clones in leg discs, inducing recombination by expressing the FLPase under the control of a heat shock promoter (Fig 5B and 5B') (see Material and methods). Some animals were allowed to reach the adult stage, finding that 4% of the first leg of males analyzed have less than nine sex comb teeth (compared to a mean of 10.5 teeth per comb in wild type), phenotype caused by *Scr* loss-of-function (Table 2). tna^- (GFP^-) clones from leg discs of animals of the same experiment were immunostained for Scr (Fig 5C and 5C', red signal) and, as for the $tna^1/tna^{EY22029}$ discs, we could not find any tna^- clone where the signal of Scr immunostaining was reduced.

Osa is a subunit of the BRAHMA chromatin remodeling complex BAP. The *osa* gene interacts strongly with *tna* in a genetic assay of Hox gene expression in pharates and adults [5]. Thus, we also made osa^- (RFP^-) clones in haltere (Fig 4E and 4E', and S3 Fig) discs by inducing recombination of the strong loss-of-function osa^{308} allele [31]. In these Osa^- clones, as in the ones for *tna*, Ubx levels, estimated by immunostaining are not affected (Fig 4F and 4F' green signal), indicating that the requirement of Osa, in the majority of these cells, is not essential for keeping the levels of these Hox proteins.

The penetrance of the *Ubx* and *Scr* loss-of-function phenotypes in animals derived from the experiments where the tna^- clones were induced, was very low (in the best of cases, 14% of halteres with an ectopic bristles, when tna^- clones were induced with Ubx-FLPase, Table 2), and we wondered whether we were not being able to detect by immunostaining the specific cells

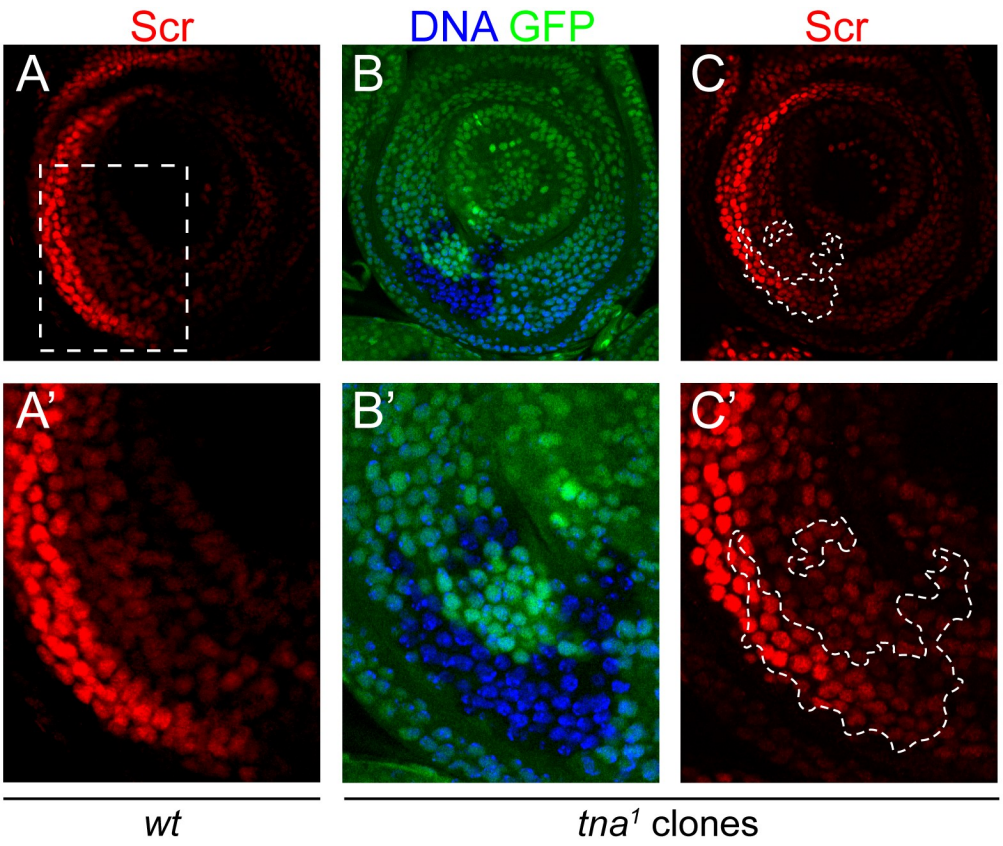

Fig 5. Scr proteins are present in TnaA defective mitotic clones in prothoracic T1 leg imaginal discs. Scr immunostaining pattern in wild type *OreR* prothoracic leg discs (**A**). The disc region from where the sex combs in the first leg are originated in the male is labeled by a pointed rectangle (**A**) and amplified in **A'**. TnaA (GFP$^-$ in **B**-**B'** and Fig 4B) defective mitotic clones induced by expressing FLPase from the *hs-FLP* chromosome in T1 leg imaginal discs. Scr protein was immunostained with the monoclonal antibody 6H4.1 [19] (red signal in **A**-**A'**, and **C**-**C'**). Note that no decrease or absence of Scr is observed in the TnaA$^-$ clones (labeled with pointed white shapes **C**, and amplified in **C'**).

https://doi.org/10.1371/journal.pone.0206587.g005

affected in the haltere or leg discs that would give origin to the transformed tissue in each case (the ectopic bristle found in the transformed halteres or the reduction of the number of sex comb teeth in the first leg of males, Table 2). Thus, we studied the effect of *tna* mutations in a derepressed homeotic background caused by loss of function of Polycomb.

Ubx is normally expressed in the haltere disc while in the wing disc (Fig 6A, shows wing disc organization), *Ubx* expression is observed only in discrete areas such as the peripodial membrane [18] and it is not expressed in the epithelia. *Scr* is normally expressed in the first prothoracic leg imaginal disc (T1), but not in the second and third thoracic leg discs (T2 and T3) (Fig 7A). *Ubx* and *Scr* expression is derepressed in imaginal discs of animals harboring PcG loss-of-function mutations such as Pc^3 (Figs 6C, 6C' and 7B) [32, 33]. Derepression of both, *Ubx* (compare Fig 6B, 6C and 6C') and *Scr* (compare Fig 7A and 7B) can be observed in wing, T2 and T3 leg discs of Pc^3 heterozygote animals respectively. *tna* mutations suppress derepression of both Hox genes evaluated in cuticles from Pc^3 pharate animals [5]. To investigate how *tna* influences *Ubx* and *Scr* expression in this context, we immunostained Ubx and Scr proteins in imaginal discs derived from Pc^3 (Figs 6C, 6C' and 6H and 7B and 7E respectively) and $Pc^3/tna^{EY22929}$ (Figs 6C, 6D, 6D' and 6G and Fig 7C and 7E respectively) animals. As expected, we found ectopic production of both Ubx [94% (44/47) of Pc^3 wing discs with

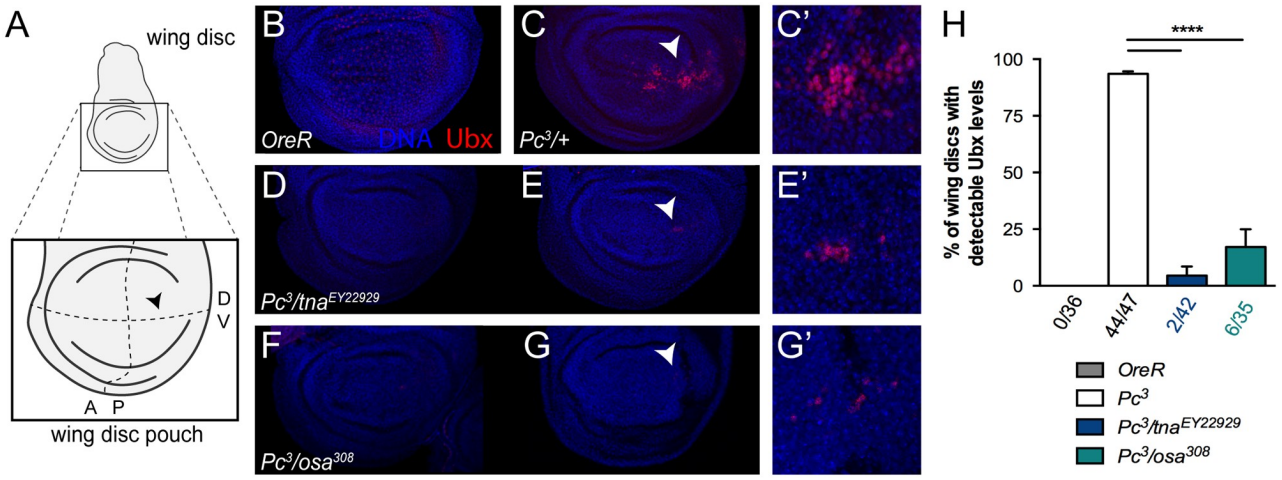

Fig 6. TnaA and Osa are necessary for ectopic presence of Ubx protein in wing Pc^3 imaginal discs. (**A**) Wing disc organization. The posterior dorso-ventral margin is indicated (black arrowhead). Immunostaining of Ubx protein (red) with the FP3.38 [18] antibody in wild type *OreR* (**B**), Pc^3 (**C**, and **C'**), $Pc^3/tna^{EY22929}$ (**D, E-E'**), and Pc^3/osa^{308} (**F, G-G'**) wing discs. Discs were also stained with Hoechst to observe nuclei (blue). The region amplified in **C'**, **E'** and **G'** is labeled in **C**, **E** and **G** (white arrowheads). (**H**) Quantification of wing discs with positive Ubx immunostaining (Ubx^+). The number of Ubx^+/Total wing discs counted is indicated at the *x*-axis of the graphic. At least 40 discs of each genotype are counted derived from at least three independent replicas. There is statistical significance (t-test, $P<0.05$) in the proportions of discs with detectable Ubx among different genotypes (bottom) are indicated with an asterisk (*). Note that ectopic Ubx expression in Pc^3 wing discs (**B, B'**) is suppressed by *tna* (**C-D'**) or *osa* (**E-F'**) haploinsufficiency.

https://doi.org/10.1371/journal.pone.0206587.g006

Ubx signal, Fig 6B, 6B' and 6G] and Scr proteins [93 (40/43) and 85% (33/39) of T2 and T3 Pc^3 leg discs respectively with Scr signal, Fig 7B and 7E], while in discs from $Pc^3/tna^{EY22929}$ animals, *tna* haploinsufficiency suppresses close to 95% (2/42) *Ubx* ectopic expression (Fig 6D and 6H) and 83 to 87% *Scr* ectopic expression (9/52, and 6/47, positive Scr T2 and T3 immunostained leg discs, respectively) (Fig 7C and 7E). In a few cases [6% (2/42), Fig 6E and 6H], *Ubx* suppression was not total. A few cells remain that still have detectable Ubx immunostaining signal, (Fig 6E and 6E'). In the case of *Scr*, the suppression was clearly observed in both $Pc^3/tna^{EY22929}$ T2 and T3 leg discs (Fig 7C, in comparison to Fig 7B and 7E), while *Scr* expression in T1 leg disc looks normal (Fig 7 compare Fig 7A or 7B and 7C, see also Fig 7E).

In the same way, we tested whether *osa* haploinsufficiency was able to suppress Hox protein immunostaining in Pc^3 discs. Indeed, we found that ectopic expression of *Ubx* (Fig 6B) and *Scr* (Fig 7B) in Pc^3 wing discs was almost totally suppressed when a copy of osa^{308} was introduced (Pc^3/osa^{308} discs) [83% (6/35) of suppression for Ubx, Fig 6F–6H, and 75% (12/49), and 78% (11/51) Scr suppression in T2 and T3 leg discs respectively, Fig 7D–7E].

In summary *tna* and *osa* are required to finely tune Hox expression and these subtle differences are not observed in the endogenous regions of Hox expression in the imaginal discs. A different situation is observed when *Ubx* and *Scr* expression is forced out of these regions and then, the requirements of *tna* and *osa* genes are revealed by the strong suppression of the ectopic Hox expression when these TrxG genes are inactivated.

Discussion

In this work we studied the role of the TrxG gene *tna* on Hox gene expression in larval imaginal discs. First, we characterized the production of TnaA isoforms in different *tna* mutant genetic backgrounds. We also analyzed the Hox loss-of-function phenotypes present in adults with some of these *tna* mutant backgrounds. We found that the $TnaA_{123}$ isoform is essential for larval, pupal, and adult survival. In contrast, we found, through mitotic clonal analyses,

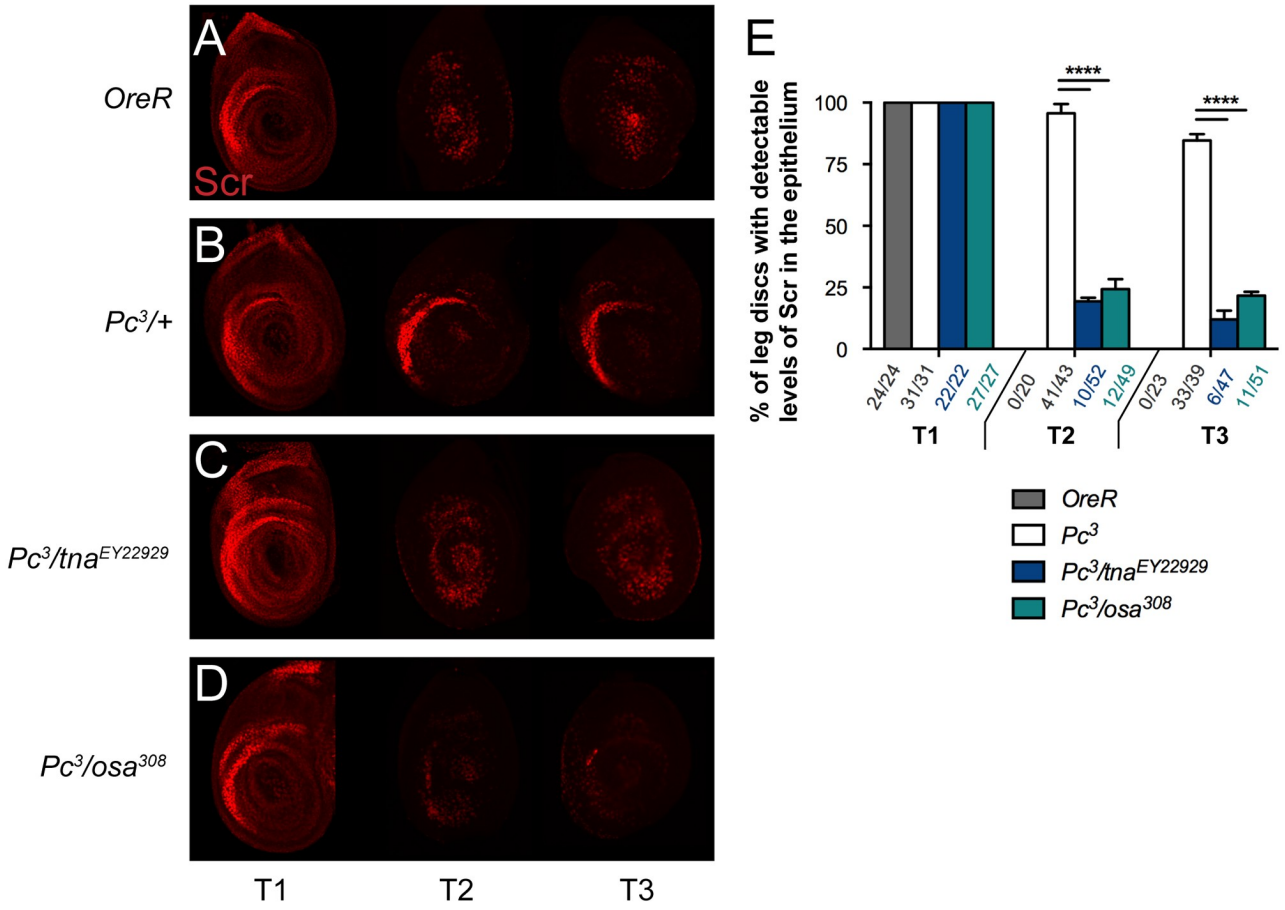

Fig 7. TnaA and Osa are necessary for ectopic presence of Scr protein in T2 and T3 Pc^3 leg imaginal discs. Immunostaining of Scr protein (red) with the 6H4.1 [19] antibody in wild type *OreR* (**A**), Pc^3 (**B**), $Pc^3/tna^{EY22929}$ (**C**), and Pc^3/osa^{308} (**D**) T1-3 leg discs. (**E**) Quantification of haltere discs with positive Scr immunostaining (Scr^+). The number of Scr^+/Total haltere discs counted is indicated at the *x*-axis of the graphic. At least 40 discs of each genotype are counted derived from at least three independent replicas. Significant differences (t-test, $P<0.05$) in the proportions of discs with detectable Ubx among different genotypes (bottom) are indicated with an asterisk (*). Genotypes of discs counted are indicated in the bottom. Note that ectopic Scr expression in Pc^3 T2 and T3 leg discs (**B**) is suppressed by *tna* (**C**) or *osa* (**D**) haploinsufficiency.

https://doi.org/10.1371/journal.pone.0206587.g007

that *tna* is not required for individual cell survival in imaginal discs. Neither, we found decreased Hox expression in these *tna*-defective imaginal cells, although adult animals derived from these experiments do present the already characterized Hox loss-of-function phenotypes. We found that *tna*-defective function suppresses ectopic Hox expression in imaginal discs in a *Pc*-defective background. indicating that *tna* is a fine modulator of Hox gene expression. Below we discuss some possible mechanisms to explain how *tna* might be implicated in the expression of Hox and other genes.

TnaA isoforms have dedicated functions related to the survival of post-embryonic stages

TrxG genes comprehend a functional diverse group that include among others, regulators of transcriptional initiation and elongation to maintain developmental gene expression (recently reviewed in [1]). *tna* encodes a group of proteins present in multicellular organisms, with a zinc SP-RING finger, characteristic of a type of SUMO E3-ligases. Besides the inherent complexity of the TrxG genes, biochemical studies are revealing that as *tna*, some genes of the

group, encode several protein isoforms that may have dedicated functions. Up to date, we have detected at least three different protein products (two of them being $TnaA_{130}$ and $TnaA_{123}$) that may be the result of the expression from different promoters, alternative splicing, or post-translational modifications ([6] and this work). We have characterized that in embryos, $TnaA_{130}$ is cytoplasmic, while $TnaA_{123}$ is mainly nuclear [6]. One of the questions derived from this evidence is to determine whether or not these different isoforms are equivalent in function. In this work, we characterized the effect of reducing the main TnaA proteins ($TnaA_{130}$ and $TnaA_{123}$) on the expression of the Hox genes *Ubx* and *Scr* in imaginal discs. Through analyses of, first, the lethality shown by *tna* mutant animals that die since larval and pupal stages, second, the presence of homeotic transformations in the survivors with some of these genotypes, and third, the protein characterization produced by animals with different *tna* mutant alleles, we were able to make the following observations discarding previous hypotheses. $TnaA_{123}$ is not a processing product of $TnaA_{130}$. We can eliminate $TnaA_{130}$ and still be able to observe $TnaA_{123}$. $TnaA_{130}$ does not affect the organism survival significantly, while $TnaA_{123}$ must be at least detectable, to allow animals to reach the adult stages revealing for the first time a dedicated function for this isoform.

What proved to be more difficult was to determine whether the larval or pupal lethality in these *tna* mutant animals, was caused by a problem in Hox gene expression in imaginal discs at these developmental stages. Nevertheless, adult cuticles of *tna* mutant survivors do show Hox loss-of-function phenotypes. Third instar larvae with stronger *tna* alleles show no detectable $TnaA_{130}$ and $TnaA_{123}$ isoforms and die as late larvae or early pupal stages. In that sense, from these experiments we cannot discard the possibility that both, $TnaA_{130}$ and $TnaA_{123}$, could be contributing for proper Hox expression.

It is probable that TnaA may be required in two phases during development. In the first phase, the maternal deposition of TnaA might be important to establish the early chromatin landscape for Hox gene expression, in a similar way as the TrxG gene *Utx*. The Utx protein (Ubiquitously transcribed tetratricopeptide repeat protein X chromosome) is a demethylase of the lysine 27 of histone H3 deposited by the PcG [34, 35]. Animals without both, maternal and zygotic *Utx*, die as larvae and do not maintain Hox expression, attributed to the fact that some cells cannot initiate the maintenance of Hox gene expression at early stages during the onset of zygotic gene transcription [34, 35]. Animals carrying maternal but no zygotic Utx reach adulthood, have weak loss-of-function phenotypes of diverse Hox, and die just after eclosing, revealing the Utx requirement for viability [34, 35].

Previously, we showed that loss of maternal *tna* function is completely rescued paternally and loss of both maternal and zygotic functions caused lethality primarily at the third larval instar [5]. It will be important to determine whether depleting TnaA at early stages could result in a reduction in Hox expression. In this work we show that *tna* is required for viability at larval, pupal and adult stages, and for ectopic Hox expression in imaginal discs. Is *tna* a gene necessary to initiate the maintenance of Hox gene expression as *Utx*? It is probable that *tna* could participate in this mechanism and later on for viability. This would explain the weak Hox phenotypes and the lethality at late developmental stages of *tna* mutant animals, resembling the ones observed in individuals lacking *Utx* zygotic expression.

Robust regulatory networks allow proper Hox gene expression that masks fine regulation mediated by TnaA

A central contribution of the present work is that wild-type domains of Hox gene expression are not visibly altered in *tna* mutant larval imaginal discs, in spite of the adult mutant Hox phenotypes presented by these animals. These results make us consider that first, robust regulatory

networks protect proper Hox gene expression and that the role of fine modulators such as TnaA is difficult to analyze in this scenario. Second, *tna* might be required in particular stages of development that we did not explore here, and third, that the *tna* mutant cells in imaginal discs that will produce the cuticular adult mutant phenotypes, might be reading very subtle differences in the Hox protein levels that we could not detect by immunostaining.

An argument to explain why the effect of *tna* mutations can only be observed in ectopic but not on wild-type regions of Hox expression derives from the robustness of regulatory networks. For example, *Ubx* has several enhancers (and at the end, all Hox genes) that ensure proper *Ubx* expression in time and space. Some of them are active in haltere discs in redundant spatial patterns which allows to buffer changes in *Ubx* expression levels due to natural variation [36]. Then it is possible that TnaA modulates the expression of only some components of these regulatory networks in imaginal discs, and when those components fail to function, the other ones "compensate" for Hox gene expression. This compensation mechanism has been observed in experiments studying the effect of loss-of-function alleles of TrxG genes. In these experiments, although the TrxG function is totally removed in mitotic clones, Hox expression (particularly *Ubx*) is partially restored in a "patchy" way, probably by these compensation mechanisms [34, 37]. Taking in account this situation it makes sense that it was in a *Pc*-defective background where we were able to observe the suppression by *tna* mutations of *Ubx* and *Scr* ectopic expression in imaginal discs.

That *tna* suppresses the extra-sex-combs adult cuticular phenotype in *Pc*-defective individuals caused by derepression of *Scr* is known [5], but this effect in imaginal discs was analyzed until this work. The suppression effect was observed in imaginal discs harboring the $tna^{EY22029}$ allele that affects primarily the production of the $TnaA_{130}$ isoform (this work), or in adult animals harboring the tna^{1} allele [5], that lack both $TnaA_{130}$ and $TnaA_{123}$ isoforms (this work). This is also similar to the effect of a null *brm* mutation in the suppression ectopic *Scr* expression caused by *Pc* mutants in imaginal discs [2].

To study the developmental window of *tna* requirement for Hox gene expression, we made clones at different stages of development, finding that *tna* may be required at early stages (3–4 h AEL). Animals with clones generated at this time did not survive. In contrast, clones generated later (24–48 h AEL) do survive, and adults present a reduced number of sex comb teeth similarly to the *Scr* loss-of-function phenotype presented by *tna* hypomorphic and knocked down mutants. This suggests that *tna* requirements may be biphasic as has been shown for other TrxG genes such as *Utx* (discussed in the previous section).

Individuals with mutations in RNA polymerase II and transcriptional factors that facilitate initiation [38], or elongation [39] present, as *tna* mutant individuals, Hox loss-of-function phenotypes. Of these, *kismet* (*kis*) is a TrxG gene involved in elongation that was identified because it suppresses ectopic expression of *Scr* in *Pc* heterozygotes [40]. *kis* clones induced during larval development do not show homeotic transformations, meanwhile clones induced earlier at the cellular blastoderm stage, show a reduction on sex comb teeth [41]. Many evidences points towards the possibility that TnaA could be required as a co-factor of the BRAHMA BAP chromatin remodeling complex, but it will also be possible that it targets other components of the general transcriptional machinery.

TnaA on gene expression mediated by the BAP complex, and other general transcription factor targets

The BRAHMA BAP complex is required for the expression of multiple genes at different times of development [42]. TnaA physically interacts with the E2 Ubc9 SUMO-conjugating enzyme and with the subunits of the BRAHMA BAP complex, Osa and Brm [6]. TnaA could be

modifying the assembly, the recruitment, or the remodeling function of the complex by stimulating the SUMOylation of one or more BAP subunits to facilitate Hox gene expression at a specific time, or cell-type. In fact, we have shown that TnaA co-localizes sometimes with the BAP subunit Osa in polytene chromosome bands of third instar larvae, but not in others [6], meaning that TnaA is required for function of the BAP complex at some gene targets but not in others, or that the co-localization of TnaA with Osa is transient. On the other side, TnaA may act on targets other than the BRAHMA BAP complex, meaning that epistatic relationships at different levels can contribute to the phenotypes derived from TnaA function(s) (S4 Fig).

Although TnaA itself is not a subunit of the BAP complex, *tna* defective clones in imaginal discs, resemble the behavior of defective clones in some subunits of the BAP complex. We compared our results particularly with the ones obtained with *brm* and *osa* clones, because TnaA physically and genetically interacts with the BAP subunits Brahma and Osa [5, 6]. Kassis *et al*., (2017) have recently published an excellent summary of results involving the clonal analyses of TrxG genes, and we only note here that germ line and/or somatic clones for mutant *brm*, *osa*, *Snf5-related 1* (*Snr1*), and *moira* (*mor*) [3, 4, 31, 43, 44], all of them encoding BAP subunits, do not present the same phenotypes, and show requirements at different times of development. For example, analyses of *brm* clones suggest defects in cell division and in adult peripheral nervous system [43]. *osa* clones in the germ line produce embryos with segmentation defects [4], and somatic clones in the wing imaginal discs, have defects in venation, and in cell growth and viability [31]. These clones do not present homeotic transformations although adult individuals with hypomorphic *brm* or *osa* mutations do have homeotic phenotypes, e. g. [40]. All these evidences, indicates that the BAP complex acts on different gene targets influenced by other factors, including TnaA.

In conclusion, these and other differences and mechanisms, may account for the diverse developmental requirements observed in the clonal analyses of different TrxG genes. As other TrxG genes which have functions in the regulation of genes other than the Hox, *tna* could have targets not related to Hox expression that are essential for larval or pupal survival. *tna* epistatic relationships, may involve different TnaA isoforms that could be required for the expression of different gene targets or at diverse times of development (S4 Fig).

If TnaA is influencing BRAHMA BAP complex function, it may act close to the promoter or on regulatory elements such as enhancers where BAP complexes are remodeling chromatin. TnaA may also have other targets than the BAP complex and have a wider target specificity as has been shown for other E3 SUMO ligases (reviewed in [8]). These are questions still unanswered and for example, chromatin immunoprecipitation experiments with TnaA antibodies that recognize specific isoforms at different times of development, will be helpful to start to determine the range of action of these TrxG proteins.

Supporting information

S1 Fig. Cell survival is not affected in TnaA defective mitotic clones. (**A**) tna^{1}/tna^{1} ($GFP^{-/-}$), and tna^{+}/tna^{+} ($GFP^{+/+}$) clones in a wing disc showing an example of the areas affected by clone-induction. (**B**) Comparison of the area of 13 tna^{1}/tna^{1} ($GFP^{-/-}$), and tna^{+}/tna^{+} ($GFP^{+/+}$) adjacent clones from independent events of clone-induction in wing discs. There were no significant (NS) differences between correspondant areas (t-test, $P>0.05$).
(TIF)

S2 Fig. TnaA level does not affect Scr immunostaining in leg imaginal discs. TnaA (red) and Scr (green) immunostaining (red) of $tna^{1}/+$ or $tna^{EY22029}/+$ (upper panel), or $tna^{1}/tna^{EY22029}$ (lower panel) leg discs. DNA is stained with Hoescht (left) and images with merged

TnaA and Scr signals is shown (extreme right). Note that TnaA level diminishes in tna^{1}/$tna^{EY22029}$ leg discs, although the Scr signal looks normal, and 77% of adult $tna^{1}/tna^{EY22029}$ animals present a loss-of-function Scr phenotype (Table 2).
(TIF)

S3 Fig. Osa defective mitotic clones in haltere discs. osa^{308} mitotic clones were induced with the Ubx-FLPase. Immunostaining of Osa with the anti-Osa15A8 (dil. 1:200) in a haltere disc where mitotic clones were induced. DNA was stained with Hoechst (blue) to show nuclear presence. RFP (red) marks the osa^{+}/osa^{-} cells that did not recombine (middle red intensity), and the osa^{+}/osa^{+} cells result of the recombination event (strong red intensity). RFP^{-} marks the osa^{308}/osa^{308} clone, as corroborated by the absence of Osa immunostaining (green).
(TIF)

S4 Fig. Possible TnaA targets that can influence gene expression involved in organism survival and Hox loss-of-function phenotypic outcomes. Representation of TnaA target proteins that can influence the transcription of different genes. Epistatic relationships, can contribute to the Hox loss-of-function and organism survival phenotypes studied in this work.
(TIF)

Acknowledgments

We thank the Bloomington *Drosophila* Stock Center for providing stocks. We thank Jim Kennison for the stock with the tna^{1} *FRT2A* chromosome. We also thank Carmen Muñoz, and Laboratorio Nacional de Microscopía Avanzada, Instituto de Biotecnología, UNAM for technical assistance.

Author Contributions

Conceptualization: Marco Rosales-Vega, Martha Vázquez.

Formal analysis: Marco Rosales-Vega, Adriana Hernández-Becerril, Mario Zurita, Martha Vázquez.

Funding acquisition: Martha Vázquez.

Investigation: Marco Rosales-Vega, Juan Manuel Murillo-Maldonado, Martha Vázquez.

Methodology: Adriana Hernández-Becerril.

Resources: Mario Zurita.

Writing – original draft: Martha Vázquez.

Writing – review & editing: Marco Rosales-Vega, Adriana Hernández-Becerril, Juan Manuel Murillo-Maldonado, Mario Zurita, Martha Vázquez.

References

1. Kassis JA, Kennison JA, Tamkun JW. Polycomb and Trithorax group genes in *Drosophila*. Genetics. 2017; 206:1699–1725. https://doi.org/10.1534/genetics.115.185116 PMID: 28778878
2. Tamkun JW, Deuring R, Scott MP, Kissinger M, Pattatuci AM, Kaufman TC, Kennison JA. *brahma*: a regulator of *Drosophila* homeotic genes structurally related to the yeast transcriptional activator SNF2/SWI2. Cell. 1992; 68:561–572. PMID: 1346755
3. Brizuela BJ, Kennison JA. The *Drosophila* homeotic gene *moira* regulates expression of *engrailed* and HOM genes in imaginal tissues. Mech Dev. 1997; 65:209–220. PMID: 9256357

4. Vázquez M, Moore L, Kennison JA. The trithorax group gene *osa* encodes an ARID-domain protein that genetically interacts with the Brahma chromatin-remodeling factor to regulate transcription. Development. 1999; 126:733–742. PMID: 9895321.
5. Gutierrez L, Zurita M, Kennison JA, Vázquez M. The Drosophila trithorax group gene *tonalli* (*tna*) interacts genetically with the Brahma remodeling complex and encodes an SP-RING finger protein. Development. 2003; 130:343–354. PMID: 12466201.
6. Monribot-Villanueva J, Juarez-Uribe A, Palomera-Sánchez, Gutiérrez-Aguiar L, Zurita M, Kennison JA, Vázquez M. TnaA, an SP-RING protein, interacts with Osa, a subunit of the chromatin remodeling complex BRAHMA and with the SUMOylation pathway in *Drosophila melanogaster*. PLoS ONE. 2013; 8:1–12. https://doi.org/10.1371/journal.pone.0062251 PMID: 23620817
7. Gramates LS, Marygold SJ, dos Santos G, Urbano JM, Antonazzo G, Mathews BB, et al. FlyBase at 25: looking to the future. Nucleic Acids Research. 2017; 45(D1):D663–D671. https://doi.org/10.1093/nar/gkw1016 PMID: 27799470
8. Monribot-Villanueva J, Zurita M, Vázquez M. Developmental transcriptional regulation by SUMOylation, an evolving field. Genesis. 2017; 55:e23009.
9. Rytinki MM, Kaikkonen S, Pehkonen P, Jaaskelainen T, Palvimo JJ. PIAS proteins: pleiotropic interactors associated with SUMO. Cell Mol Life Sci. 2009; 66:3029–3041. https://doi.org/10.1007/s00018-009-0061-z PMID: 19526197
10. Mann RS, Carroll SB. Molecular mechanisms of selector gene function and evolution. Curr Opin Genet Dev. 2002; 12:592–600. PMID: 12200165
11. dos Santos G, Schroeder AJ, Goodman JL, Strelets VB, Crosby MA, Thurmond J, et al. Flybase: Introduction of the *Drosophila melanogaster* Release 6 reference genome assembly and large-scale migration of genome annotations. Nucl Ac Res. 2014; 43:D690–D697.
12. Bellen HJ, Levis RW, Liao G, He Y, Carlson JW, Tsang G, et al. The BDGP gene disruption project: single transposon insertions associated with 40% of Drosophila genes. Genetics. 2004; 167:761–81. https://doi.org/10.1534/genetics.104.026427 PMID: 15238527
13. Dietzl G, Chen D, Schnorrer F, Su KC, Barinova Y, Fellner M, et al. A genome-wide transgenic RNAi library for conditional gene inactivation in Drosophila. Nature. 2007; 448:151–6. https://doi.org/10.1038/nature05954 PMID: 17625558
14. Ni JQ, Markstein M, Binari R, Pfeiffer BD, Liu LP, Villalta C, et al. Vector and parameters for targeted transgenic RNA interference in *Drosophila melanogaster*. Nature Methods. 2008; 5:49–51. https://doi.org/10.1038/nmeth1146 PMID: 18084299
15. Ito K, Awano W, Suzuki K, Hiromi Y, Yamamoto D. The Drosophila mushroom body is a quadruple structure of clonal units each of which contains a virtually identical set of neurones and glial cells. Development. 1997; 124:761–777. PMID: 9043058
16. Capdevila J, Guerrero I. Targeted expression of the signalling molecule Decapentaplegic induces pattern duplications and growth alterations in Drosophila wings. EMBO J. 1994; 13:4459–4468. PMID: 7925288
17. Haerry TE, Khalsa O, O'Connor MB, Wharton KA. Synergistic signaling by two BMP ligands through the SAX and TKV receptors controls wing growth and patterning in Drosophila. Development. 1998; 125:3977–3987. PMID: 9735359
18. White RAH, Wilcox M. Protein products of the Bithorax complex in *Drosophila*. Cell. 1984; 39:163–171. PMID: 6091908
19. Glicksman MA, Brower DL. Expression of the Sex combs reduced protein in Drosophila larvae. Dev Biol. 1988; 127:113–118. PMID: 2896135
20. Treisman JE, Luk A, Rubin GM, Heberlein U. *eyelid* antagonizes *wingless* signaling during *Drosophila* development and has homology to the Bright family of DNA-binding proteins. Genes Dev. 1997; 11:1949–1962. PMID: 9271118
21. Cunningham MD, Gause M, Cheng Y, Noyes A, Dorsett D, Kennison JA, Kassis JA. Wapl antagonizes cohesin binding and promotes Polycomb group silencing in Drosophila. Development. 2012; 139:4172–4179. https://doi.org/10.1242/dev.084566 PMID: 23034634
22. Golic KC, Lindquist SL. The FLP recombinase of yeast catalyzes site-specific recombination in the *Drosophila* genome. Cell. 1989; 59:499–509. PMID: 2509077
23. Christen B, Bienz M. Imaginal disc silencers from *Ultrabithorax*: evidence for Polycomb response elements. Mech Dev. 1994; 48:255–266. PMID: 7893606
24. Emery G, Hutterer A, Berdnik D, Mayer B, Wirtz-Peitz F, Gonzalez-Gaitan M, Knoblich JA. Asymmetric Rab11 endosomes regulate delta recycling and specify cell fate in the *Drosophila* nervous system. Cell. 2005; 122:763–773. https://doi.org/10.1016/j.cell.2005.08.017 PMID: 16137758

25. Beuchle D, Struhl G, Müller J. Polycomb group proteins and heritable silencing of *Drosophila* Hox genes. Development. 2001; 128:993–1004. PMID: 11222153

26. Blair SS. Imaginal discs. Chapter 10. In: Sullivan W, Ashburner M, Hawley RS, editors. Drosophila Protocols. Cold Spring Harbor, N. Y.: Cold Spring Harbor Laboratory Press; 2000. p. 159–173.

27. Bender W., Akam M, Karch F, Beachy PA, Peifer M, Spierer P, Lewis EB, Hogness DS. Molecular genetics of the Bithorax complex in *Drosophila melanogaster*. Science. 1983; 221:23–29. https://doi.org/10.1126/science.221.4605.23 PMID: 17737996

28. Menéndez J, Perez-Garijo A, Calleja M, Morata G. A tumor-suppressing mechanism in *Drosophila* involving cell competition and the Hippo pathway. Proc Natl Acad Sci U S A. 2010; 107:14651–14656. https://doi.org/10.1073/pnas.1009376107 PMID: 20679206

29. White RAH, Wilcox M. Regulation of the distribution of Ultrabithorax proteins in Drosophila. Nature. 1985; 318:563–569.

30. Weatherbee SD, Halder G, Kim J, Hudson A, Carroll S. Ultrabithorax regulates genes at several levels of the wing-patterning hierarchy to shape the development of the Drosophila haltere. Genes Dev. 1998; 12:1474–82. PMID: 9585507

31. Terriente-Félix A, De Celis JF. Osa, a subunit of the BAP chromatin-remodelling complex, participates in the regulation of gene expression in response to EGFR signalling in the *Drosophila* wing. Dev Biol. 2009; 329:350–361. https://doi.org/10.1016/j.ydbio.2009.03.010 PMID: 19306864

32. Beachy PA, Helfand SL, Hogness DS. Segmental distribution of bithorax complex proteins during *Drosophila* development. Nature. 1985; 313:545–551. PMID: 3918274

33. Lewis EB. A gene complex controlling segmentation in *Drosophila*. Nature. 1978; 276:565–570. PMID: 103000

34. Copur O, Müller J. The histone H3-J27 demethylase Utx regulates HOX gene expression in *Drosophila* in a temporally restricted manner. Development. 2013; 140:3478–3485. https://doi.org/10.1242/dev.097204 PMID: 23900545

35. Copur O, Müller J. Histone demethylase activity of Utx is essential for viability and regulation of *HOX* gene expression in *Drosophila*. Genetics. 2018; 208:633–637. https://doi.org/10.1534/genetics.117.300421 PMID: 29247011

36. Crickmore MA, Ranade V, Mann RS. Regulation of *Ubx* expression by epigenetic enhancer silencing in response to Ubx levels and genetic variation. PLoS Genetics. 2009; 5:1–10.

37. Klymenko T, Müller J. The histone methyltransferases Trithorax and Ash1 prevent transcriptional silencing by Polycomb group proteins. EMBO Rep. 2004; 5:373–377. https://doi.org/10.1038/sj.embor.7400111 PMID: 15031712

38. Gutiérrez L, Merino C, Vázquez M, Reynaud E, Zurita M. RNA polymerase II 140wimp mutant and mutations in the TFIIH subunit XPB differentially affect homeotic gene expression in Drosophila. genesis. 2004; 40:58–66. https://doi.org/10.1002/gene.20066 PMID: 15354295

39. Chopra VS, Hong JW, Levine M. Regulation of Hox gene activity by transcriptional elongation in *Drosophila*. Curr Biol. 2009; 19:688–693. https://doi.org/10.1016/j.cub.2009.02.055 PMID: 19345103

40. Kennison JA, Tamkun JW. Dosage-dependent modifiers of *Polycomb* and *Antennapedia* mutations in *Drosophila*. Proc Natl Acad Sci U S A. 1988; 85:8136–8140. PMID: 3141923

41. Daubresse G, Deuring R, Moore L, Papoulas O, Zakrajsek I, Waldrip WR, et al. The *Drosophila kismet* gene is related to chromatin-remodeling factors and is required for both segmentation and segment identity. Development. 1999; 126:1175–1187. PMID: 10021337

42. Armstrong JA, Papoulas O, Daubresse G, Sperling AS, Lis JT, Scott MP, Tamkun JW. The *Drosophila* BRM complex facilitates global transcription by RNA polymerase II. EMBO J. 2002; 21:5245–5254. https://doi.org/10.1093/emboj/cdf517 PMID: 12356740

43. Elfring L, Daniel C, Papoulas O, Deuring R, Sarte M, Moseley S, et al. Genetic analysis of *brahma*: the *Drosophila* homolog of the yeast chromatin remodeling factor SWI2/SNF2. Genetics. 1998; 148:251–265. PMID: 9475737

44. Zraly CB, Marenda DR, Nanchal R, Cavalli G, Muchardt C, Dingwall AK. SNR1 is an essential subunit in a subset of *Drosophila* BRM complexes, targeting specific functions during development. Dev Biol. 2003; 253:291–308. PMID: 12645932

Supporting information

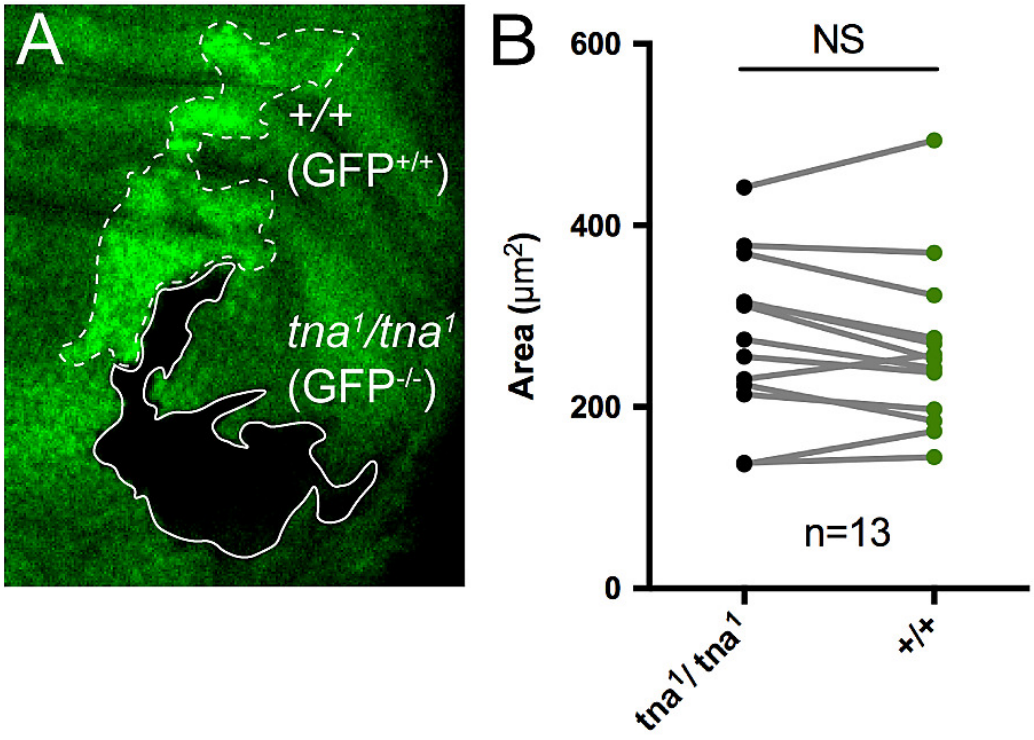

S1 Fig. Cell survival is not affected in TnaA defective mitotic clones. (**A**) *tna1/tna1* ($GFP^{-/-}$), and *tna+/tna+* ($GFP^{+/+}$) clones in a wing disc showing an example of the areas affected by clone-induction. (**B**) Comparison of the area of 13 *tna1/tna1* ($GFP^{-/-}$), and *tna+/tna+* ($GFP^{+/+}$) adjacent clones from independent events of clone-induction in wing discs. There were no significant (NS) differences between correspondant areas (t-test, P>0.05).

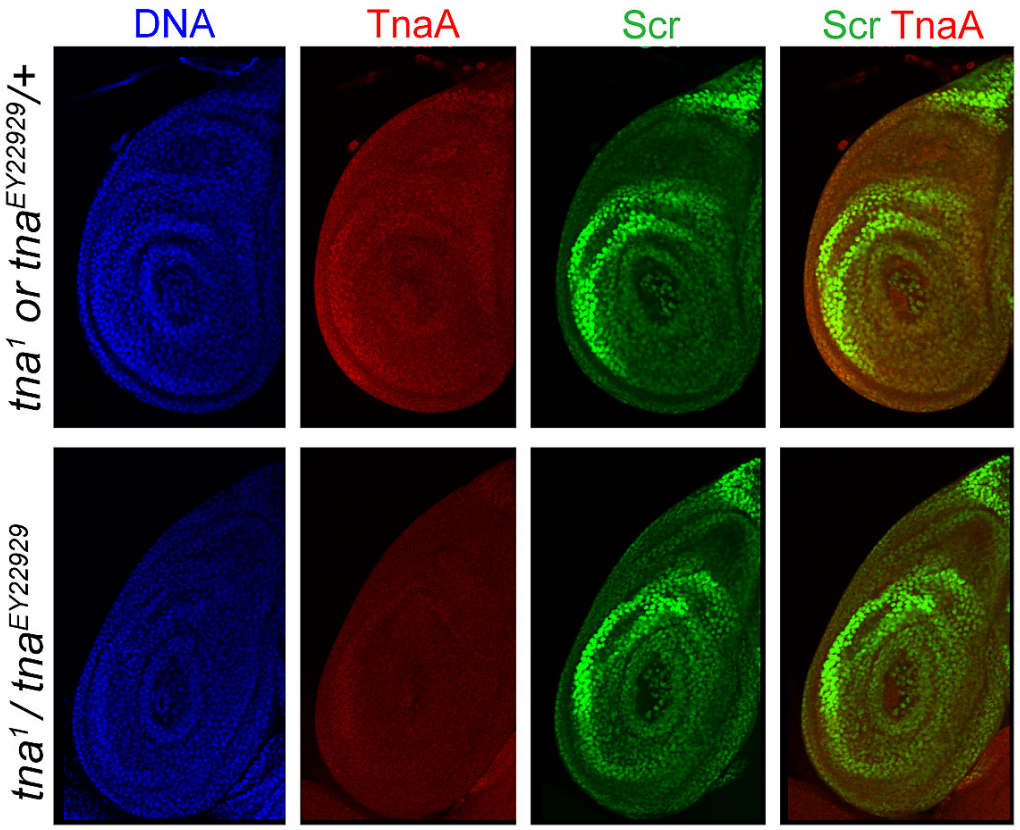

S2 Fig. TnaA level does not affect Scr immunostaining in leg imaginal discs. TnaA (red) and Scr (green) immunostaining (red) of *tna*^{1}/+ or *tna*^{EY22029}/+ (upper panel), or *tna*^{1}/*tna*^{EY22029} (lower panel) leg discs. DNA is stained with Hoescht (left) and images with merged TnaA and Scr signals is shown (extreme right). Note that TnaA level diminishes in *tna*^{1}/*tna*^{EY22029} leg discs, although the Scr signal looks normal, and 77% of adult *tna*^{1}/*tna*^{EY22029} animals present a loss-of-function Scr phenotype (Table 2).

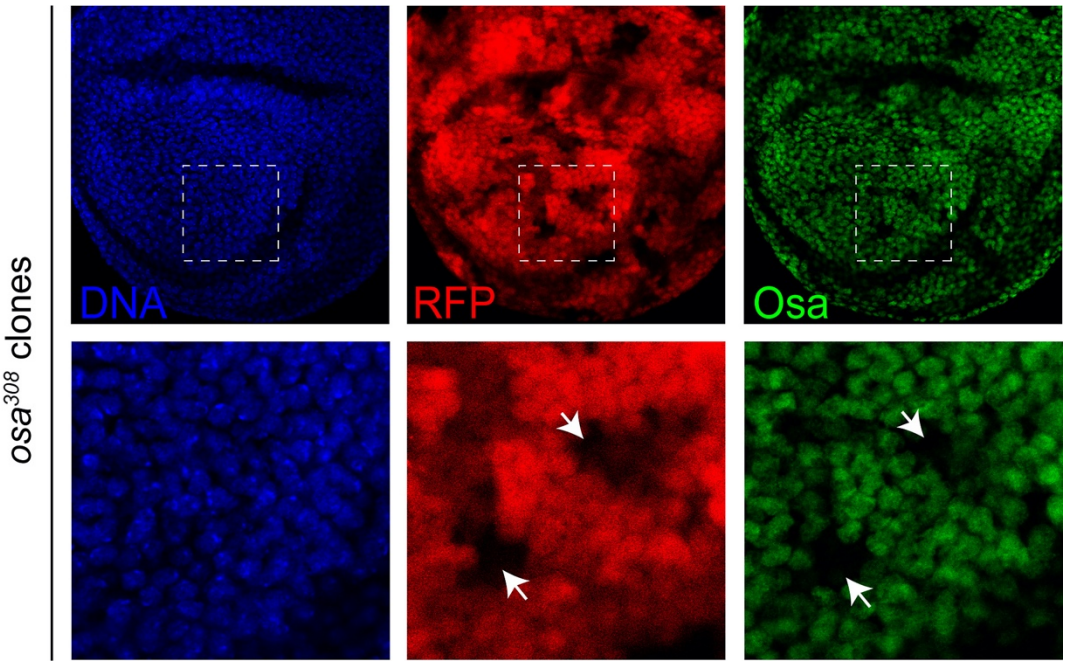

S3 Fig. Osa defective mitotic clones in haltere discs. *osa*^{308} mitotic clones were induced with the Ubx-FLPase. Immunostaining of Osa with the anti-Osa15A8 (dil. 1:200) in a haltere disc where mitotic clones were induced. DNA was stained with Hoechst (blue) to show nuclear presence. RFP (red) marks the *osa*$^{+}$/*osa*$^{-}$ cells that did not recombine (middle red intensity), and the *osa*$^{+}$/*osa*$^{+}$ cells result of the recombination event (strong red intensity). RFP^{-} marks the *osa*^{308}/*osa*^{308} clone, as corroborated by the absence of Osa immunostaining (green).

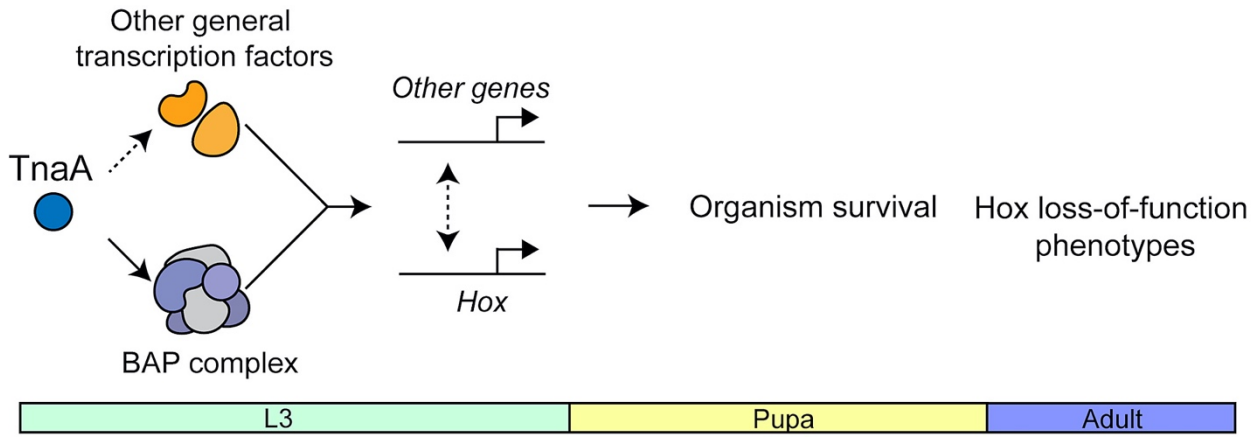

S4 Fig. Possible TnaA targets that can influence gene expression involved in organism survival and Hox loss-of-function phenotypic outcomes. Representation of TnaA target proteins that can influence the transcription of different genes. Epistatic relationships, can contribute to the Hox loss-of-function and organism survival phenotypes studied in this work.

Posteriormente, derivado de los experimentos de ChIP-seq de TnaA en discos de ala (información que aún no se publica en su totalidad), nos enfocamos en el hallazgo de que TnaA se encuentra en un “enhancer” de *wg*, un gen maestro en los programas de desarrollo.

Analizamos el papel de TnaA en la expresión de *wg* en los discos de ala y encontramos que TnaA regula la expresión de *wg* específicamente en el límite D/V y el IR del disco de ala. Además, mostramos que TnaA se encuentra presente en la cromatina del “enhancer” del IR para modular la expresión de *wg*. Lo anterior resultó en una segunda publicación donde soy primer autor y se anexa a continuación:

Rosales-Vega, M., Reséndez-Pérez, D., Zurita, M. y Vázquez, M. (2023). TnaA, a trithorax group protein, modulates *wingless* expression in different regions of the *Drosophila* wing imaginal disc. *Scientific Reports* **13**, 1-13.

scientific reports

Check for updates

OPEN

TnaA, a trithorax group protein, modulates *wingless* expression in different regions of the *Drosophila* wing imaginal disc

Marco Rosales-Vega[1], Diana Reséndez-Pérez[2], Mario Zurita[1] & Martha Vázquez[1]✉

wingless **expression is exquisitely regulated by different factors and enhancers in the imaginal wing discs of** ***Drosophila melanogaster*** **in four domains: the dorsal band, the dorso-ventral boundary, and the inner and outer ring domains.** ***tonalli*** **is a trithorax group gene that encodes a putative SUMO E3 ligase that binds to chromatin to regulate the expression of its targets, including the** ***Hox*** **genes. However, its role in modulating gene expression is barely known. Here, we show that TnaA modulates the** ***wingless*** **expression at two domains of the wing disc, the dorso-ventral boundary and the inner ring. At first,** ***tonalli*** **interacts genetically with** ***Notch*** **to form the wing margin. In the inner ring domain, TnaA modulates** ***wingless*** **transcription. When the dosage of TnaA increases in or near the inner ring since early larval stages, this domain expands with a rapid increase in** ***wingless*** **expression. TnaA occupies the** ***wingless Inner Ring Enhancer*** **at the wing disc, meanwhile it does not affect** ***wingless*** **expression directed by the** ***Ventral Disc Enhancer*** **in leg discs, suggesting that TnaA acts as a** ***wingless*** **enhancer-specific factor. We describe for the first time the presence of TnaA at the** ***Inner Ring Enhancer*** **as a specific regulator of** ***wingless*** **in the development of wing boundaries.**

Gene expression is exquisitely regulated in the wing disc by the Notch, Wingless, Hedgehog, and Decapentaplegic pathways, among others, to form an adult organ. Genes responding to these inputs direct tissue patterning through differentiation, proliferation, and cell death. The Notch and Wingless signaling pathways are highly conserved in metazoans. Developmental processes in which Notch is involved include lateral inhibition, lineage decisions, and boundary formation (reviewed in[1]), while Wingless works on balancing cell proliferation, cell fate specification, changes in polarity, and differential cell adhesion (reviewed in[2]).

The formation of boundaries requires Notch and Wingless signaling and is well studied at the *Drosophila* wing disc. The genes that encode the transcription factors of these pathways have, in turn, complex regulatory regions that differentially respond according to the position of the cell in the wing imaginal disc and consequently activate the appropriate developmental programs to give rise to the adult wing.

Notch signaling defines the identity of dorsoventral (D/V) boundary cells and is required for the localized expression of genes involved in the formation and patterning of the wing margin, such as *wingless* (*wg*), *cut* (*ct*), and *vestigial* (*vg*)[3–5]. The Notch pathway is activated through a cell–cell signaling process between the Notch receptor and its ligand of the DSL family (Delta, Serrate, Lag-2), leading to the nuclear import of the Notch Intracellular Domain (NICD). In the nucleus, there are complexes with the DNA-binding protein Suppressor of Hairless [Su(H)], also known as CSL [named after CBF1, Su(H), and Lag-1], to activate or repress target gene transcription[1,6].

Different regulators control the expression of *wg* to define the boundaries and domains on the wing disc[7,8]. In the late third instar wing disc, *wg* is expressed in a broad band located at the notum, along the D/V boundary, and in two concentric ring-like patterns at the hinge region called the inner (IR) and the outer (OR) ring domains[9]

[1]Departamento de Genética del Desarrollo y Fisiología Molecular, Instituto de Biotecnología, Universidad Nacional Autónoma de México, 62210 Cuernavaca, Morelos, Mexico. [2]Departamento de Inmunología y Virología, Facultad de Ciencias Biológicas, Universidad Autónoma de Nuevo León, San Nicolás de los Garza, Nuevo León, Mexico. ✉email: martha.vazquez@ibt.unam.mx

(Fig. 1A). The D/V boundary domain will contribute to the formation of the adult wing margin, while the IR is necessary for the formation of the hinge[5].

The Notch pathway regulates the expression of *wg* at the D/V boundary[4,5], while Rotund and Nubbin are two key players in the regulation of *wg* expression in the IR domain[7]. *wg* has several known enhancers and at least two of them are differentially expressed in the imaginal discs. The *Inner Ring Enhancer* (*IRE*) acts on the wing disc[10], while the *Ventral Disc Enhancer* (*VDE*) functions on the leg and eye-antennal discs[8]. However, the precise mechanisms that activate these enhancers and the factors that regulate their functions are poorly understood.

SUMOylation is a post-translational modification that modify the activity, location, and/or interaction of nuclear target proteins (reviewed in[11]). SUMO ligases favor the SUMOylation of specific target proteins. *tonalli* (*tna*) is a trithorax-group gene that is essential during larval and pupal development[12,13]. It encodes several TnaA isoforms with putative E3 SUMO ligase activity in the subunits of the BRAHMA complex, Osa and Brahma[13,14] and probably in other nuclear proteins in imaginal discs.

In this work, we show that TnaA influences *wg* expression in the wing imaginal disc. We found that *tna* genetically interacts with *Notch* (*N*) to regulate *wg* expression at the D/V boundary domain. In the IR domain, we show through genetic and ChIP-qPCR experiments that TnaA favors *wg* expression since early larval stages and that it physically interacts with the *IRE*. In summary, the experiments presented here reveal TnaA as a positive modulator of *wg* expression, and its physical presence at the *IRE* describes for the first time a protein that may contribute to the function of this complex regulatory element.

Results

tonalli genetically interacts with _Notch_ at the D/V boundary wing disc to form the wing margin. The wing disc is divided into different regions according to complex gene expression patterns. One of the genes that is expressed in these regions is *wg* (Fig. 1A).

In previous work, we identified modifiers of the BRAHMA complex that include *tna*[12]. Individuals with mutations in some of these BRAHMA modifiers, which did not include *tna* at that time, have notched wings among other phenotypes[15]. This notched wing phenotype resembles that exhibited by individuals with defects in the Notch signaling pathway at the D/V boundary of the wing disc (Fig. 1B).

To investigate whether *tna* is related to Notch signaling, we assayed the genetic interaction of *N* with *tna*, looking for the notched-wing phenotype in flies carrying the null *N* allele, N^{55e11}, in combination with different *tna* alleles that include tna^{1}, tna^{5}, $tna^{EY22929}$ and $tna^{MI01482}$ (Fig. 1B, and Table 1, for location and description of the alleles, see Sup. Fig. 1A, and "Methods"). Female heterozygote individuals carrying any of the tested *tna* alleles have normal wings (e. g. tna^{1}/+, Fig. 1B, Table 1). Most N^{55e11}/+ females (82%) have wings with notches located at the distal tip of the wing blade (weak phenotype), while in the presence of tna^{1} (N^{55e11}/+; tna^{1}/ +), the flies show extensive notches located mainly along the posterior wing margin with strong (74%) or weak (7%) expressivity. Individuals with the other tested *tna* alleles also show the notched-wing phenotype with different penetrance and expressivity (Table 1). N^{55e11}/+; tna^{1}/+ mutant flies present a strong notched-wing phenotype, as

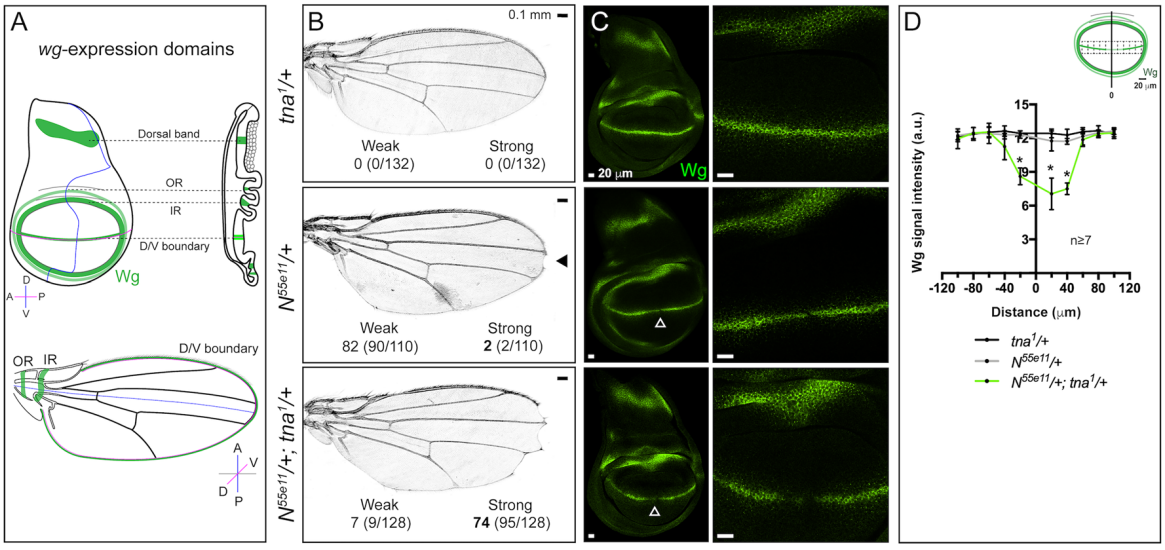

Figure 1. Genetic interaction of *tna* with *Notch* and *wg* expression in the wing disc. (**A**) Schemes of *wg* expression domains in the wing disc (green, upper panel) and their developmental fate in an adult wing (bottom panel). (**B**) Adult wings with *N* and/or *tna* mutant genotypes. Penetrance and expressivity of the notched-wing phenotype are classified as weak or strong when a single or several notches, respectively, are present in a wing margin. Quantification of each class is shown in Table 1. (**C**) Wingless signal in wing discs of *N* and/or *tna* mutant genotypes. Note that Wingless is further reduced at the D/V boundary domain in N^{55e11}/+; tna^{1}/+ wing discs (solid arrowhead, magnified in the right panels). (**D**) Quantification of Wingless in wing discs of the indicated genotypes (see Sup. Fig. 4B). Student's *t*-test was performed for signal intensity in each bin ($P < 0.05$*).

Genotype[a]	Individuals with notched wings/total[b]	
	Weak	Strong
tna^{1}/+	0/132 (0)	0/132 (0)
tna^{5}/+	0/178 (0)	0/178 (0)
$tna^{MI01482}$/+	0/125 (0)	0/125 (0)
$tna^{EY22929}$/+	0/149 (0)	0/149 (0)
N^{55e11}/+	90/110 (82)	2/110 (2)
$Su(H)^{1}$	2/72 (3)	0/72 (0)
N^{55e11}/+; tna^{1}/+	9/128 (7)	95/128 (74)
N^{55e11}/+; $tna^{MI01482}$/+	13/129 (10)	55/129 (43)
N^{55e11}/+; tna^{5}/+	18/161 (11)	56/161 (35)
N^{55e11}/+; $tna^{EY22929}$/+	12/147 (8)	35/147 (24)
$Su(H)^{1}$/+; tna^{1}/+	15/91 (16)	0/91 (0)
$Su(H)^{1}$/+; $tna^{EY22929}$/+	7/86 (8)	0/86 (0)

Table 1. *tna* interacts genetically with *N* and *Su(H)*. [a]N^{55e11}/*FM0* female virgins were crossed with males carrying different *tna* alleles. [b]Number of individuals with the notched-wing phenotype. Penetrance and expressivity of the notched-wing phenotype are classified as weak or strong when a single or several notches, respectively, are present in a wing margin (see Fig. 1B). The percentages are indicated in parentheses. The results are a compilation of F1 of at least four independent crosses. Statistical significance in each case was determined with x^2 ($P < 0.05$) as stated in "Methods".

the more evident loss-of-function phenotype of *N*, suggesting that TnaA is required for activities of the Notch pathway related to the formation of the wing dorso-ventral boundary.

We also tested the genetic interaction between *tna* and *Su(H)* by combining the loss-of-function $Su(H)^{1}$[16] and the alleles tna^{1} and $tna^{EY22929}$. We found that wing-notching in transheterozygote $Su(H)^{1}$/+; *tna*/+ individuals increases slightly with respect to notched wings of individuals carrying only the $Su(H)^{1}$ allele (16% for $Su(H)^{1}$/+; tna^{1}/+, 8% for $Su(H)^{1}$/+; $tna^{EY22929}$/+ compared to 3% for $Su(H)^{1}$/+ individuals) (Table 1 and Sup. Fig. 2A)[17]. Thus, there is a genetic interaction between *tna* and *Su(H)* although it is not as strong as the one found in N^{55e11}/+; *tna*/+ individuals (Fig. 1B and Table 1).

Since *wg* expression is controlled by the Notch pathway at the D/V boundary[4,5], we evaluated the Wingless protein level in wing discs of N^{55e11}/+; tna^{1}/+ flies. We found that the level of Wingless decreases, in correlation with the observed phenotypes in adult wings (Fig. 1C). Although the Wingless level at the D/V boundary is intact in discs from tna^{1}/+ individuals, it is reduced in a few cells at the center of the D/V boundary in discs of N^{55e11}/+ genotype. The latter phenotype is enhanced in N^{55e11}/+; tna^{1}/+ animals (Fig. 1C) and in all combinations of *tna* alleles tested (Table 1). Quantification of this phenotype is presented in Fig. 1D and Sup. Fig. 4A.

To further test this finding, we asked whether the Wingless protein level decreased in tna^{1} clones (Sup. Fig. 3) that cross the D/V boundary since the expression of *wg* is controlled by NICD in this region[4,5]. In fact, we found that this is the case (Fig. 2A). Consistently, quantification of the Wingless signal is reduced almost 50% in these tna^{-} clones (Fig. 2B), and adult wings derived from these wing discs present notches (Sup Fig. 2B).

Next, we directed the expression of an epitope-tagged version of $TnaA_{123}$ that we will name from now on TnaA-Flag, to the D/V boundary. As wild-type TnaA, TnaA-Flag is nuclear (Sup. Fig. 1B), binds to the same bands in polytene chromosomes (Sup. Fig. 1C), and, albeit partially, complements the lethality of tna^{-} individuals (see "Methods"). We found that in the presence of TnaA-Flag, Wingless show a two-fold increase along the D/V boundary (Fig. 2C,D and Sup. Fig. 4B), in contrast to the Wingless decrease found in this domain in tna^{-} clones (Fig. 2B), further supporting the notion that TnaA regulates *wg* expression.

We also analyzed the effect of TnaA-Flag presence at the D/V boundary on the levels of Cut whose expression is controlled by NICD in this region[5] (Fig. 3A). We observed that Cut diminishes considerably at the D/V boundary of these wing discs (Fig. 3A,C, and Sup. Fig. 4B) that develop into defective adult wings (Sup. Fig. 2C). These results are similar to those observed by others in *Su(H)* mutant individuals[18,19], suggesting a functional relationship between *tna* and *Su(H)*.

Next, we tested whether TnaA directly affects Notch-mediated transcriptional activation. We measured GFP expression in flies bearing a Notch pathway reporter construct *NRE-GFP* (*Notch Responsive Element*, *NRE*)[20]. We found that in the presence of TnaA-Flag, the expression of *NRE-GFP* is substantially reduced, indicating that TnaA interferes with the CSL complex-mediated activation of the *NRE-GFP* reporter in this specific region of the wing disc (Fig. 3B,C).

We conclude from the loss-of-function experiments that *tna* is interacting with the Notch pathway to control the level of Wingless at the D/V boundary domain of the wing disc. In addition, the positive and negative effects of TnaA-Flag on *wg* and *ct,* respectively, agree with the reported formation of Su(H)-CSL activating and repressor complexes on the promoters of these genes under *Su(H)* overexpression[18,19] (see "Discussion").

TnaA modulates the expression of *wg* in the IR domain of the wing disc. We previously established that *tna* genetically interacts with the Notch pathway to control the level of Wingless protein at the D/V boundary. Next, we knocked-down TnaA (a decrease of approximately 70% with respect to the wild-type level),

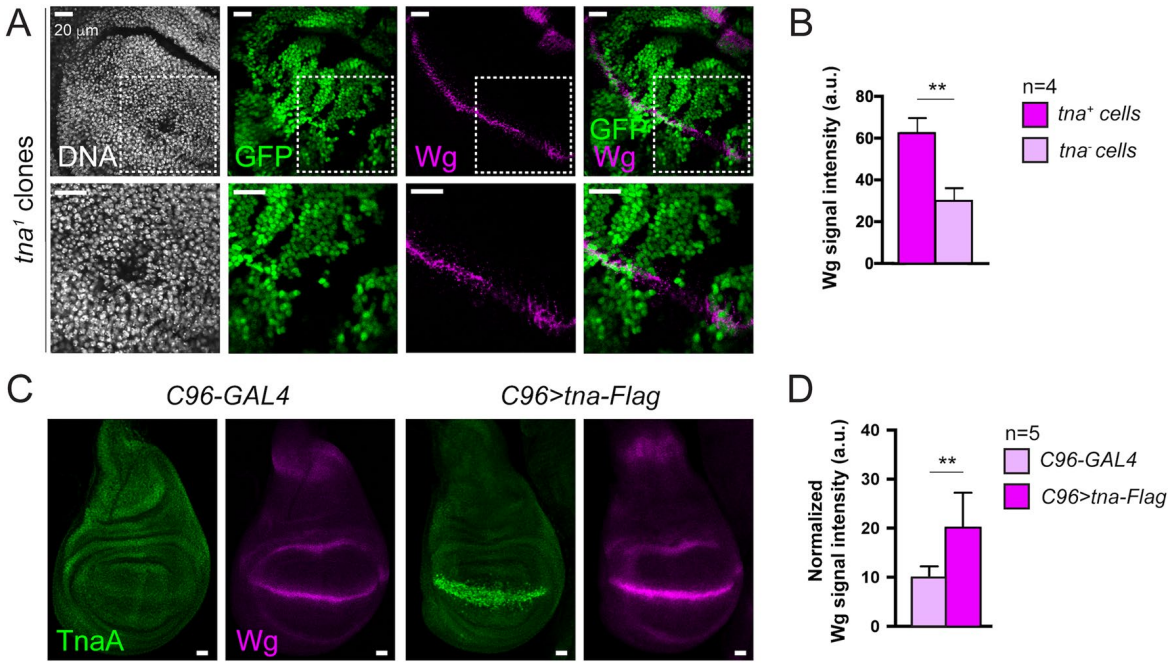

Figure 2. Wingless at the D/V boundary in *tna*-deficient and *tna-Flag* expressing wing discs. (**A**) Wingless signal in tna^1 clones (non-GFP cells) induced in the D/V boundary with *Ubx-FLP*[46]. Dashed squares in the images in the upper panel indicate the amplified region in the lower panel. (**B**) Quantification of the intensity of the Wingless signal at the D/V boundary in tna^+ and tna^- cells (**C**) Wingless signal in *tna-Flag* expressing discs at the D/V boundary driven by the *C96-GAL4* driver[59]. The discs were immunostained for TnaA and Wingless with the corresponding antibodies ("Methods"). (**D**) Quantification of Wingless in tna^+ and tna^- cells as indicated in Sup. Fig. 4B. Student's *t*-test was performed for the intensity of the signal in (**B**) and (**D**) ($P < 0.01^{**}$).

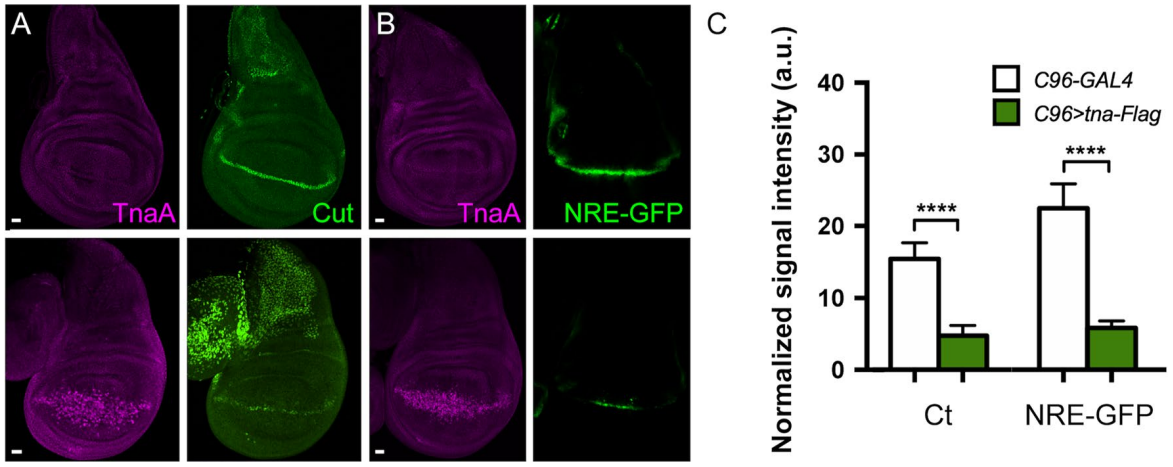

Figure 3. Cut and NRE-GFP signal in wing discs expressing *tna-Flag* along the D/V boundary. The expression of *tna-Flag* was driven to the D/V boundary with *C96-GAL4*[59]. (**A**) TnaA and Cut signals on *C96-GAL4* wing discs (upper panel), or in *C96 > tna-Flag* wing discs (lower panel). (**B**) TnaA and NRE-GFP signals in wing discs of genotypes as in (**A**). Note the reduction of Cut and NRE-GFP signals along the D/V boundary domain (**C**) Quantification of Cut and NRE-GFP in the D/V boundary of wing discs of the indicated genotypes ($n \geq 5$ discs). See also Sup. Fig. 4B. Student's *t*-test was performed for signal intensity in each case ($P < 0.0001^{****}$).

by expressing a *tna* RNAi ($tna^{JF02536}$,[13,21]) in the anterior compartment of the wing disc (Sup. Fig. 5) and assessed Wingless levels in their different expression domains (IR and D/V boundary) in this compartment. In this otherwise wild-type background, we did not observe any Wingless fluctuation in any of the evaluated regions, compared to the correspondent regions at the posterior compartment that are expressing wild-type TnaA levels (Sup. Fig. 5).

We reasoned that the TnaA knockdown level reached by the expression of $tna^{JF02536}$ RNAi may not be enough to knock down the robust Wingless expression in the different regions of the disc. We hypothesized that TnaA may act on a particular *wg*-regulatory element. *wg* has several embryonic and larval enhancers. One of the larval enhancers is the wing disc IR enhancer (*IRE*), located about 9 kb upstream the *wg* promoter[10].

We chose to test the TnaA requirements for the function of this enhancer in an *IRE* sensitized background. We used a line that carries the $wg^{spd\text{-}fg}$ allele, which is a small deletion that removes the *IRE* region. Wing discs where the deletion is homozygous lack *wg* expression at the IR while the one at the D/V boundary remains unchanged[10]. When the *IRE* is haploinsufficient, the Wingless signal looks normal in the IR and in the D/V (Fig. 4A, $wg^{spd\text{-}fg}$/+). The quantification of the Wingless and TnaA signals in each of these regions is shown in Fig. 4B. In contrast, when TnaA is knocked down in the anterior compartment of the wing disc ($wg^{spd\text{-}fg}$/+, $ci > tna^{JF02536}$), there is a decrease in the Wingless signal in the anterior half of the IR (Fig. 4A, $wg^{spd\text{-}fg}$/+, $ci > tna^{JF02536}$). An internal control of this experiment is the normal Wingless signal observed in the posterior IR region where $tna^{JF02536}$ is not expressed. Moreover, in this $wg^{spd\text{-}fg}$/+ background, Wingless is not reduced at the D/V boundary as expected, since the *IRE* does not control the *wg* expression in this domain. The quantification of the TnaA and Wingless levels in these discs is shown in Fig. 4B.

To complement these data, we directed *tna-Flag* expression to the anteroposterior (A/P) margin of the wing disc (Fig. 4C,D). In this case, we did observe TnaA-Flag effects on *wg* expression at both the D/V boundary and the IR (Fig. 4C**,** open and solid arrows, and quantification of the Wingless signal for each region in Fig. 4D and Sup. Fig. 4C). In response to TnaA-Flag, *wg* expression increases at the D/V boundary (Fig. 4C, open arrowhead). At the IR, *wg* expression is also increased, and its expression domain is expanded (Fig. 4C solid arrows). Adult wings derived from these discs show defects along the A/P boundary, including the hinge (Sup. Fig. 2D).

In conclusion of these experiments, in addition to influencing the expression of *wg* at the D/V boundary, TnaA also modulates its expression at the IR possibly through some direct or indirect action on the *IRE*.

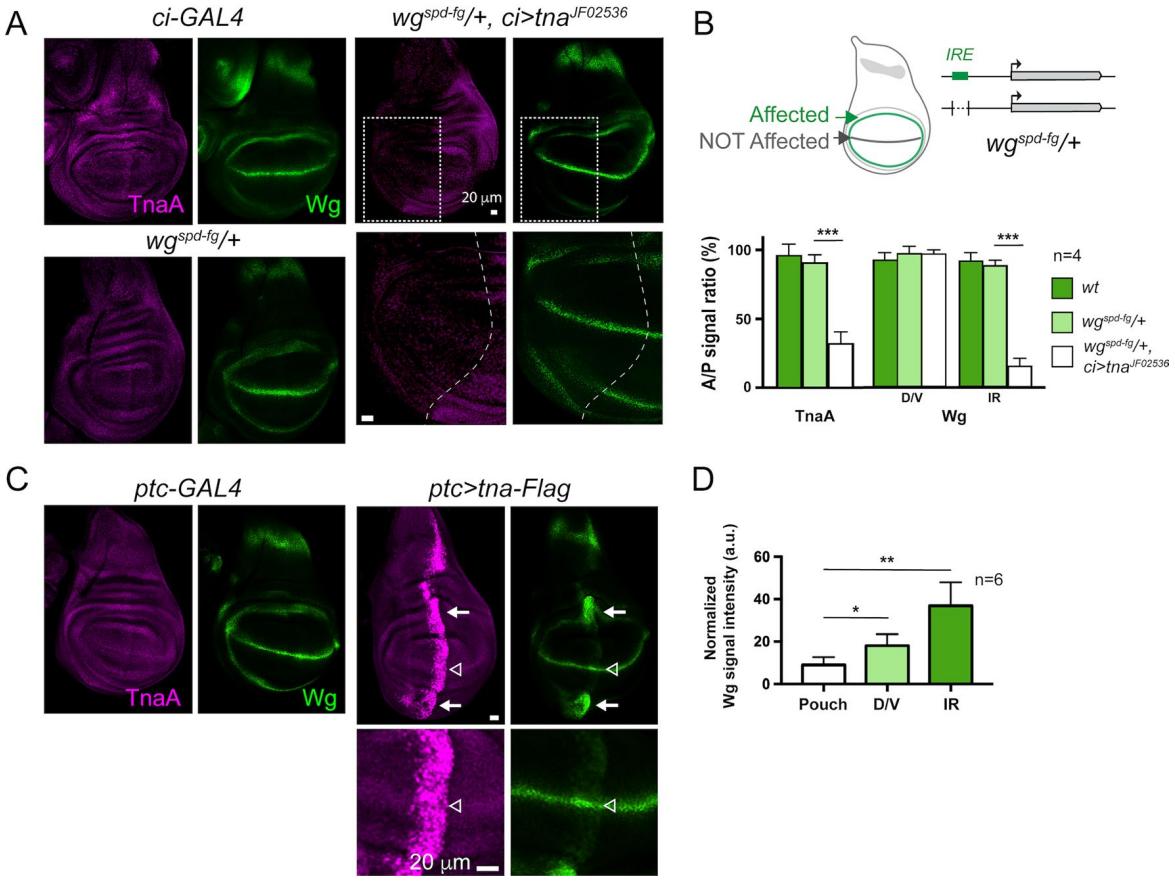

Figure 4. Effect of the dosage of TnaA on *wg* expression in the IR (**A**) The Wingless signal in the IR decreases when TnaA is knocked down in $wg^{spd\text{-}fg}$/+ wing discs. Immunostainings of TnaA and Wingless in wing discs of the indicated genotypes. TnaA was knocked down in the anterior compartment with the expression of the $tna^{JF25036}$ RNAi driven by the *ci-GAL4* in $wg^{spd\text{-}fg}$/+ discs ($wg^{spd\text{-}fg}$/+; $ci > RNAi\text{-}tna^{JF02536}$). The dashed rectangles (right upper panels) show the amplified region (right lower panels) where the A/P margin is indicated. (**B**) The $wg^{spd\text{-}fg}$ allele is a small deletion that removes the *IRE* region (upper diagram) and directs the expression of *wg* to the IR (green), but not to the D/V boundary (grey). Quantification of TnaA and Wingless A/P signal ratio in the D/V boundary and IR in discs with the indicated genotypes (lower panel). (**C**) TnaA and Wingless signals in wing discs that express *tna-Flag* at the anteroposterior margin driven by *ptc-GAL4*[60] that is active since the early second instar stage[61]. The IR (white arrows) and the D/V boundary (empty arrowhead) regions on the A/P axis are indicated (**D**) Quantification of the Wingless signal in the pouch, D/V and IR in $ptc > tna\text{-}Flag$ wing discs ($n \geq 6$ discs). See also Sup. Figure 4C. Student's *t*-test was performed for signal intensity in (**B**) and (**D**) in each case ($P < 0.05^{*}$, $P < 0.01^{**}$, $P < 0.001^{***}$).

The presence of TnaA-Flag in various developmental stages induces a rapid expansion of the Wingless IR domain. The characteristic pattern of *wg* expression in the third instar wing discs results from the activation of different enhancers along earlier larval stages. The larval expression of *wg* begins at the second instar (48 h after egg laying, AEL) in a ventral anterior region of the wing discs[26] directed by a well characterized early enhancer[27]. In early third instar larvae, the expression of *wg* is detectable in the D/V boundary and the IR[7,27] (Fig. 5A).

We investigated whether TnaA acts at a specific time of larval wing disc development. For this goal, we used the TARGET system, which inactivates the GAL4 repressor (GAL80ts) with temperature shifts[28]. We applied temperature shifts to inactivate GAL80ts at specific times along the development of the wing discs. This allowed us to accurately control the induction of *tna-Flag* expression in the *MS1096-GAL4* driver pattern between second and third instar larval stages (72 h AEL)[29,30] (Fig. 5A, see "Methods"). We found that as a result of *tna-Flag* expression since the first instar larval stage (36 h AEL), there is a strong expansion of the IR towards the pouch (Fig. 5A,B). At the third instar larval stage (90 h AEL), induction of *tna-Flag* expression causes a milder expansion of the IR domain than the one observed when induced at an earlier developmental stage (Fig. 5B, solid arrow).

We also studied whether cells in different regions of the wing disc could induce *wg* expression in response to TnaA dose. To approach this question, we induced clones expressing *tna-Flag* on the entire disc at 82 h AEL using the FLP-out technique (Fig. 5C and "Methods"). As previously shown, there is an expansion of the IR towards the pouch or the hinge when clones locate at/or near the IR (Fig. 5C, solid arrowheads). We also noticed that these cells rapidly increase the Wingless level in response to TnaA-Flag since the clones were induced only 24 h before dissection. In contrast, clones far from the IR, in other regions of the wing disc, such as the notum or ventral pouch (Fig. 5C empty arrowhead), do not show almost any increase in the level of Wingless. This indicates that proximity to the IR domain is important for the regulation of *wg* transcription mediated by TnaA.

These results show that TnaA-Flag can activate the expression of *wg* in the IR even before this domain is resolved in early to mid-third instar larvae. This TnaA-Flag effect is milder but is still observed when its expression is induced after the IR formation. Moreover, TnaA-Flag can rapidly increase *wg* expression, particularly in cells at or near the IR, with expansion of this domain. Altogether these results suggest that regulatory regions that modulate *wg* expression in the IR are available and highly sensitive to TnaA doses in specific stages of larval development.

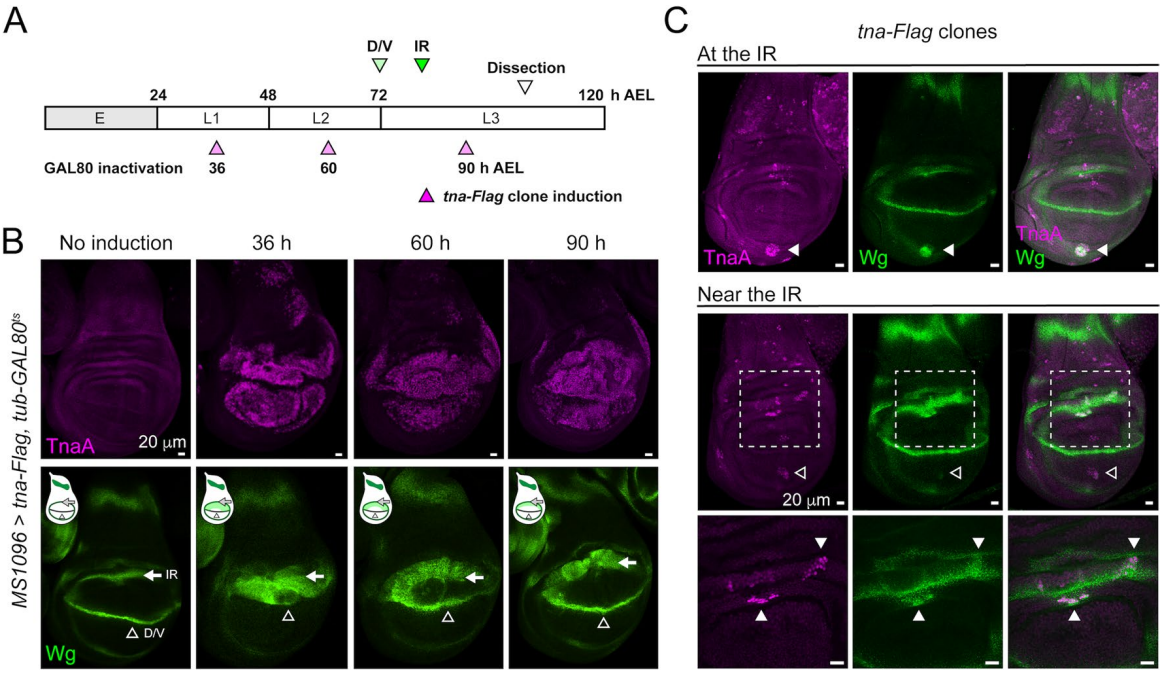

Figure 5. The TnaA-Flag effect depends on its timing of appearance and proximity to the IR during larval development. (**A**) Developmental timeline (E, Embryo, L1-L3 larval stages) according to hours after egg laying (h AEL). The time when the expression of *wg* is resolved in the D/V and IR domains (green arrowheads), and the temperature shift times applied to inactivate Gal80ts to allow expression of *MS1096 > tna-Flag* at the dorsal hinge (pink arrowheads) are indicated. (**B**) TnaA and Wingless distribution in wing discs expressing *tna-Flag* at specific times from 36 to 90 h AEL. Note the expansion of the Wingless signal from the IR (white arrow) but not from the D/V boundary domain (empty arrowhead). (**C**) Expression of *wg* in TnaA-Flag clones in different regions of the wing disc. TnaA and Wingless immunostainings are indicated, and merged images are shown (right panels). Images from two discs show a TnaA-Flag clone at the IR (upper panel) or near the IR (middle and lower panels). A TnaA-Flag clone in the pouch does not cause an induction of *wg* expression (middle panel, empty arrowhead). TnaA-Flag clones at/or adjacent to the *wg* IR domain present the induction of *wg* expression (middle and lower panels, solid arrowheads). Dashed squares (middle panel) indicate the region amplified in the lower panel.

TnaA localizes at the IR enhancer to modulate *wg* transcription. Next, we investigated whether TnaA directly affects *wg* transcription at the IR. We followed the expression of the *wg-lacZ* reporter[22] at the IR in wing discs where *tna-Flag* expression was directed to the dorsal hinge with the *MS1096-GAL4* driver[23]. This allowed us to monitor the expansion of the IR domain on the dorsal side of the wing disc, leaving the ventral side as an internal control (Fig. 6A,B). We found that under this condition, the expression of *tna-Flag* increases *wg* transcription (Fig. 6C). This causes a strong expansion of the dorsal IR domain towards the pouch, making it hard to distinguish it from the D/V boundary. As *tna-Flag* is not expressed in this region, the ventral IR looks normal (Fig. 6C). We also corroborated that both the A/P and D/V boundary domains remained intact in these wing discs, by monitoring the expression of *dpp-lacZ*[24] and *Dll-lacZ*[25], respectively (Fig. 6D,E). These results reinforce the notion that TnaA specifically influences the transcription of *wg* at the IR domain.

The *wg* locus has several enhancers that control its expression in different regions or stages of development. Imaginal *wg* enhancers include the *IRE* that controls *wg* expression in the IR domain of wing and haltere discs[10], and the *VDE* which controls the antero-ventral *wg* expression in leg and eye-antennal discs[8] (Fig. 7A). When the expression of TnaA is knocked down, the Wingless signal decreases in the IR in wing discs that harbor only one functional copy of the *IRE* ($wg^{spd\text{-}fg}$/+, Fig. 4), suggesting that TnaA is involved in the regulation of *wg* expression through this enhancer.

To further test the idea that TnaA acts on specific regulatory regions of *wg* to modulate *wg* transcription in the IR domain, we expressed *tna-Flag* on T3 leg and wing discs using the *rn-GAL4* driver[31], and we compared the effect of TnaA-Flag on *wg* expression in both types of discs (Fig. 7B). We found that in the presence of TnaA-Flag, the Wingless level increases significantly at the wing (Fig. 7B, left), where the *IRE* and the putative D/V enhancers are active. In contrast, in the T3 leg discs, where *wg* expression is driven by the *VDE*[8], the Wingless level is not altered or expanded (Fig. 7B, right), suggesting that TnaA influences specifically the *IRE* and not the *VDE*.

Then, we investigated whether TnaA and TnaA-Flag are present in the *IRE* in the chromatin of the larval wing discs. To determine this, we performed ChIP-qPCR assays of both proteins in the *wg IRE* and *VDE* enhancers (Fig. 7C). Chromatin from wing discs with wild-type TnaA or TnaA-Flag driven by *MS1096* genotypes was immunoprecipitated with anti-$TnaA_{TAIL}$ (Sup. Fig. 1D) or anti-FLAG antibodies, respectively. The presence of TnaA in both enhancers was evaluated by qPCR amplification with the appropriate oligonucleotides (Fig. 7A). We found that both TnaA and TnaA-Flag are enriched in the *IRE* compared to their mock fractions (see "Methods"). Additionally, TnaA enrichment was not found in the *VDE* compared to its mock sample (Fig. 7C), showing that TnaA is present in the *IRE* but not in the *VDE* in the chromatin of the wing discs.

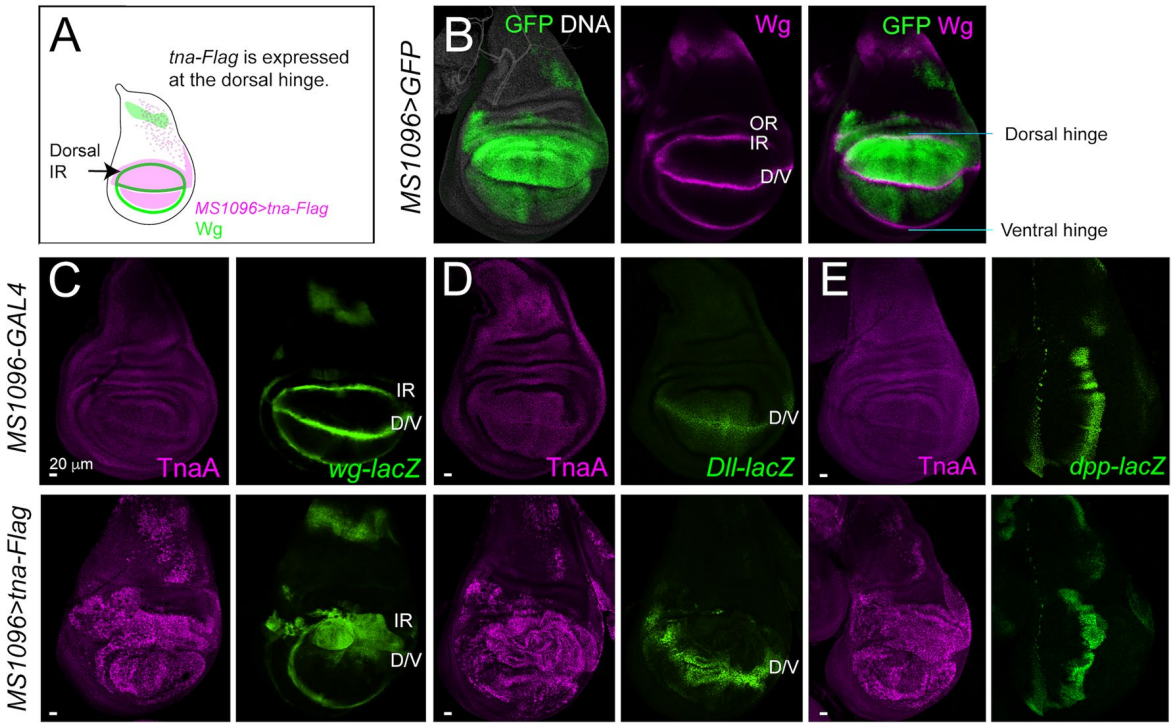

Figure 6. TnaA-Flag transcriptional effect on *wg* expression in the IR. The expression of *tna-Flag* was driven to the dorsal hinge with *MS1096-GAL4*[23]. (**A**) Scheme of the expression domain of *MS1096 > tna-Flag* (magenta) and the *wg* expression pattern (green) in a wing imaginal disc. Under this condition, the expression of *tna-Flag* overlaps only with the *wg* IR dorsal side and not with the ventral side, which could be used as a control in the same disc. (**B**) *MS1096 > GFP* wing discs showing GFP expression on the dorsal hinge (left), Wingless signal (middle) and merged image (right). (**C–E**) *MS1096-GAL4* and *MS1096 > tna-Flag* wing discs, immunostained for TnaA (magenta) or LacZ (green). (**C**) Expression of the transcriptional reporter *wg-lacZ*[62]. Note that the ventral *wg* IR domain is not affected since the driver is not active in this region. (**D**) The D/V boundary followed by the *Dll-lacZ* reporter[25]. (**E**) The A/P boundary followed by the expression of *dpp-lacZ*[24].

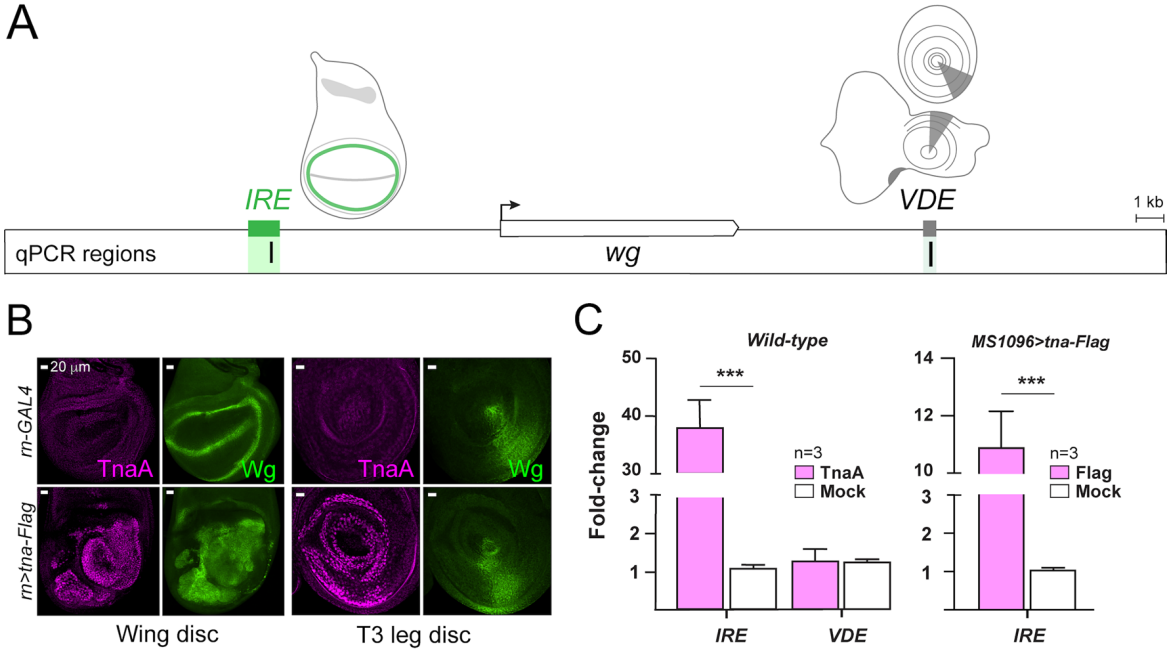

Figure 7. TnaA and TnaA-Flag are in the *IRE* in the wing disc. (**A**) Scheme of the *wg* locus showing the *IRE* and *VDE* that control *wg* expression in the wing and T3 leg discs (upper panel). The localization of the regions used (green lines) to evaluate the presence of TnaA by ChIP-qPCR with the anti-$TnaA_{TAIL}$ antibody is indicated. (**B**) TnaA and Wingless immunostainings of the *rn-GAL4* and *rn > tna-Flag* wing and T3 leg discs (upper and lower panels, respectively). The expression of *tna-Flag* was directed to the distal part of the discs with *rn-GAL4* which is active since the late second instar stage[31]. Note that the TnaA-Flag wing disc shows expansion of the IR domain (green) that is correlating with the presence of TnaA in the *IRE* in the wing discs. In contrast, the morphology and the Wingless expression pattern are normal in the TnaA-Flag T3 leg disc, where the *IRE* is not active. (**C**) TnaA ChIP-qPCRs of the *wg IRE* and *VDE* in chromatin from wild type wing discs (left). The presence of TnaA-Flag in the *IRE* was determined by ChIP-qPCR with a FLAG antibody in *MS1096 > tna-Flag* discs (right). qPCR reactions with immunoprecipitated DNA samples with anti-$TnaA_{TAIL}$, anti-FLAG, or with irrelevant antibodies (rabbit and mouse IgG for TnaA and TnaA-Flag, respectively; see "Methods") were performed with the indicated primer sets to amplify the selected *IRE* or *VDE* regions indicated in (**A**) (black vertical lines). Results are shown as fold enrichment over the background signals. Student's *t*-test was performed on qPCR enrichments in the regions tested ($P < 0.001$***).

We conclude from these experiments that TnaA and TnaA-Flag are physically present in the *IRE* probably to modulate *wg* expression in the IR domain in the wing disc.

Discussion

In this work, we found that TnaA modulates the expression of *wg* at the D/V boundary and the IR domains in the wing disc. At the D/V boundary domain, TnaA modulates *wg* expression interacting with the Notch pathway, and at the IR domain, it promotes *wg* transcription probably through its specific binding to the *wg IRE*.

Several pieces of evidence in this work indicate that TnaA is involved in the transcription of Notch target genes expressed in the D/V boundary. TnaA plays a role in the transcriptional activation of *wg* in the D/V boundary domain mediated by CSL, the effector complex of the Notch pathway. The CSL complex consists of NICD, Mam, and Su(H). According to models based on genetic and biochemical data, NICD acts as a permissive signal (e.g., *wg* transcription), alleviating the repression imposed by corepressors bound to Su(H), while in others (e.g., *ct* and *NRE-GFP* transcription), NICD acts as an instructive signal by directly recruiting transcription factors to activate gene expression[32]. In this model, overexpression of *Su(H)* reduces *ct* expression, presumably because excessive Su(H) can titrate available NICD as well as any co-repressors[18,19]. ChIP-seq analyses[33] and studies on protein-enhancer dynamics[34,35] showed that NICD binding has different effects on the dwell time of CSL subunits in regulatory regions and on transcriptional outcomes depending on enhancer priming and the chromatin landscape.

Our data suggest that TnaA may facilitate the formation of CSL complexes at their dedicated promoters. Loss of TnaA decreases the Wingless signal in the D/V boundary in *tna* clones and enhances the decrease in *wg* caused by mutations in Su(H) or NICD[4,5]. Conversely, TnaA-Flag increases *wg* expression and reduces *ct* and *NRE-GFP* (Fig. 3), in a behavior similar to that found in wing discs with misexpression of *Su(H)*.

Although the precise mechanism of the TnaA function remains elusive, these results fit the interpretation that TnaA is acting in the same direction as the CSL activator complex to facilitate *wg* expression in this region. Moreover, it is likely that TnaA could be involved in the regulation of the dynamics of CSL complexes or in the chromatin landscape around its target genes.

TnaA also modulates the expression of *wg* in the IR (Figs. 4, 5, 6). The loss of TnaA diminishes the Wingless signal specifically in the IR in $wg^{spd\text{-}fg}$/+ wing discs that are haploinsufficient for the *wg* IR enhancer[10] (Fig. 4a). In contrast, TnaA-Flag rapidly increases the Wingless signal at the IR, particularly before the *wg* IR domain is resolved in early to mid-third instar larvae. Its effect is milder after the IR formation. These results suggest that at least some regulatory regions that modulate *wg* expression in the IR are available and highly sensitive to TnaA doses throughout the development of the wing disc and may reflect the intrinsic ability of TnaA to interact with transcriptional activators and/or to find or influence chromatin changes to make its target regions available for preparation (as for enhancer priming), activation, or maintenance of *wg* expression in the IR.

TnaA is nuclear in all cells of the wing disc (this work, and[14]). However, it modulates specifically the expression of *wg* at the D/V boundary and the IR domains. This indicates that TnaA is not promiscuous and that it probably targets regulatory elements of *wg* that are functional only in specific regions within the wing disc. The complex spatial pattern of *wg* in the wing disc is regulated through multiple regulatory regions. The broad band enhancer at the notum of the wing disc and the *VDE* ventral disc enhancer are very close to each other and together with the *IRE* are accurately located[5,8]. Furthermore, enhancers that specify wings and respond to damage have recently been located close to each other[27]. In contrast, the location of the D/V boundary enhancer that is controlled by the Notch pathway[4,5] is not known.

We found that TnaA and TnaA-Flag are in the *IRE* (Fig. 7C), influencing the expression of *wg*. To the best of our knowledge, there is not yet a compilation of which proteins are in this enhancer under wild-type conditions when the enhancer is primed, active, or inactive. Good candidates are key factors for the initiation and establishment of *wg* expression in the IR domain. These are Nubbin, Rotund, Vestigial, and Scalloped[7,36,37]. Until now, there is little evidence supporting the direct binding of any of these proteins to the *IRE* and it will be important to determine whether any of them collaborate with TnaA.

The precise location of the Notch-responsive D/V boundary enhancer remains unknown, making it difficult to test whether TnaA binds to it. However, a region located at or near the *IRE* may mediate Notch regulation of *wg*. Under conditions with ubiquitous activation of the Notch pathway, NICD and Su(H) are in a region that includes the *IRE* and an *IRE-GFP* reporter construct responds to Notch activation[33,38]. When *Su(H)* is overexpressed, there is an increase in *wg* expression in the IR[18]. This evidence indicates that there is a Notch-responsive region at or near the *IRE* that could mediate the Notch regulation of *wg* at the D/V boundary. According to this, TnaA would modulate the expression of *wg* in the IR and in the D/V boundary domains by binding to a single region that comprises the *IRE* and, at least partially, the putative D/V boundary enhancer in the wing disc. Nevertheless, our own data show that there is no change in the Notch-regulated D/V *wg* expression in animals with a reduced dose of *tna* upon *IRE* haploinsufficiency (Fig. 4). Altogether, these data leave open the possibilities that the Notch-responsive regulatory region is not affected by the deletion harbored by the $wg^{spd\text{-}flag}$ allele or that it is located elsewhere.

We do not know whether TnaA is in the *IRE* in all cells of the wing disc or only in cells of the IR since our ChIP-qPCR experiments were carried out with chromatin from whole discs (Fig. 7C). In the wing disc, the *IRE* should only be active in the stripe of cells that form the IR (and probably in the ones that form the D/V boundary), but it is not known in which activity state the *IRE* is in other nuclei outside these *wg* expression domains.

Finally, it is interesting to discuss the role of TnaA in the function of the *wg IRE* and the D/V enhancers. TnaA is a putative SUMO E3 ligase whose targets could be protein factors recruited to the enhancer and/or histones in particular nucleosomes, histone modifiers, or chromatin remodelers surrounding it. In fact, TnaA has been implicated in the SUMOylation of subunits of the BRAHMA complex[12,14]. The BRAHMA complex has already been implicated in Notch signaling in *Drosophila* and vertebrates[39–41].

Complexes recruited in enhancers must be very dynamic to respond to signaling at dedicated locations. The study of the mechanisms that help chromatin render a functional environment for the action of these complexes is of particular interest. SUMOylation can modify the activity, location and/or interaction of nuclear target proteins (reviewed in[11]), and TnaA has two domains that are relevant in this context[12,14]. One is the 300 aminoacidic XSPRING domain with a signature zinc finger of a kind of SUMO E3 ligases and a glutamine-rich region that can help recruit transcription-related factors that also have glutamine-rich regions[42]. Although the specific role of TnaA in *wg* transcription is not clear, one possibility is that it helps one or more regulatory factors to facilitate their exchange on enhancers such as the *wg IRE* at the wing disc.

Our data suggest that TnaA is an enhancer-specific factor of *wg*, modulating only the *wg* D/V and IR enhancer(s) of the wing imaginal disc. We do not know whether this effect is caused by the interaction of TnaA with a factor that is common to both enhancers or whether they bind to different proteins. Furthermore, if the *wg IRE* is subjected to the same kind of dynamics discovered for the CSL enhancers, TnaA may play a role in the mechanisms that determine the timing and exchange of the proteins recruited to switch the enhancer to its active or inactive forms. It remains a challenge to determine, in the tightly regulated multiple-tier network of wing disc proliferation and patterning processes, the different elements that help TnaA find, engage and exert its function at specific target genes in different wing disc domains. This will be important in understanding the role of TnaA in this context and in a genome-wide perspective.

Methods

Ethics statement. *Drosophila melanogaster* handling was approved by the Instituto de Biotecnología, UNAM, Bioethics Committee, Permit Number 359, which follows NOM-062 animal welfare Mexican law. No other animals were used in this study. All efforts were made to minimize animal suffering. Flies were sacrificed by CO2 euthanasia.

Fly strains, growth, and genetic procedures. The lesions of *N*, *Su(H)*, *wg*, *tna* alleles, *lacZ* reporters for some genes, and GAL4 driver lines used in this work are, unless otherwise noted, described in Flybase[43]. The mutant alleles of *tna* used in this work are shown in Sup. Fig. 1A. Briefly, tna^{1}, tna^{5} are dominant negative and null EMS-derived alleles, respectively. $tna^{EY22929}$ is a hypomorphic *P{EPgy2}* element insertion-derived allele[44]. These three alleles are described in[13]. $tna^{MI01482}$ is a *MiMIC* element insertion-derived allele[45]. *tna* knockdown was achieved by expressing interference RNA (RNAi) from the $tna^{JF02536}$ line from Perrimon's pVALIUM10-derived TRiP collection[21], using different drivers. The efficacy of *tna* knockdown of this line ($tna^{JF02536}$) was previously characterized[13].

The reporter construct *NRE-GFP* (*Notch Responsive Element*, *NRE*) has three Grainy Head (Grh) binding sites, followed by two pairs of Su(H)-binding sites from the *Enhancer of split m8* [*E(spl)m8*] gene which is regulated by Notch as an instructive signal[20].

The $wg^{spd\text{-}fg}$ allele is a small deletion that removes the *IRE* region that, hence, lacks *wg* expression at the IR but the one at the D/V boundary appears to remain unaltered[10].

Fly culture and crosses were performed according to standard procedures. Flies were raised in yeast-molasses media at 25 °C unless otherwise noted.

Notched-wing phenotypes were scored in adult animals with *tna* mutant alleles under a Notch loss-of-function genetic background. Penetrance and expressivity of the notched-wing phenotype were classified as weak or strong depending on the presence of single or several notches respectively in a wing margin (see Fig. 1B and Table 1). Adult wings were dissected in 70% ethanol, mounted onto slides in isopropanol, and immediately imaged with an Amscope UCMOS05100 camera attached to a Nikkon Eclipse E600 microscope. The statistical significance of the Notch loss-of-function phenotypes was determined using a *t*-test ($P < 0.05$) in animals obtained from at least three independent crosses for each genotype.

tna^{1} homozygous clones were generated by homologous recombination using *Ubx-FLP*[46] as described in[13]. Clones expressing *tna-Flag* were generated with the FLP-out technique[47]. To remove the stop cassette in *hs-FLP, UAS-mCD8::GFP; UAS-tna-Flag/+; Act5C-STOP-GAL4* larvae, we induced a heat-shock in these animals at 82 h AEL in a water-bath for 15 min at 35 °C. In both cases, the wing imaginal discs were dissected from wandering third instar larvae at 96 h AEL and immunostained as described in the following section.

To induce the expression of *tna-Flag* at different stages of development, we used the Temporal and Regional Gene Expression Targeting (TARGET) system[28]. *MS1096-GAL4, UAS-GFP; UAS-tna-Flag/+; tub-GAL80^{ts}/+* animals were grown at 18 °C and then shifted to 29 °C at 36, 60 and 90 h AEL. Temperature changes were applied at least 12 h before and after the appearance Wingless in the pouch (48 h AEL) and IR (72 h AEL). Wing discs were dissected at around 96 h AEL and *tna-Flag* expression was corroborated by immunostaining with anti-$TnaA_{TAIL}$ antibody (1:250, see ahead). The results were compared with the ones obtained with flies without induction (grown at 18 °C) or with full induction (grown at 29 °C).

Characterization of epitope-tagged TnaA-Flag *Drosophila* transgenic lines. TnaA-Flag is a tagged version of $TnaA_{123}$ from the *Iso*1 strain, which is the main nuclear isoform derived from the *tna* locus[13,14]. The FLAG epitope (DYKDDDDK) was inserted into the carboxy-termini of $TnaA_{123}$, precisely after the last amino acid (Asp1109). The correct tagging was confirmed by DNA sequencing of the construct. The epitope-tagged TnaA version was subcloned in the p*UAST* plasmid, where its expression is controlled by the GAL4-*UAS* system[48]. The correct molecular weight of TnaA-Flag was confirmed by Western analysis of soluble protein extracts from wing discs using the anti-$TnaA_{XSPRING}$ antibody (Sup. Fig. 1E).

Independent transgenic *yw; UAS-tna-Flag* lines were obtained, and the different insertions of the transgene (w^{+}) were mapped to different *Drosophila* chromosomes with subsequent balancing using classical genetic techniques. The TnaA-Flag protein from several transgenic lines, expressed with different strong and weak drivers, was tested for complementation of lethality caused by heteroallelic *tna* mutant alleles. It partially rescues adult viability (2% of the expected progeny), probably due to incorrect time/space dosages of the TnaA-Flag version in the whole fly. TnaA-Flag, as the wild-type form, is nuclear in imaginal discs, as corroborated by immunostaining of imaginal discs of third instar larvae with the anti-Flag antibody (Sup. Fig. 1B). TnaA-Flag binds to the same polytene bands as wild-type $TnaA_{123}$ bands (Sup. Fig. 1C).

TnaA antibodies and Western blot analyses. To detect TnaA in this work, we used affinity purified anti-$TnaA_{XSPRING}$ and anti-$TnaA_{TAIL}$ antibodies. Briefly, antibodies were raised in rabbits against different regions of the $TnaA_{123}$ isoform encoded by the *tna-RD* transcript (Sup. Fig. 1D), identified and sequenced by[49], and reported by Flybase[49]. The anti-$TnaA_{XSPRING}$ is described in Rosales-Vega et al.[13], and the anti-$TnaA_{TAIL}$ was raised against the 21-mer DVDPMEILSYLDPQPDLNTPPS peptide (aminoacids 1070–1091 of $TnaA_{123}$) by ProSci, Inc. Both antibodies were affinity-purified from total sera. Western blot analyses of TnaA and actin in soluble protein extracts from wing discs (Sup. Fig. 1E) were performed in duplicate from two different biological replicates with soluble protein extracts from 30 wing discs of each genotype with the appropriate antibodies and were performed as specified in[13]. The membrane chemiluminescence imaging was acquired using a BioRad ChemiDoc imaging system. The raw images were not processed in any manner, and the average level of the normalized signal intensity of the indicated bands with respect to the wild-type levels (dashed line), is represented as bars with standard deviation in Sup. Fig. 1E. These proteins were detected with anti-$TnaA_{XSPRING}$ and mouse anti-Actin (JLA20, Developmental Studies Hybridoma Bank) antibodies, used at 1:250 and 1:3000 dilutions, respectively. Secondary antibodies used were anti-rabbit HRP goat IgG (H + L) (62–6129), and anti-mouse HRP goat IgG/IgA/IgM (H + L) (A106868) (Invitrogen) used both, at 1:5000 dilutions.

Immunostaining of polytene chromosomes and imaginal discs. To determine the colocalization between endogenous TnaA and TnaA-Flag on polytene chromosomes, we induced the expression of *tna-Flag* in the salivary glands of third instar larvae with the *Sgs3-GAL4* driver[50] and immunostained these chromosomes (Sup. Fig. 1C). For immunostaining of polytene chromosomes, we followed the protocol of[51], with modifications as described in[14]. Affinity purified anti-$TnaA_{XSPRING}$ (1:50), and anti-FLAG (M2 Invitrogen) (1:100) antibodies were used in the indicated dilutions. Imaginal discs immunostaining was performed according to the protocol of[52], with some modifications as described in[13]. To detect TnaA and TnaA-Flag, imaginal discs were immunostained with anti-$TnaA_{TAIL}$ antibodies used at a 1:50 dilution unless otherwise specified. Other antibodies used were anti-Wg 4D4 (1:25)[53], anti-NICD (C17.9C6) (1:200)[54], anti-Ct 2B10 (1:50)[55], anti-βGAL 40-1a (1:50)[56], anti-Su(H) C-9 (Santa Cruz # sc-398453) (1:200) and anti-FLAG antibody (M2, Sigma) (1:100). Secondary antibodies anti-rabbit, anti-mouse Alexafluor 568 and anti-rat Alexafluor 594 (Invitrogen) were used for confocal microscopy. Fluorescent images of immunostained polytene chromosomes and/or imaginal discs were acquired with an Olympus Inverted FV1000, or 2P Upright FV1000 confocal microscopes with a 20X, NA 0.75 or 60X, NA 1.3 objectives. The images were processed with Fiji (ImageJ) v. 1.0, and Adobe Photoshop CS software.

Quantification of signal intensity in confocal images. The presence of Wingless, Cut, and NRE-GFP was quantified using the plot profile tool from Fiji (ImageJ) v. 1.0. The mean grey value was used as a measure of the intensity of the signal in rectangular areas and its average value was obtained with measurements of at least six wing discs of each genotype. Statistical analyses of differences in signal intensity, were performed using Student's *t*-test (with P-values ≤ 0.05*).

To measure the differences in *wg* expression in the genetic interaction between *tna* and *N*, we measured the intensity of the signal in ten bins of 20 µm in width around the center of the wing disc (Sup. Fig. 4A). To measure changes in the levels of Wingless, Cut, and *NRE-GFP* in *C96 > tna-Flag* wing discs, we normalized the signal intensity values by subtracting the signal intensity in TnaA-Flag (+) cells from that in TnaA-Flag (−) cells. (Sup. Fig. 4B). To quantify changes in *wg* expression in *ptc > tna-Flag* wing discs, we applied the same normalization procedure as in Sup. Fig. 4. The signal intensity was quantified in the pouch, IR, and D/V (Sup. Fig. 4C).

ChIP-qPCR analyses. Chromatin immunoprecipitation was performed on 60 wing imaginal discs from *Ore*R wandering third instar larvae per biological sample as described in[57] with minor changes. IgA- and IgG-coupled Dynabeads (Invitrogen), were used in a 1:1 ratio for chromatin immunoprecipitation in place of protein A or G agarose/salmon sperm DNA beads. Immunoprecipitations were performed with irrelevant antibodies that do not bind nuclear proteins and serve as Mock samples (rabbit IgG, Invitrogen #02-6102, and mouse IgG, Invitrogen #02-6502), or with 5 µg of affinity purified anti-$TnaA_{TAIL}$. Three biological samples were obtained in each case and quantitative PCR (qPCR) reactions with the appropriate oligonucleotides were performed to amplify the selected *IRE* or *VDE* regions (indicated in Fig. 7). The experiments were carried out with three replicates of each biological sample.

qPCR reactions of different *wg* regions immunoprecipitated with the anti-$TnaA_{TAIL}$ antibody were performed as described by[58], in a Lightcycler 480 Real-time PCR system (Roche Applied Science) using the Maxima SYBR Green/Rox qPCR Master Mix (2X) (Thermo Scientific). The *wg* regions targeted for qPCR amplification are shown in Fig. 7. Oligonucleotide sequences to amplify a 128-bp region within the *IRE* are Fwd 5′-AAAGTTATG GGCCTCCGTCT-3′ and Rev 5′- CTGGCCGAAGAGAAGTCATC-3′, and those used to amplify a 149-bp region of the *VDE*, used as a negative control, are Fwd 5′-GGACTGGAGTGGACGGATTT-3′ and Rev 5′-CCTAAT TCACGCGCCAAAGT-3′. The quantification of TnaA by ChIP-qPCR on *wg IRE* in wing discs was calculated as fold enrichment over background signal and is the average of three independent biological samples with three replicates each. Statistical analyses of differential accumulation of TnaA between samples were performed using Student's *t* test, P-values ≤ 0.05.

Data availability

Stocks and reagents are available upon request to Martha Vázquez. The authors affirm that all data necessary for confirming the conclusions of the article are present within the article, Figures, and Table.

Received: 9 February 2023; Accepted: 6 September 2023
Published online: 13 September 2023

References

1. Bray, S. J. Notch signalling: A simple pathway becomes complex. *Nat. Rev. Mol. Cell Biol.* **7**, 678–689 (2006).
2. Wiese, K. E., Nusse, R. & van Amerongen, R. Wnt signalling: Conquering complexity. *Development* **145**, 1–9. https://doi.org/10.1242/dev.165902 (2018).
3. Couso, J. P., Knust, E. & Martinez-Arias, A. *Serrate* and *wingless* cooperate to induce *vestigial* gene expression and wing formation in *Drosophila*. *Curr. Biol.* **5**, 1437–1448 (1995).
4. de Celis, J. F., Garcia-Bellido, A. & Bray, S. J. Activation and function of *Notch* at the dorsal-ventral boundary of the wing imaginal disc. *Development* **122**, 359–369 (1996).
5. Neumann, C. J. & Cohen, S. M. A hierarchy of cross-regulation involving *Notch*, *wingless*, *vestigial* and *cut* organizes the dorsal/ventral axis of the Drosophila wing. *Development* **122**, 3477–3485 (1996).
6. Barolo, S., Stone, T., Bang, A. G. & Posakony, J. W. Default repression and Notch signalling: Hairless acts as an adaptor to recruit the corepressors Groucho and dCtBP to Suppressor of Hairless. *Genes Dev.* **16**, 1964–1976 (2002).
7. del Alamo-Rodríguez, D., Terriente, J., Galindo, M. I., Couso, J. P. & Diaz-Benjumea, F. J. Different mechanisms initiate and maintain *wingless* expression in the *Drosophila* wing hinge. *Development* **129**, 3995–4004 (2002).
8. Pereira, P. S., Pinho, S., Johnson, K., Couso, J. P. & Casares, F. A 3' *cis*-regulatory region controls *wingless* expression in the *Drosophila* eye and leg primordia. *Dev. Dyn.* **235**, 225–234 (2006).

9. Baker, N. E. Transcription of the segment-polarity gene *wingless* in the imaginal discs of *Drosophila*, and the phenotype of a pupal-lethal *wg* mutation. *Development* **102**, 489–497 (1988).
10. Neumann, C. J. & Cohen, S. M. Distinct mitogenic and cell fate specification functions of *wingless* in different regions of the wing. *Development* **122**, 1781–1789 (1996).
11. Monribot-Villanueva, J., Zurita, M. & Vázquez, M. Developmental transcriptional regulation by SUMOylation, an evolving field. *Genesis* **55**, e23009 (2017).
12. Gutierrez, L., Zurita, M., Kennison, J. A. & Vazquez, M. The *Drosophila* trithorax group gene *tonalli* (*tna*) interacts genetically with the Brahma remodeling complex and encodes an SP-RING finger protein. *Development* **130**, 343–354 (2003).
13. Rosales-Vega, M., Hernández-Becerril, A., Murillo-Maldonado, J. M., Zurita, M. & Vázquez, M. The role of the trihorax group TnaA isoforms in Hox gene expression, and in *Drosophila* late development. *PLoS ONE* **13**, 1–22. https://doi.org/10.1371/journal.pone.0206587 (2018).
14. Monribot-Villanueva, J. *et al.* TnaA, an SP-RING protein, interacts with Osa, a subunit of the chromatin remodeling complex BRAHMA and with the SUMOylation pathway in *Drosophila melanogaster*. *PLoS ONE* **8**, 1–12. https://doi.org/10.1371/journal.pone.0062251 (2013).
15. Vázquez, M., Cooper, M. T., Zurita, M. & Kennison, J. A. {gamma}Tub23C interacts genetically with Brahma chromatin-remodeling complexes in *Drosophila melanogaster*. *Genetics* **180**, 835–843. https://doi.org/10.1534/genetics.108.093492 (2008).
16. Schweisguth, F. & Posakony, J. W. *Suppressor of Hairless*, the Drosophila homolog of the Mouse Recombination signal-binding protein gene, controls sensory organ cell fates. *Cell* **69**, 1199–1212. https://doi.org/10.1016/0092-8674(92)90641-o (1992).
17. Singh, A., Paul, M. S., Dutta, D., Mutsuddi, M. & Mukherjee, A. Regulation of Notch signaling by the chromatin-remodeling protein Hat-trick. *Development* **146**, 1–11. https://doi.org/10.1242/dev.170837 (2019).
18. Furriols, M. & Bray, S. Dissecting the mechanisms of Supressor of Hairless function. *Dev. Biol.* **227**, 520–532 (2000).
19. Klein, T., Seugnet, L., Haenlin, M. & Martínez Arias, A. Two different activities of *Suppressor of Hairless* during wing development in *Drosophila*. *Development* **127**, 3553–3566 (2000).
20. Furriols, M. & Bray, S. A model Notch Response Element detects Supressor of Hairless-dependent molecular switch. *Curr. Biol.* **11**, 60–64 (2001).
21. Ni, J. Q. *et al.* Vector and parameters for targeted transgenic RNA interference in *Drosophila melanogaster*. *Nat. Methods* **5**, 49–51 (2008).
22. Ingham, P. W., Taylor, A. M. & Nakano, Y. Role of the *Drosophila patched* gene in positional signalling. *Nature* **353**, 184–187 (1991).
23. Capdevila, J. & Guerrero, I. Targeted expression of the signalling molecule Decapentaplegic induces pattern duplications and growth alterations in *Drosophila* wings. *EMBO J.* **13**, 4459–4468 (1994).
24. Zecca, M., Basler, K. & Struhl, G. Sequential organizing activities of Engrailed, Hedgehog and Decapentaplegic in the *Drosophila* wing. *Development* **121**, 2265–2278 (1995).
25. Kaphingst, K. & Kunes, S. Pattern formation in the visual centers of the *Drosophila* brain: *Wingless* acts via *decapentaplegic* to specify the dorsoventral axis. *Cell* **78**, 437–448 (1994).
26. Couso, J. P., Bate, M. & Martinez-Arias, A. A wingless-dependent polar coordinate system in the imaginal discs of Drosophila. *Science* **259**, 484–489 (1993).
27. Gracia-Latorre, E., Pérez, L., Muzzopappa, M. & Milán, M. A single WNT enhancer drives specification and regeneration of the *Drosophila* wing. *Nat. Commun.* **13**, 4794–4809. https://doi.org/10.1038/s41467-022-32400-2 (2022).
28. McGuire, S. E., Le, P. T., Osborn, A. J., Matsumoto, K. & Davis, R. L. Spatiotemporal rescue of memory dysfunction in *Drosophila*. *Science* **302**, 1765–1768 (2003).
29. Mirth, C. K., Truman, J. W. & Riddiford, L. M. The ecdysone receptor controls the post-critical weight switch to nutrition-independent differentiation in Drosophila wing imaginal discs. *Development* **136**, 2345–2353 (2009).
30. Paul, R. *et al.* Hox dosage contributes to flight appendage morphology in Drosophila. *Nat. Commun.* **12**, 2892–2905 (2021).
31. St Pierre, S., Galindo, M. I., Couso, J. P. & Thor, S. Control of *Drosophila* imaginal disc development by *rotund* and *roughened eye*: Differentially expressed transcripts of the same gene encoding functionally distinct zinc finger proteins. *Development* **129**, 1273–1281 (2002).
32. Bray, S. & Furriols, M. Notch pathway: Making sense of Supressor of Hairless. *Curr. Biol.* **11**, R217–R221 (2001).
33. Djiane, A. *et al.* Dissecting the mechanisms of Notch induced hyperplasia. *EMBO J.* **32**, 60–71 (2013).
34. Falo-Sanjuan, J., Lammers, N. C., Garcia, H. G. & Bray, S. J. Enhancer priming enables fast and sustained transcriptional responses to Notch signaling. *Dev. Cell* **50**, 411–425 (2019).
35. Gomez-Lamarca, M. *et al.* Activation of the Notch signaling pathway *in vivo* elicits changes in CSL nuclear dynamics. *Dev. Cell* **44**, 611–623 (2018).
36. Liu, X., Grammont, M. & Irvine, K. D. Roles for *scalloped* and *vestigial* in regulating cell affinity and interactions between the wing blade and the wing hinge. *Dev. Biol.* **228**, 287–303 (2000).
37. Williams, J. A., Paddock, W. W. & Carroll, S. B. Pattern formation in a secondary field: A hierarchy of regulatory genes subdivides the developing wing disc into discrete subregions. *Development* **126**, 109–117 (1993).
38. Chan, S. K. K. *et al.* Role of co-repressor genomic landscapes in sharing the Notch response. *PLoS Genet.* https://doi.org/10.1371/journal.pgen.1007096 (2017).
39. Armstrong, J. A. *et al.* Genetic screens for enhancers of *brahma* reveal functional interactions between the BRM chromatin-remodeling complex and the Delta-Notch signal transduction pathway in *Drosophila*. *Genetics* **170**, 1761–1774 (2005).
40. Pillidge, Z. & Bray, S. J. SWI/SNF chromatin remodeling controls Notch-responsive enhancer accessibility. *EMBO Rep.* **20**, 1–16 (2019).
41. Takeuchi, J. K. *et al.* Baf60c is a nuclear Notch signaling component required for the establishment of left-right asymmetry. *Proc. Natl. Acad. Sci. U.S.A.* **104**, 846–851 (2007).
42. Stroebele, E. & Erives, A. Integration of orthogonal signaling by the Notch and Dpp pathways in *Drosophila*. *Genetics* **203**, 219–240 (2016).
43. Gramates, L. S. *et al.* FlyBase at 25: Looking to the future. *Nucleic Acids Res.* **45**(D1), D663–D671 (2017).
44. Bellen, H. J. *et al.* The BDGP gene disruption project: Single transposon insertions associated with 40% of Drosophila genes. *Genetics* **167**, 761–781 (2004).
45. Venken, K. J. *et al.* MiMIC: A highly versatile transposon insertion resource for engineering *Drosophila melanogaster* genes. *Nat. Methods* **8**, 737–743 (2011).
46. Emery, G. *et al.* Asymmetric Rab11 endosomes regulate Delta recycling and specify cell fate in the *Drosophila* nervous system. *Cell* **122**, 763–773 (2005).
47. Struhl, G. & Basler, K. Organizing activity of Wingless protein in *Drosophila*. *Cell* **71**, 527–540 (1993).
48. Brand, A. H. & Perrimon, N. Targeted gene expression as a means of altering cell fates and generating dominant phenotypes. *Development* **118**, 401–415 (1993).
49. dos Santos, G. *et al.* Flybase: Introduction of the *Drosophila melanogaster* Release 6 reference genome assembly and large-scale migration of genome annotations. *Nucleic Acids Res.* **43**, D690–D697 (2014).
50. Zhimulev, I. F. *et al.* Intercalary heterochromatin in *Drosophila melanogaster* polytene chromosomes and the problem of genetic silencing. *Genetica* **117**, 259–270 (2003).

51. Corona, D. F., Armstrong, J. A. & Tamkun, J. W. Genetic and cytological analysis of *Drosophila* chromatin-remodeling factors. *Methods Enzymol.* **377**, 70–85 (2004).
52. Blair, S. S. In *Drosophila Protocols* (eds Sullivan, W. *et al.*) 159–173 (Cold Spring Harbor Laboratory Press, 2000).
53. Brook, W. J. & Cohen, S. M. Antangonistic interactions between Wingless and Decapentaplegic responsible for dorsal-ventral pattern in the Drosophila leg. *Science* **273**, 1373–1377 (1996).
54. Fehon, R. G. *et al.* Molecular interactions between the protein products of the neurogenic *loci Notch* and *Delta*, two EGF-homologous genes in *Drosophila*. *Cell* **61**, 523–534 (1990).
55. Blochlinger, K., Bodmer, R., Jan, L. Y. & Jan, Y. N. Patterns of expression of Cut, a protein required for external sensory organ development in wild-type and *cut* mutant *Drosophila* embryos. *Genes Dev.* **4**, 1322–1331 (1990).
56. Ghattas, I. R., Sanes, J. R. & Majors, J. E. The encephalomyocarditis virus internal ribosome entry site allows efficient coexpression of two genes from a recombinant provirus in cultured cells and embryos. *Mol. Cell. Biol.* **11**, 5848–5859 (1991).
57. Agrawal, P. & Shashidhara, L. S. In *Hox Genes: Methods and Protocols* Vol. 1196 (eds Yacine, G. & René, R.) 241–253 (Springer Science+Business Media, 2014).
58. Schmittgen, T. D. & Livak, K. J. Analyzing real-time PCR data by the comparative *CT* method. *Nat. Protoc.* **3**, 1101–1108. https://doi.org/10.1038/nprot.2008.73 (2008).
59. Gustafson, K. & Boulianne, G. L. Distinct expression patterns detected within individual tissues by the GAL4 enhancer trap technique. *Genome* **39**, 174–182 (1996).
60. Hinz, U., Giebel, B. & Campos-Ortega, J. The basic-helix-loop-helix domain of *Drosophila* Lethal of Scute protein is sufficient for proneural function and activates neurogenic genes. *Cell* **76**, 77–87. https://doi.org/10.1016/0092-8674(94)90174-0 (1994).
61. Matsuda, S. & Affolter, M. Dpp from the anterior stripe of cells is crucial for the growth of the *Drosophila* wing disc. *eLife* https://doi.org/10.7554/eLife.22319 (2017).
62. Kassis, J. A., Noll, E., VanSickle, E. P., Odenwald, W. F. & Perrimon, N. Altering the insertional specificity of a *Drosophila* transposable element. *Proc. Natl. Acad. Sci. USA* **89**, 1919–1923 (1992).

Acknowledgements

We thank Jim Kennison for his valuable insights in the initial part of this work. We thank the Bloomington *Drosophila* Stock Center for providing stocks. We thank Carmen Muñoz and Laboratorio Nacional de Microscopía Avanzada, Instituto de Biotecnología, UNAM for technical assistance, and M. R.-V for drawings. This work was supported by funds from UNAM-PAPIIT IN202220 grant to M. V., CONACyT-Infraestructura No. 316070 to M. Z, and CONACyT-Ciencia de Frontera, FONIS Project No. 2280 to D. R-P., M. Z. and M. V. M. R.-V. is a Ph. D. student from Programa de Doctorado en Ciencias Bioquímicas, Universidad Nacional Autónoma de México (UNAM). M. R.-V. The investigation was carried out thanks to the Programa de Apoyo a Proyectos de Investigación e Innovación Tecnológica (PAPIIT) of UNAM IN202220. He thanks DGAPA-UNAM for his scholarship and also to the 307929 scholarship from CONACyT.

Author contributions

M.R.-V., M.V. and M.Z. conceived and designed the study. M.R.-V. and M.V. performed the formal experiments and analyses. M.R.-V. prepared the figures. M.V. and M.Z and D.R.-P provided the resources for the study. M.V. wrote the original manuscript. M.R.-V., M. V., M.Z. and D.R.-P reviewed and edited the manuscript. All authors read and approved the final manuscript.

Competing interests

The authors declare no competing interests.

Additional information

Supplementary Information The online version contains supplementary material available at https://doi.org/10.1038/s41598-023-42169-z.

Correspondence and requests for materials should be addressed to M.V.

Reprints and permissions information is available at www.nature.com/reprints.

Publisher's note Springer Nature remains neutral with regard to jurisdictional claims in published maps and institutional affiliations.

Supplementary figures

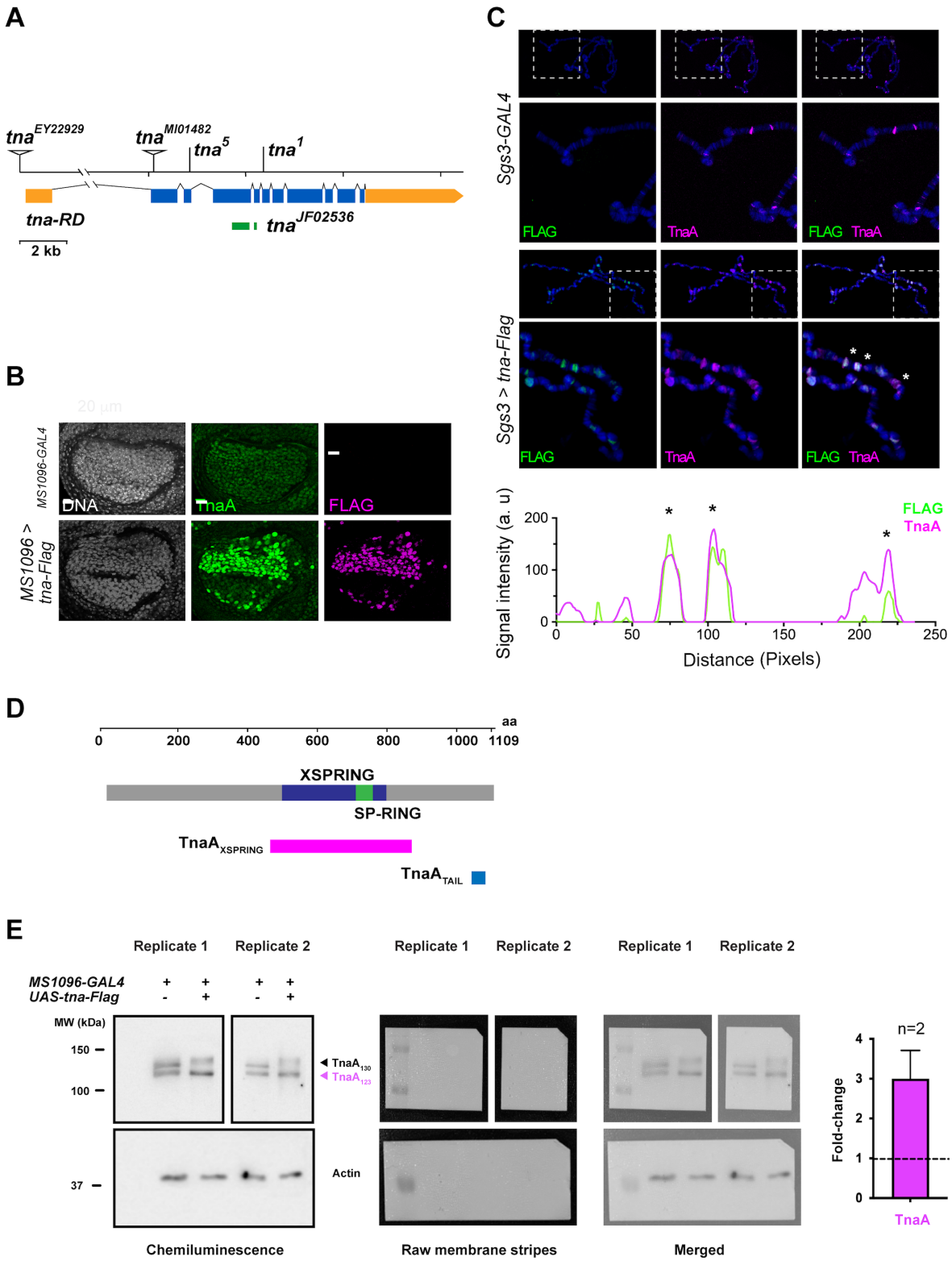

Sup. Fig. 1. *tna* mutant alleles, antibodies, and expression of *tna-Flag* in imaginal disc cells. (**A**) *tna* genomic region of the *tna-RD* transcript, (untranslated and translated exons in yellow and blue, respectively), indicating the lesions (triangle for insertion and vertical black lines for point mutations) and the $tna^{JF02536}$ RNAi (target region, green) used in this work. (**B**) Endogenous TnaA and TnaA-Flag localize to the nuclei of imaginal disc cells. Immunostaining of TnaA (anti-$TnaA_{TAIL}$ antibody, green) and TnaA-Flag (anti-FLAG antibody, magenta) driven by *MS1096-GAL4*, compared to *MS1096-GAL4* haltere discs (upper panel). (**C**) TnaA and TnaA-Flag colocalize in polytene chromosome bands. The endogenous TnaA signal detected with the anti-$TnaA_{XSPRING}$ antibody (magenta) is shown in *Sgs3-GAL4* polytene chromosomes (*Sgs3-GAL4* panels, amplified region indicated by a dashed square). The colocalization of TnaA, and TnaA-Flag (FLAG antibody, green) driven by *Sgs3-GAL4* is shown in *Sgs3>tna-Flag* panels. To assess the colocalization of bands detected with anti-$TnaA_{XSPRING}$ and anti-FLAG antibodies, we traced the signal intensity along a line in a chromosomal region (dashed square, *Sgs3>tna-Flag* panels) with the ImageJ plot profile tool and represented the data in a graph (bottom panel). (**D**) $TnaA_{123}$ protein (grey, 1109 residues) indicating the XSPRING (purple) and SP-RING (green). The regions targeted by the polyclonal antibodies are shown, $TnaA_{XSPRING}$ (pink) and $TnaA_{TAIL}$ (blue). (**E**) Western blot analysis of *MS1096>tna-Flag* wing discs compared to control *MS1096* wing discs. To quantify the changes in TnaA between the *MS1096* and *MS1096>tna-Flag* wing discs, the full-length blot membrane with samples from two independent biological replicas, was cut into two membrane stripes to immunodetect TnaA with the anti-$TnaA_{XSPRING}$ (upper panels), and one stripe to immunodetect actin as a loading control from replicas 1 and 2 (lower panel). Each set of corresponding TnaA and actin images shown in replica 1 and 2, come from the same gel lanes and they were processed in parallel. After immunodetection, chemiluminescent images were acquired with the ChemiDoc imaging system (BioRad). Chemiluminescence images (left), raw membrane stripes (center) and the merged images of both replicas (right) are shown. The experiment was performed by duplicate, showing at least a three-fold increase in TnaA-Flag levels (magenta bar).

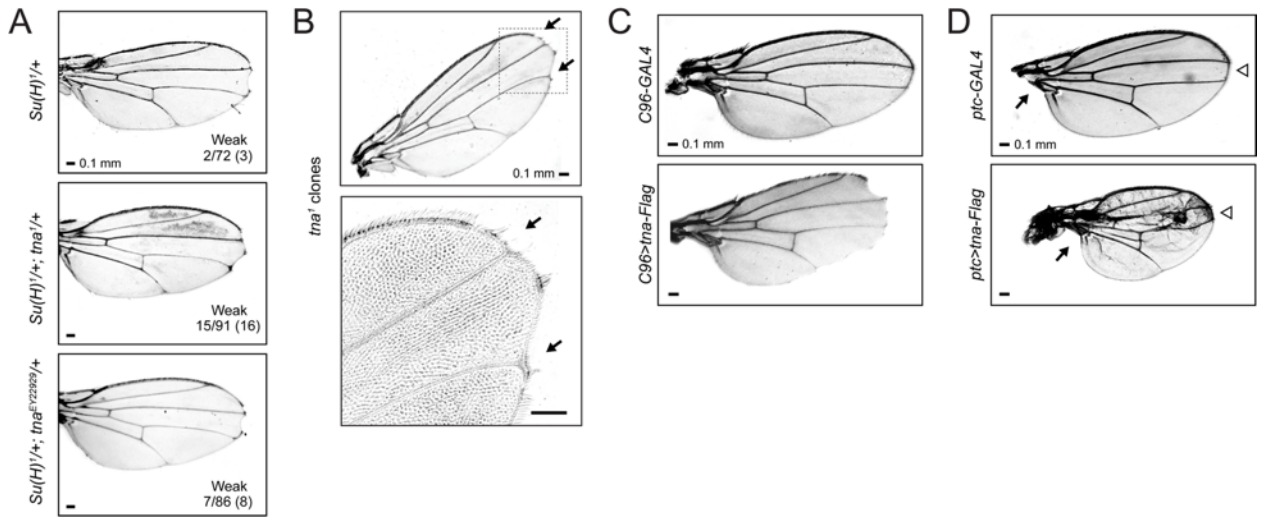

Sup. Fig. 2. Adult wings derived from experiments in this study. (**A**) Genetic interaction of *tna* with *Su(H). Su(H)*^{1} wings alone or in combination with *tna* alleles (*tna*^{1} and *tna*^{EY22929}). *tna*^{1} and *tna*^{EY22929} wings do not have notching, while *Su(H)*/+; *tna/*+ transheterozygotes have notched wings. The penetrance and expressivity of the notched-wings phenotype are indicated in Table 1. (**B**) Adult wings with notches from animals in which *tna*^{1} clones of the wings discs were induced. The lower panel shows an amplification of the observed notches. (**C**) The expression of *tna-Flag* driven by *C96-GAL4* (lower) causes strong notching in adult wings compared to the *C96-GAL4* control (upper); (**D**) *ptc-GAL4* (upper) and *ptc>tna-Flag* adult wings (lower), indicating the hinge (arrow) and the D/V boundary (empty arrowhead).

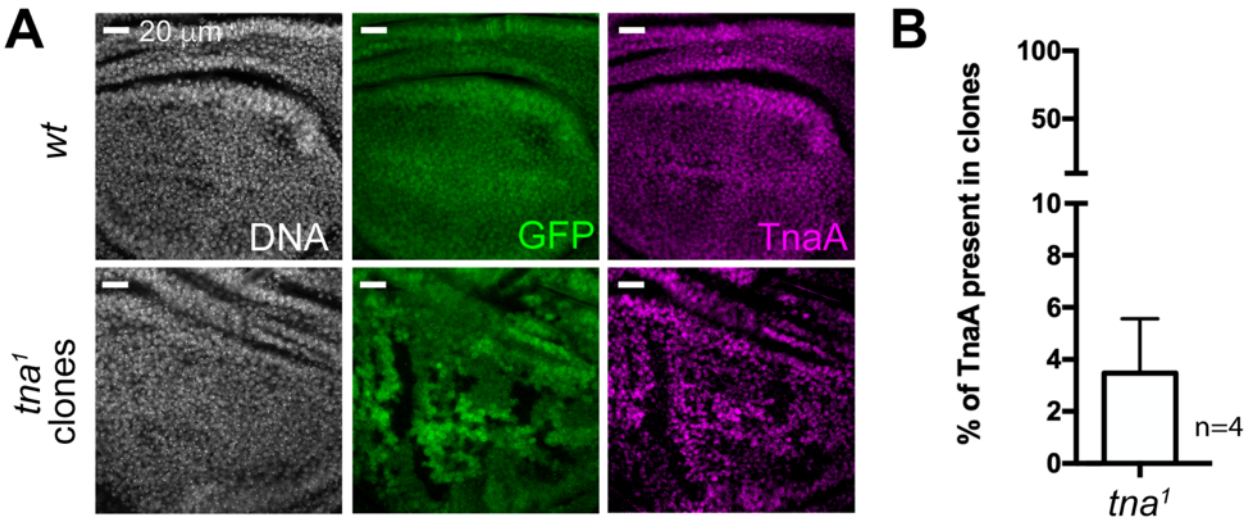

Sup. Fig. 3. TnaA signal in *tna*^{1} clones. (**A**) Mitotic clones (non-GFP cells) were induced with *Ubx-FLP* in wing imaginal discs. DNA, TnaA (magenta), and GFP (green) are shown. (**B**) *tna*^{1} clones show only 5% of the wild-type TnaA signal when immunostained with the anti-TnaA$_{TAIL}$ antibody.

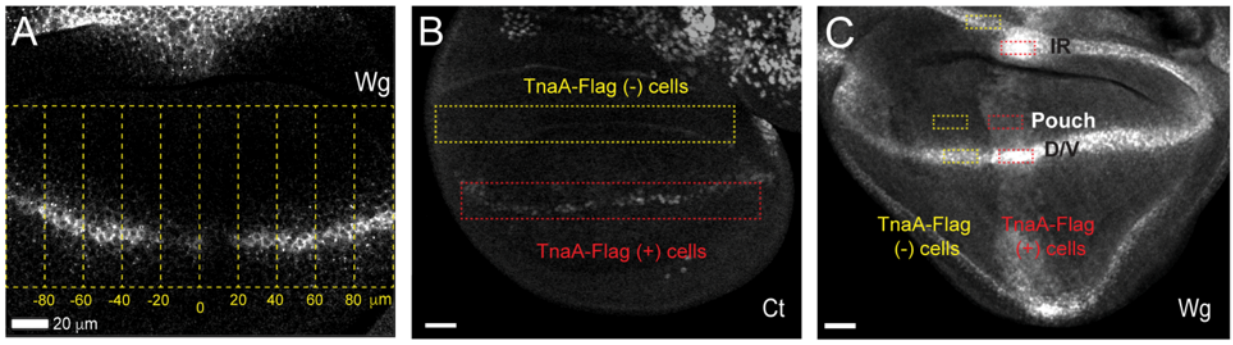

Sup. Fig. 4. Quantification of Wingless and Cut signal intensities in immunostainings of wing imaginal discs. (**A**) Example of a N^{55e11}/+; tna^{1}/+ wing disc divided into 10 regions (20 µm in width) along the *wg* D/V boundary domain. These regions allow quantification of the Wingless signal around the center of the D/V boundary compared to the Wingless signal found in a similar region in a wild-type disc. (**B**) Example of quantification of Cut signal intensity in a *C96>tna-Flag* wing disc. To make an accurate quantification of the signal, we normalized the Cut signal intensity by subtracting the signal in the TnaA-Flag (-) cells from the signal obtained in TnaA-Flag (+) cells. (**C**) Example of quantification of the intensity of the Wingless signal in a *ptc>tna-Flag* wing disc. Signal intensity was normalized as in (**B**) for each of the D/V, IR, and pouch regions.

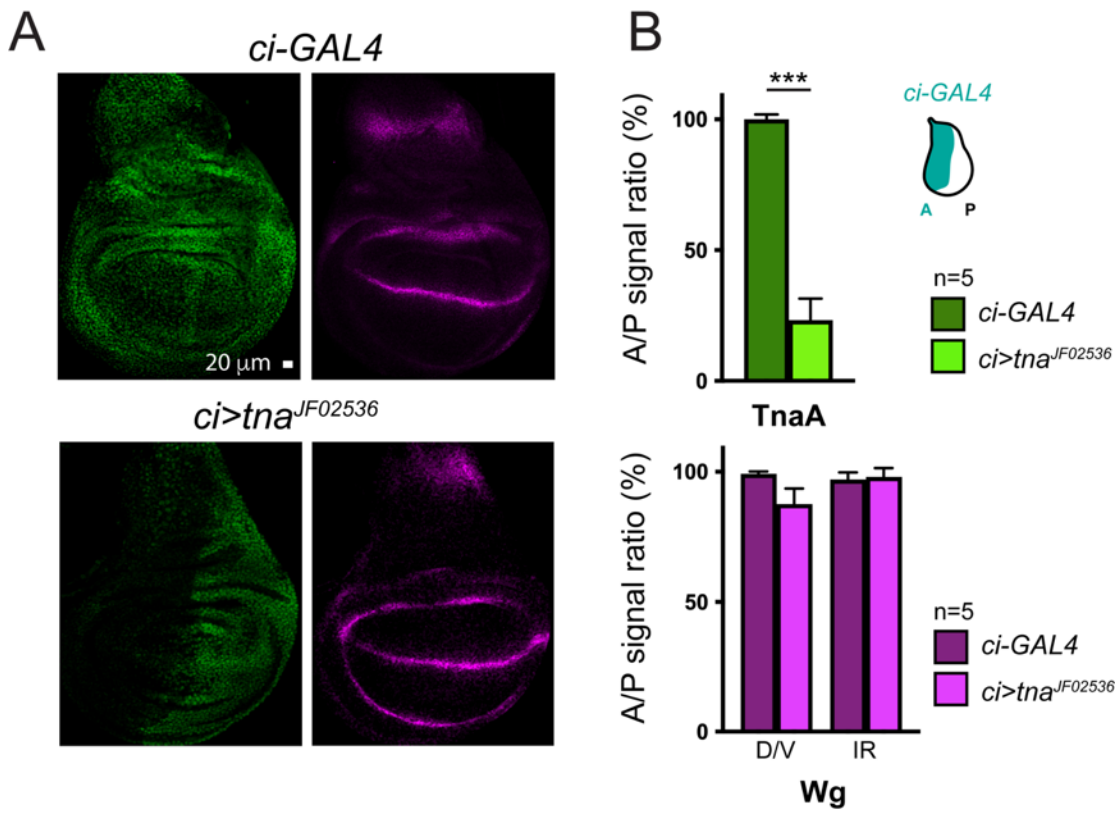

Sup. Fig. 5. Effectiveness of TnaA knockdown and its effect on Wingless signal in the D/V and IR regions. (**A**) TnaA (green) was knockdowned in the anterior compartment by the expression of a RNAi from the *tna*^{JF25036} allele driven by the *ci-GAL4*. Wingless signal (magenta) was analyzed in this genotype. (**B**) Quantification of the A/P signal ratio of TnaA (upper panel) and Wingless (lower panel). Note that on average TnaA is reduced to 20% of the wild type signal compared to 5% of the signal observed in *tna*^{1} clones from Sup. Fig. 3. Student's *t*-test was performed for A/P signal ratios ($P<0.001^{***}$).

6. DISCUSIÓN ADICIONAL

6.1 La regulación de la expresión de *tna* durante el desarrollo

En este trabajo encontramos que las isoformas $TnaA_{123}$ y $TnaA_{130}$ proceden de distintos transcritos (*RD* y *RA*, respectivamente). Es probable que ambas isoformas se regulen de manera diferencial durante el desarrollo. De hecho, el análisis de los promotores de *tna* en bases de datos experimentales del EPD ("Eukaryotic Promoter Database", Meylan et al., 2020), muestra que el promotor del transcrito *RA* es un promotor "enfocado" y contiene un motivo DPE, el cual está presente en diversos genes regulados durante el desarrollo (revisado en Sloutskin et al., 2021), mientras que el promotor del transcrito *RD* es "disperso".

Estudios de proteómica en diversos modelos muestran que miles de proteínas son ubiquitinadas por cientos de E3 ligasas de ubiquitina (Li et al., 2008). En contraste, cientos a miles de proteínas son SUMOiladas en un momento dado (Hendriks y Vertegaal, 2016), a pesar de que solo se han identificado alrededor de una decena de genes que codifican E3 ligasas de SUMO. Por lo tanto, la especificidad de las E3 ligasas de SUMO puede depender de otras estrategias, por ejemplo, de la regulación de la expresión de múltiples isoformas codificadas por un solo gen (revisado en Pichler et al., 2017).

Nosotros mostramos que *tna* codifica al menos dos transcritos que resultan en la expresión de dos isoformas proteicas distintas (Rosales-Vega et al., 2018). Las isoformas $TnaA_{123}$ y $TnaA_{130}$ provienen de transcritos distintos y poseen promotores diferentes, lo que permite que su expresión se regule de manera diferencial en tiempo y espacio durante el desarrollo. Por lo tanto, es probable que cada isoforma regule blancos específicos al modularse su localización espacio-temporal.

Para que TnaA favorezca la SUMOilación de sus blancos, es probable que deba coexistir con sus interactores en un ambiente donde la vía de SUMOilación esté activa. El papel de cada isoforma de TnaA depende de que se localice en el lugar apropiado en el tiempo y espacio. Una forma de regular la unión de TnaA con sus interactores es modulando su localización subcelular. Una posibilidad es que las isoformas de TnaA se unan a otras proteínas mediante su región amino terminal diferencial, lo anterior podría explicar por qué durante la embriogénesis $TnaA_{130}$ es citoplásmica, mientras que $TnaA_{123}$ es preferentemente nuclear (Monribot-Villanueva et al., 2013). Esto sugiere que si los interactores cambian durante el desarrollo también podría cambiar la distribución subcelular. Otra posibilidad es que se regule la estabilidad o la localización de los transcritos de *tna* mediante sus regiones 3' y 5' UTR diferenciales, favoreciendo así la presencia de cierta isoforma de TnaA en distintas regiones subcelulares, como se ha reportado en otras proteínas durante el desarrollo de *D. melanogaster* (Chekulaeva et al., 2006). Un análisis tejido-específico de los transcritos durante el desarrollo podría ayudar a comprender si la abundancia de las isoformas de TnaA juega un papel crucial en ciertos tejidos.

6.2 Los posibles interactores de TnaA en la cromatina

TnaA es una E3 ligasa de SUMO que interacciona físicamente con el complejo BRAHMA y con enzimas de la vía de SUMOilación (Monribot-Villanueva et al., 2013) y, por lo tanto, las subunidades de este remodelador son interactores de TnaA, pero no son los únicos. TnaA no tiene un dominio de unión a DNA, sino que se une indirectamente al interaccionar con proteínas de la cromatina. Actualmente no hay evidencias que sugieran que TnaA tiene un dominio de unión a DNA (Gutiérrez et al., 2003; Monribot-Villanueva et al., 2013).

Es probable que TnaA funcione como un cofactor transcripcional al favorecer la SUMOilación de proteínas de la cromatina como FTs, enzimas modificadoras o histonas que se encuentran en regiones regulatorias específicas. Aunque no podemos descartar la posibilidad de que TnaA posea algún dominio desconocido que le permita actuar como un cofactor independiente de la vía de SUMOilación, como se ha descrito en otras E3 ligasas de SUMO (revisado en Sharrocks, 2006). En humanos, las proteínas ZMIZ1 y ZMIZ2 son E3 ligasas de SUMO que poseen un dominio XSPRING altamente conservado y se ha reportado que poseen alrededor de un 60% de homología con el XSPRING de TnaA (Gutiérrez et al., 2003). Sin embargo, estas proteínas presentan otros dominios que no están presentes en TnaA, como un dominio TPR (de 34 aminoácidos) y regiones ricas en prolina y arginina (revisado en Lomelí, 2022). Los alineamientos de TnaA con estas proteínas muestran que no posee estos dominios. Los únicos dominios descritos de TnaA en la región amino-terminal son sus regiones de poli-glutamina (pQ) (Figura 3). Sin embargo, una posibilidad es que las E3 ligasas de SUMO usen estos dominios localizados alrededor del XSPRING para estabilizar su interacción con otras proteínas (ver más adelante).

Para saber cuál es el papel de TnaA en la cromatina, realizamos experimentos de ChIP-seq con la cromatina de glándulas salivales y discos de ala de larvas de tercer instar de *D. melanogaster* (datos no publicados). En congruencia con nuestros datos de inmunotinción de TnaA en cromosomas politénicos, en los datos obtenidos mediante ChIP-seq encontramos que TnaA se encuentra en la cromatina de alrededor de 100 sitios del genoma de cada uno de los tejidos analizados. Además, es notorio que no todos los sitios son compartidos en las muestras de los tejidos analizados, lo que indica que la localización de TnaA en la cromatina de diferentes regiones genómicas es específica. Por otro lado, no todos los genes en cuya cromatina se encuentra TnaA se expresan en los tejidos analizados, lo cual sugiere que TnaA podría estar relacionado tanto con activadores como con represores de la transcripción.

TnaA posee un dominio SP-RING, el cual es característico de un tipo de E3 ligasas de SUMO. Las E3 ligasas de SUMO permiten la SUMOilación especifica de un grupo reducido de blancos al aumentar la especificidad de la enzima E2 (revisado en

Pichler et al., 2017). Hasta ahora no sabemos si la capacidad de TnaA de unirse a la cromatina y/o de regular a sus genes blanco está ligada a su actividad de E3 ligasa de SUMO, por lo que sería interesante generar una mutante en el dedo de zinc del XSPRING de *tna* para analizar dichas funciones. El papel de TnaA en la cromatina de los promotores aún no está claro, sin embargo, se ha mostrado que la SUMOilación es importante para el recambio de algunos FTs (revisado en Rosonina et al., 2017). Por lo tanto, dado que es una E3 ligasa de SUMO, es probable que TnaA participe en algún mecanismo para modular la expresión de los genes donde se encuentra al permitir el recambio entre activadores/represores (ver adelante) y/o al interaccionar con la maquinaria transcripcional en asas conformadas por las regiones promotor-"enhancer".

TnaA también se encuentra en algunas regiones intergénicas que son posibles "enhancers". En este trabajo se demostró que TnaA modula la expresión de *wg* en el límite D/V y el IR del disco de ala. Estos experimentos se hicieron disminuyendo las dosis de ambas isoformas de TnaA. Dado que las isoformas podrían tener funciones particulares (Rosales-Vega et al., 2018), sería interesante explorar el papel de cada una de las isoformas en la expresión de *wg* en el disco de ala.

En el límite D/V, *wg* es regulado por la vía de Notch (revisado en Bray, 2006). El complejo efector de la vía de Notch (conocido como complejo CSL) está formado por el dominio intracelular de Notch (NICD), Suppressor de Hairless [Su(H)], Mastermind (Mam) y diversos coactivadores o correpresores. Los genes que se regulan por este complejo responden de manera diferencial dependiendo del contexto de cada "enhancer". Para explicar este fenómeno se planteó inicialmente el modelo de interruptor, donde los "enhancers" se clasificaron como permisivos o instructivos a NICD (revisado en Bray y Furriols, 2001). Este modelo se refinó más tarde al analizar la unión de Notch y Su(H) a la cromatina (Djiane et al., 2013) y con estudios sobre la dinámica de unión de las subunidades del complejo a los "enhancers" (Gomez-Lamarca et al., 2018; Falo-Sanjuan et al., 2019). Con estos datos, surgió un modelo más refinado, donde la unión del NICD al "enhancer" depende del tiempo de permanencia de algunos cofactores, de que ciertas proteínas se unan previamente a los "enhancers" (fenómeno conocido como "priming" del "enhancer") y del paisaje de la cromatina. Dado que TnaA es importante para la expresión de *wg* a través del *IRE*, es probable que TnaA permita el recambio de activadores y/o represores para modular de manera precisa la transcripción de *wg* en el disco de ala. Una posibilidad es que TnaA favorezca la SUMOilación de las subunidades del complejo CSL, alterando la estequiometría y/o función del complejo de manera similar a la ganancia de función de Su(H) (Furriols y Bray, 2000).

Además, TnaA posee al menos dos regiones ricas en pQ en su región amino terminal (Gutiérrez et al., 2003). Las regiones ricas en pQ largas poseen una alta plasticidad estructural (revisado en Barbosa Pereira et al., 2023) y son cruciales para aumentar la estabilidad de las interacciones proteína-proteína (revisado en Atanesyan

et al., 2012). Se ha reportado que las regiones ricas en pQ suelen estar ubicadas cerca de “coiled-coils”, las cuales son estructuras de interacción proteína-proteína. Lo anterior sugiere que las regiones ricas en pQ permiten extender la longitud de los “coiled-coils” para aumentar la estabilidad de ciertas interacciones intra- e inter-moleculares (Fiumara et al., 2010). Aunque no se ha analizado experimentalmente si TnaA tiene estructuras tipo “coiled-coil” cerca de sus regiones ricas en pQ, una posibilidad es que estas regiones permitan estabilizar la unión con sus interactores. Por ejemplo, TnaA podría interaccionar con proteínas del complejo CSL, cuyos interactores poseen múltiples regiones ricas en pQ (Stroebele y Erives, 2016).

La formación de algunos organelos sin membranas en la célula depende de interacciones débiles que resultan en la formación de condensados biomoleculares causados por una separación de fases líquido-líquido. TnaA podría participar en la formación de condensados biomoleculares dentro de la célula con ayuda de sus regiones ricas en pQ y/o al favorecer la SUMOilación de sus blancos. Se sabe que la SUMOilación es importante para la formación de diversos organelos nucleares sin membrana que están involucrados en la regulación de la transcripción y el mantenimiento de la estabilidad del genoma (revisado en Banani et al., 2017). Estudios *in vitro* e *in vivo* han mostrado que las proteínas con múltiples tractos de SUMO (poli-SUMO) en conjunto con proteínas que tienen dominios de interacción con SUMO (poli-SIM) pueden formar condensados biomoleculares (Banani et al., 2016). Es probable que la SUMOilación mediada por TnaA, además de regular la transcripción de sus genes blanco, sea crucial para generar condensados biomoleculares, estabilizando su formación mediante sus regiones ricas en pQ.

Ya que TnaA y las subunidades del complejo CSL de *D. melanogaster* tienen ortólogos en otros organismos multicelulares, incluido el ser humano, los hallazgos en este trabajo contribuyen a la comprensión de elementos adicionales que modulan la complejidad funcional que gobierna a este complejo. Por ejemplo, se ha reportado que la función del complejo CSL modularse por la SUMOilación de Notch1 en células epiteliales (Zhu et al., 2017; Antila et al., 2018) y que un homólogo de TnaA en humanos (ZMIZ1) interacciona con Notch1 durante el desarrollo temprano de los linfocitos T (Wang et al., 2018). Los modelos computacionales sugieren que una forma SUMOilada del NICD pueden ser parte de complejo CSL [Su(H)-NICD-Mam] y unirse de manera estable al DNA (Antila et al., 2018), en este modelo, el receptor Notch SUMOilado podría reclutar FTs o enzimas modificadoras.

Otra posibilidad es que TnaA interaccione en algún circuito donde estén involucradas histonas con alguna modificación específica o con las enzimas modificadoras que depositan dichas marcas. En *D. melanogaster*, la histona acetiltransferasa *chameau* es responsable de depositar la marca H3K14Ac, la cual reconoce directamente el complejo BRAHMA (Regadas et al., 2021). La reducción de los niveles de *chameau* tiene el mismo efecto sobre *wg* que el observado por la expresión de la TnaA-Flag, lo cual sugiere que TnaA podría estar involucrada en la

regulación de la expresión de los blancos del complejo CSL al participar en el mecanismo de deposición de marcas epigéneticas o al modular la apertura de la cromatina en regiones regulatorias específicas.

6.3 El papel de TnaA en el desarrollo de *D. melanogaster.*

tna es un gen esencial en etapas tardías del desarrollo de *D. melanogaster*. La pérdida de función de *tna* causa fenotipos desde estadios larvarios que incluyen, además de la letalidad, defectos en el desarrollo de los discos imagales como lo son las transformaciones homeóticas o defectos en la formación de patrones ("patterning"). Muchas de las cascadas transcripcionales que se presentan en los discos imagales se entrecruzan, por ejemplo, las desencadenadas por los genes Hox y por los genes de "patterning" (como *wg*). Por lo tanto, muchos de los mecanismos que regulan a todos estos genes pueden tener elementos comunes. TnaA podría participar en los mecanismos que se requieran para el recambio de proteínas que actúan en sitios específicos del genoma. Es por ello que los experimentos de ChIP-seq muestran que TnaA se encuentra en promotores y "enhancers" de diferentes genes. En el caso de *wg*, TnaA regula su expresión de manera "enhancer"-específica en una región particular del disco de ala. Una posibilidad es que señales transitorias permitan que TnaA favorezca la SUMOilación de sus interactores localizados en los "enhancers" y/o en promotores de manera etapa- y/o tejido-específica, permitiendo así su activación o represión durante momentos cruciales del desarrollo. Se ha reportado que la SUMOilación de múltiples proteínas ocurre en oleadas para regular programas genéticos complejos de manera coordinada durante el desarrollo, como en el caso de la proliferación y la diferenciación de distintos tipos celulares (Paakinaho et al., 2021; Zhao et al., 2022). En vertebrados, algunas hormonas provocan cambios en la selección de "enhancers" activos, lo cual permite la SUMOilación simultanea de varios FTs unidos al DNA para activar o reprimir la expresión desencadenada por glucocorticoides (Paakinaho et al., 2021), andrógenos (Dufour et al., 2022) o durante la diferenciación de adipocitos (Zhao et al., 2022). Queda como un desafío determinar el papel que ejerce TnaA sobre sus interactores para modular la expresión de sus genes blanco en el tiempo y espacio, en la intrincada red de regulación de estos "enhancers".

7. CONCLUSIONES

Sobre las isoformas de TnaA:

1. Las isoformas $TnaA_{123}$ y $TnaA_{130}$ provienen de los transcritos *tna-RD* y *tna-RA,* respectivamente.

2. Evidencias genéticas sugieren que $TnaA_{123}$ es esencial para alcanzar las etapas

tardías del desarrollo mientras que $TnaA_{130}$ es dispensable en estas etapas.

Sobre la función de TnaA:

1. Modula la expresión de *Ubx* y *Scr* en los discos imagales por lo menos desde la etapa de larvas de tercer estadío.

2. Regula la expresión de *wg* específicamente en el límite D/V y el IR del disco de ala.

3. Se encuentra en el *IRE* para modular la expresión de *wg* en el IR.

8. PERSPECTIVAS

1. Analizar los datos de ChIP-seq para determinar la localización genómica de TnaA en la cromatina de los tejidos de interés en diversas etapas de *D. melanogaster.*

2. Determinar los posibles FTs con los que interacciona TnaA en la cromatina buscando motivos de unión a DNA de dichos FTs en las regiones de cromatina donde se une TnaA de manera indirecta.

3. Realizar un análisis tejido-específico de los transcritos de *tna* durante el desarrollo con los datos de RNA-seq en célula única de discos de ala (Everetts et al., 2021), embriones (Calderon et al., 2022) y adultos (Li et al., 2022).

4. Buscar interactores de TnaA mediante fluorescencia de complementación bimolecular (revisado en Kerppola, 2008), para encontrar proteínas que interaccionen con ella tanto en la cromatina como en el citoplasma.

9. REFERENCIAS ADICIONALES

Antila C. J. M., Rraklli V., Blomster H. A., Dahlström K. M., Salminen T.A., Holmberg J., Sistonen L. y Sahlgren C. (2018). SUMOylation of Notch1 represses its target gene expression during cell stress. *Cell Death Differentiation* **25**, 600-615.

Atanesyan, L., Günther, V., Dichtl, B., Georgiev, O. y Schaffner, W. (2012). Polyglutamine tracts as modulators of transcriptional activation from yeast to mammals. *Biological Chemistry* **393**, 63-70.

Banani, S. F., Lee, H. O., Hyman, A. A. y Rosen, M. K. (2017). Biomolecular condensates: organizers of cellular biochemistry. *Nature Reviews Molecular Cell Biology* **18**, 285-298.

Banani, S. F., Rice, A. M., Peeples, W. B., Lin, Y., Jain, S., Parker, R. y Rosen, M. K. (2016). Compositional control of phase-separated cellular bodies. *Cell* **166**, 651-663.

Barbosa Pereira, P. J., Manso, J. A. y Macedo-Ribeiro, S. (2023). The structural plasticity of polyglutamine repeats. *Current Opinion in Structural Biology* **80**, 1-11.

Bray, S. y Furriols, M. (2001). Notch pathway: making sense of *suppressor of hairless*. *Current Biology* **11**, 217-221.

Bray, S. J. (2006). Notch signalling: a simple pathway becomes complex. *Nature Reviews Molecular Cell Biology* **7**, 678-689.

Bryant, P. J. (1975). Pattern formation in the imaginal wing disc of *Drosophila melanogaster*: fate map, regeneration and duplication. *Journal of Experimental Zoology* **193**, 49-77.

Calderon, D., Blecher-Gonen, R., Huang, X., Secchia, S., Kentro, J., Daza, R. M., Martin, B., Dulja, A., Schaub, C., Trapnell, C., et al. (2022). The continuum of *Drosophila* embryonic development at single-cell resolution. *Science* **377**, 1-12.

Chalkley, G. E., Moshkin, Y. M., Langenberg, K., Bezstarosti, K., Blastyak, A., Gyurkovics, H., Demmers, J. A. y Verrijzer, C. P. (2008). The transcriptional coactivator SAYP is a trithorax group signature subunit of the PBAP chromatin remodeling complex. *Molecular and Cellular Biology* **28**, 2920-2929.

Chekulaeva, M., Hentze, M. W. y Ephrussi, A. (2006). Bruno acts as a dual repressor of *oskar* translation, promoting mRNA oligomerization and formation of silencing particles. *Cell* **124**, 521-533.

Clark, E., Peel, A. D. y Akam, M. (2019). Arthropod segmentation. *Development* **146**, 1-16.

del Alamo-Rodríguez, D., Terriente, J., Galindo, M. I., Couso, J. P. y Díaz-Benjumea, F. J. (2002). Different mechanisms initiate and maintain *wingless* expression in the *Drosophila* wing hinge. *Development* **129**, 3995-4004.

Djiane, A., Krejci, A., Bernard, F., Fexova, S., Millen, K. y Bray, S. J. (2013). Dissecting the mechanisms of Notch induced hyperplasia. *The EMBO Journal* **32**, 60-71.

Dufour, D., Dumontet, T., Sahut-Barnola, I., Carusi, A., Onzon, M., Pussard, E., Wilmouth, J. J., Olabe, J., Lucas, C., Levasseur, A., Damon-Soubeyrand, C., Pointud, J. C., Roucher-Boulez, F., Tauveron, I., Bossis, G., Yeh, E. T., Breault, D. T., Val, P., Lefrançois-Martinez, A. M. y Martinez, A. (2022). Loss

of SUMO-specific protease 2 causes isolated glucocorticoid deficiency by blocking adrenal cortex zonal transdifferentiation in mice. *Nature Communications* **13**, 1-18.

Everetts, N. J., Worley, M. I., Yasutomi, R., Yosef, N. y Hariharan, I. K. (2021). Single-cell transcriptomics of the *Drosophila* wing disc reveals instructive epithelium-to-myoblast interactions. *Elife* **10**, 1-25.

Falo-Sanjuan, J., Lammers, N. C., Garcia, H. G. y Bray, S. J. (2019). Enhancer priming enables fast and sustained transcriptional responses to Notch signaling. *Developmental Cell* **50**, 411-425.

Fiumara, F., Fioriti, L., Kandel, E. R., y Hendrickson, W. A. (2010). Essential role of coiled coils for aggregation and activity of Q/N-rich prions and PolyQ proteins. *Cell* **143**, 1121-1135.

Furriols, M. y Bray, S. (2000). Dissecting the mechanisms of Suppressor of Hairless function. *Developmental Biology* **227**, 520-532.

Galouzis, C. C., y Furlong, E. E. M. (2022). Regulating specificity in enhancer-promoter communication. *Current Opinion in Cell Biology* ***75***, 1-11.

Gomez-Lamarca, M. J., Falo-Sanjuan, J., Stojnic, R., Abdul Rehman, S., Muresan, L., Jones, M. L., Pillidge, Z., Cerda-Moya, G., Yuan, Z., Baloul, S., et al. (2018). Activation of the Notch signaling pathway *in vivo* elicits changes in CSL nuclear dynamics. *Developmental Cell* **44**, 611-623.

Gutiérrez, L., Zurita, M., Kennison, J. A. y Vázquez, M. (2003). The *Drosophila* trithorax group gene *tonalli* (*tna*) interacts genetically with the Brahma remodeling complex and encodes an SP-RING finger protein. *Development* **130**, 343-354.

Hendriks, I. A., y Vertegaal, A. C. (2016). A comprehensive compilation of SUMO proteomics. *Nature reviews. Molecular cell biology* **17**, 581-595.

Hendriks, I. A., Lyon, D., Young, C., Jensen, L. J., Vertegaal, A. C., y Nielsen, M. L. (2017). Site-specific mapping of the human SUMO proteome reveals co-modification with phosphorylation. *Nature Structural & Molecular Biology* **24**, 325-336.

Kassis, J. A., Kennison, J. A. y Tamkun, J. W. (2017). Polycomb and trithorax Group genes in *Drosophila*. *Genetics* **206**, 1699-1725.

Kaufman, T. C., Seeger, M. A. y Olsen, G. (1980). Molecular and genetic organization of the *Antennapedia* gene complex of *Drosophila melanogaster*. *Advances in Genetics* **27**, 309-362.

Kerppola T. K. (2008). Bimolecular fluorescence complementation (BiFC) analysis as a probe of protein interactions in living cells. *Annual review of biophysics* **37**, 465-487.

Kopan, R. e Ilagan, M. X. (2009). The canonical Notch signaling pathway: unfolding the activation mechanism. *Cell* **137**, 216-233.

Lewis, E. B. (1978). A gene complex controlling segmentation in *Drosophila*. *Nature* **276**, 565-570.

Li, H., Janssens, J., De Waegeneer, M., Kolluru, S. S., Davie, K., Gardeux, V., Saelens, W., David, F. P. A., Brbić, M., Spanier, K., et al. (2022). Fly Cell Atlas: A single-nucleus transcriptomic atlas of the adult fruit fly. *Science* **375**, 1-12.

Li, W., Bengtson, M. H., Ulbrich, A., Matsuda, A., Reddy, V. A., Orth, A., Chanda, S. K., Batalov, S., y Joazeiro, C. A. (2008). Genome-wide and functional annotation of human E3 ubiquitin ligases identifies MULAN, a mitochondrial E3 that regulates the organelle's dynamics and signaling. *PLOS ONE* **3**, 1-14

Lomelí, H. y Vázquez, M. (2011). Emerging roles of the SUMO pathway in development. *Cellular and Molecular Life Sciences* **68**, 4045-4064.

Lomelí H. (2022). ZMIZ proteins: partners in transcriptional regulation and risk factors for human disease. *Journal of molecular medicine (Berlin, Germany)* **100**, 973-983.

Meylan, P., Dreos, R., Ambrosini, G., Groux, R., y Bucher, P. (2020). EPD in 2020: enhanced data visualization and extension to ncRNA promoters. *Nucleic acids research* **48**, D65-D69.

Mohrmann, L., Langenberg, K., Krijgsveld, J., Kal, A. J., Heck, A. J. y Verrijzer, C. P. (2004). Differential targeting of two distinct SWI/SNF-related *Drosophila* chromatin-remodeling complexes. *Molecular and Cellular Biology* **24**, 3077-3088.

Monribot-Villanueva, J., Juárez-Uribe, R. A., Palomera-Sánchez, Z., Gutiérrez-Aguiar, L., Zurita, M., Kennison, J. A. y Vázquez, M. (2013). TnaA, an SP-RING protein, interacts with Osa, a subunit of the chromatin remodeling complex BRAHMA and with the SUMOylation pathway in *Drosophila melanogaster*. *PLOS ONE* **8**, 1-12.

Paakinaho, V., Lempiäinen, J. K., Sigismondo, G., Niskanen, E. A., Malinen, M., Jääskeläinen, T., Varjosalo, M., Krijgsveld, J. y Palvimo, J. J. (2021). SUMOylation regulates the protein network and chromatin accessibility at glucocorticoid receptor-binding sites. *Nucleic Acids Research* **49**, 1951-1971.

Panigrahi, A., y O'Malley, B. W. (2021). Mechanisms of enhancer action: the known and the unknown. *Genome Biology* **22**, 1-30.

Pearson, J. C., Lemons, D. y McGinnis, W. (2005). Modulating Hox gene functions during animal body patterning. *Nature Reviews Genetics* **6**, 893-904.

Pichler, A., Fatouros, C., Lee, H., y Eisenhardt, N. (2017). SUMO conjugation - a mechanistic view. *Biomolecular Concepts* **8**, 13-36.

Regadas, I., Dahlberg, O., Vaid, R., Ho, O., Belikov, S., Dixit, G., Deindl, S., Wen, J. y Mannervik, M. (2021). A unique histone 3 lysine 14 chromatin signature underlies tissue-specific gene regulation. *Molecular Cell* **81**, 1766-1780.

Rodriguez, M. S., Dargemont, C. y Hay, R. T. (2001). SUMO-1 conjugation *in vivo* requires both a consensus modification motif and nuclear targeting. *Journal of Biological Chemistry* **276**, 12654-12659.

Rosales-Vega, M., Hernández-Becerril, A., Murillo-Maldonado, J. M., Zurita, M. y Vázquez, M. (2018). The role of the trithorax group TnaA isoforms in Hox gene expression, and in *Drosophila* late development. *PLOS ONE* **13**, 1-22.

Rosales-Vega, M., Reséndez-Pérez, D., Zurita, M. y Vázquez, M. (2023). TnaA, a trithorax group protein, modulates *wingless* expression in different regions of the *Drosophila* wing imaginal disc. *Scientific Reports* **13**, 1-13.

Rosonina, E., Akhter, A., Dou, Y., Babu, J. y Sri Theivakadadcham, V. S. (2017). Regulation of transcription factors by SUMOylation. *Transcription* **8**, 220-231.

Sánchez-Herrero, E. (2013). Hox targets and cellular functions. *Scientifica (Cairo)* **2013**, 1-26.

Schubiger, G., Schubiger, M. y Sustar, A. (2012). The three leg imaginal discs of *Drosophila*: "Vive la différence". *Developmental Biology* **369**, 76-90.

Sharrocks A. D. (2006). PIAS proteins and transcriptional regulation - more than just SUMO E3 ligases?. *Genes & Development **20***, 754-758.

Sloutskin, A., Shir-Shapira, H., Freiman, R. N. y Juven-Gershon, T. (2021). The core promoter Is a regulatory hub for developmental gene expression. *Frontiers in Cell and Developmental Biology* **9**, 1-11.

Stroebele, E. y Erives, A. (2016). Integration of orthogonal signaling by the Notch and Dpp pathways in *Drosophila*. *Genetics* **203,** 219-240.

Talamillo, A., Barroso-Gomila, O., Giordano, I., Ajuria, L., Grillo, M., Mayor, U. y Barrio, R. (2020). The role of SUMOylation during development. *Biochemical Society Transactions* **48**, 463-478.

Tripathi, B. K. e Irvine, K. D. (2022). The wing imaginal disc. *Genetics* **220**, 1-36.

Varejão, N., Lascorz, J., Li, Y., y Reverter, D. (2020). Molecular mechanisms in SUMO conjugation. *Biochemical Society Transactions* **48**, 123-135.

Wang, Q., Yan, R., Pinnell, N., McCarter, A. C., Oh, Y., Liu, Y., Sha, C., Garber, N. F., Chen, Y., Wu, Q., Ku, C. J., Tran, I., Serna Alarcon, A., Kuick, R., Engel, J. D., Maillard, I., Cierpicki, T. y Chiang, M. Y. (2018). Stage-specific roles for Zmiz1 in Notch-dependent steps of early T-cell development. *Blood* **132**, 1279-1292.

Wiese, K. E., Nusse, R. y van Amerongen, R. (2018). Wnt signalling: conquering complexity. *Development* **145**, 1-12.

Zhao, X., Hendriks, I. A., Le Gras, S., Ye, T., Ramos-Alonso, L., Nguéa P, A., Lien, G. F., Ghasemi, F., Klungland, A., Jost, B., Enserink, J. M., Nielsen, M. L. y Chymkowitch, P. (2022). Waves of SUMOylation support transcription dynamics during adipocyte differentiation. *Nucleic Acids Research* **50**, 1351-1369.

Zhu X, Ding S, Qiu C, Shi Y, Song L, Wang Y, Wang Y, Li J, Wang Y, Sun Y, Qin L, Chen J, Simons M, Min W y Yu L. (2017). SUMOylation negatively regulates angiogenesis by targeting endothelial Notch signaling. *Circulation Research* **121**, 636-649.